Towards real-time sludge dewatering process optimization using ultraviolet-visible spectrophotometry and torque rheology

by

Jordan Gerber

A thesis submitted to the Faculty of Graduate and Postdoctoral Affairs in partial fulfillment of the requirements for the degree of

Master of Applied Science

in

Environmental Engineering

Department of Civil and Environmental Engineering
Ottawa-Carleton Institute for Environmental Engineering

Carleton University

Ottawa, Ontario

Abstract

The treatment of biosolids is becoming a larger focus of wastewater treatment facilities due to the growing associated costs and optimization potentials. Presently, most operations are controlled manually, which often results in sub-optimal process performance. The goals of this research were to develop systems to optimize sludge treatment processes. The first study in this thesis analyzed and improved the sensitivity of UV-Vis spectrophotometry for the detection of polymer in dewatered sludge supernatant. The second study developed a two-stage in-line and real-time optimum polymer dose monitoring system. This system employed torque rheology as the upstream monitor and UV-Vis spectrophotometry as the downstream monitor relative to the dewatering process. Laboratory scale experiments found the system to be generally reliable and accurate. The third study developed a method for nutrient recovery optimization in sludge supernatant after dewatering. This method employed UV-Vis spectrophotometry as a monitor for struvite formation through magnesium addition.

Acknowledgements

I would like to first and foremost thank my supervisor Dr. Banu Örmeci. Her knowledge, guidance, and support were incredible, and I would not have made it to this point without her help. I've learned so much from her, and she has been such a positive influence on my life.

I would also like to thank Rich Kibbee for all of his help through these past two years. His tireless efforts to be of aid were almost too generous, and I am very grateful for it all. Additionally, I would like to thank Marie Tudoret for her continuous support and help in the lab.

Lastly, I would like to thank my friends and family for all of their support throughout my Masters. They consistently kept me on track and moving towards the end goal.

Table of Contents

List of Tables

List of Figures

List of Abbreviations and Terms

A	Absorbance
α	Fraction of Mg, N, and P which can go on to form struvite
abs	Absorbance unit
BOD	Biochemical Oxygen Demand
C	Concentration
CST	Capillary Suction Time
DI	Deionized Water
DS	Dry Solids
dv/dy	Shear Rate
ε	Extinction Coefficient
η	Plastic Viscosity
FTIR	Fourier Transform Infrared Spectroscopy
I	Transmitted Radiation
I_o	Incident Radiation
K_{SO}	Conditional Solubility Product
K_{SP}	Solubility Product
l	Path Length
λ	Wavelength
μ	Dynamic Viscosity
N/I	Non-Identifiable (optimum polymer dose based on measurement)
NMR	Nuclear Magnetic Resonance
PAM	Polyacrylamide

R^2	Coefficient of Determination
RAS	Return Activated Sludge
RI	Refractive Index
ROPEC	Robert O. Pickard Environmental Centre
RSS	Residual Sum of Squares
S_a	Degree of Supersaturation
SEC	Size Exclusion Chromatography
SS	Suspended Solids
T	Transmittance
τ	Shear Stress
τ_o	Initial Yield Stress
TKN	Total Kjeldahl Nitrogen
TS	Total Solids
TSS	Total Sum of Squares
TTF	Time-To-Filter
TTQ	Totalized Torque
TWAS	Thickened Waste Activated Sludge
UV	Ultraviolet
Vis	Visible
WAS	Waste Activated Sludge
WWTP	Wastewater Treatment Plant
XRD	X-ray Diffraction

Chapter 1 – Introduction

The treatment of biosolids is rapidly becoming a larger focus of wastewater treatment facilities due to the growing associated costs and optimization potentials. Treatment and reuse costs for sludge management can amount to approximately 50% of the total operational costs of a municipal wastewater treatment facility (Nowak, 2006). This high cost can be offset through more optimization and the reuse of the products and by-products of the treatment processes. Optimization of biosolids treatment processes can also lead to improvements in process efficiency and efficacy, thus allowing for higher treatment targets and stricter regulations to be met. There is, however, an overreliance on manual control and optimization of biosolids treatment processes, which can be inaccurate and are unreliable for real-time control and optimization.

Mechanical sludge dewatering processes often employ polyacrylamide polymer conditioners to enhance the flocculation of the solids and separation of the water phase in the sludge (Dentel, 2001). Many wastewater treatment plants add more than the optimal polymer dosage in their dewatering processes in order to avoid an underdose. However, both underdosing and overdosing of polymer conditioners decreases the solids recovery of the dewatering process, and therefore maintaining an optimum polymer dose is necessary to maximize the efficacy of the process (Bolto and Gregory, 2007). Additionally, polymer conditioners can account for over 50% of the biosolids handling process cost (US EPA, 1987). Therefore, the optimization of polymer dosage can result in significant cost savings for a dewatering facility.

In order to effectively optimize the polymer dose of a dewatering process, a real-time and in-line system is required. A polymer dose optimization system utilizing both feed-forward

and feed-back controls would further improve the efficacy of a real-time system. In such a system, one in-line optimization method is employed upstream of the dewatering process and another is employed downstream. This allows for two-stage independent verification of the optimum polymer dose, thus ensuring the accuracy and reliability of the system as a whole.

The products of mechanical sludge dewatering processes are a cake stream with a high solids content and a liquid stream with a relatively low solids content. The liquid product is often simply recycled to the headworks of the treatment facility and is referred to as a side-stream. Struvite ($MgNH_4PO_4 \bullet 6H_2O$) precipitation is an excellent and often employed method for nutrient recovery in these side-streams at wastewater treatment facilities (Tchobanoglous *et al.*, 2014). This is due in part to the simplicity and cost-effectiveness of the process, as well as that struvite can be used as a fertilizer and in certain industrial applications (Fattah *et al.*, 2008; Tchobanoglous *et al.*, 2014; Vaneeckhaute *et al*., 2018). Struvite contains both nitrogen in the form of ammonium and phosphorus in the form of phosphate, and therefore its recovery removes both of these nutrients from the side-stream. In wastewaters, magnesium is generally the limiting component for struvite formation (Abel-Denee *et al.*, 2018; Doyle and Parsons, 2002; Fattah *et al.*, 2008; Jaffer *et al*., 2002). Accordingly, it is generally added to wastewater side-stream processes for struvite formation and precipitation (Doyle *et al*., 2000; Fattah *et al*., 2008).

The overall goal of this research was to develop optimization methodologies for biosolids dewatering processes which can be used in-line and in real-time. The focus was on methods utilizing UV-Vis spectrophotometry and torque rheology. This thesis is organized in the format of integrated manuscripts, with Chapters 4, 5, and 6 representing individual study

manuscripts. The first study, here Chapter 4, investigated the impact of path length and solids concentration on the sensitivity of polymer measurement using UV-Vis spectrophotometry. The second study, here Chapter 5, investigated the feasibility of using torque rheology and UV-Vis spectrophotometry within a proposed feed-forward and feed-back control system for sludge dewatering optimization. The third study, here Chapter 6, investigated the optimization of struvite formation nutrient recovery processes in sludge side-streams using UV-Vis spectrophotometry.

Chapter 2 – Literature Review

2.1 Sludge types and treatment

At a typical wastewater treatment facility, solids are removed at various stages throughout the treatment process as a high-density mixture with various liquids. This mixture is commonly referred to as sludge and its properties are dependent upon the stage of the treatment process from which is it removed as shown in Figure 2.1. As it contains most of the pathogens, organics, and toxic compounds from the wastewater influent in a highly concentrated form, sludge requires further treatment separate from the main treatment train of the facility (Tchobanoglous *et al.*, 2014). The level of this treatment is dependent upon the final disposal method of the biosolids, with some methods requiring a higher quality than others.

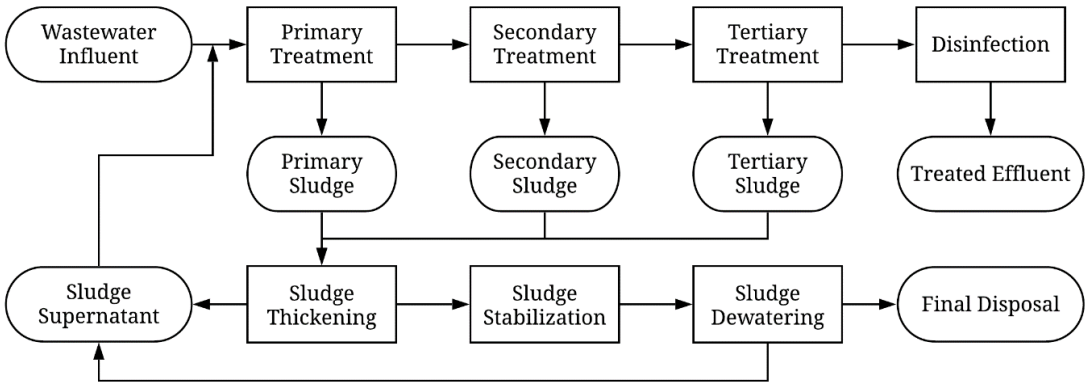

Figure 2.1: A treatment train for a typical wastewater treatment plant with sludge treatment.

2.1.1 Sludge types

A useful way to classify sludge types is by the source of the sludge in the treatment facility. For most facilities, this classifies sludge as primary, secondary, and tertiary sludge.

Primary sludge is that recovered from the primary clarifiers and is made up of the readily settleable solids from the raw wastewater. It usually has a high total solids (TS) content of 1% to 6% dry solids (DS) by weight (Tchobanoglous *et al.*, 2014). It is typically gray with a slimy texture and has an offensive odour. Primary sludge has a high pathogen content, but stabilization can be achieved through digestion processes under normal conditions.

Secondary sludge is that recovered from the secondary clarifiers following the secondary treatment processes. It is often referred to as activated sludge as the activated sludge process is the most common secondary treatment process employed at wastewater treatment facilities. The activated sludge process employs an aerated reactor in which microorganisms are kept in suspension and consume the organics in the wastewater, decreasing the biochemical oxygen demand (BOD) (Tchobanoglous *et al.*, 2014). In order to maintain an optimal food to microorganism ratio, activated sludge must be periodically recycled from the secondary clarifiers to the activated sludge process reactor. This is known as Return Activated Sludge (RAS). The excess activated sludge which is not recycled and proceeds to the sludge treatment train is the Waste Activated Sludge (WAS). WAS has a lower TS content than primary sludge in the range of 0.4% to 1.2% DS and a high organic content due to nature of the activated sludge process (Tchobanoglous *et al.*, 2014). It is typically brown in colour with a flocculant appearance and an earthy odour. However, without sufficient aeration, the microorganisms will begin to die, and the sludge will become septic, turning a darker colour and producing a more offensive odour. WAS

stabilization can be achieved by itself using aerobic digestion, or when mixed with primary sludge using either aerobic or anaerobic digestion.

Some wastewater treatment facilities employ tertiary treatment following secondary treatment and prior to disinfection for additional treatment of the wastewater. These processes can perform different treatment goals, including nutrient removal and additional BOD removal (Tchobanoglous *et al.*, 2014). As a result of this variety of potential processes, the properties of tertiary sludge are widely varied. Many tertiary treatment processes employ some form of biological treatment, and in this case can share many properties with activated sludge.

2.1.2 Sludge thickening

Due to its low TS content, WAS is often thickened to a higher TS content prior to further sludge treatment. This is done in order to reduce the total volume being treated, thus reducing the chemical and energy requirements of downstream processes such as stabilization and dewatering. Depending on the sludge properties and the facility's requirements, different methods of making thickening WAS (TWAS) can be used such as gravity thickening, flotation thickening, centrifugal thickening, gravity belt thickening, and rotary drum thickening (Tchobanoglous *et al.*, 2014). These processes are often enhanced through the use of chemical conditioners such as iron or alum salts or polymers (Tchobanoglous *et al.*, 2014).

2.1.3 Sludge stabilization

Sludge stabilization is a process performed on all sludges, usually mixed, in order to reduce pathogens, odours, and the potential for putrefaction. This is done for a few reasons including volume reduction, improved dewaterability, production of biogas for energy, and preparation for reuse of the biosolids (Tchobanoglous *et al.*, 2014).

There are a number of stabilization processes used including chemical, which uses an alkaline material such as lime, biological digestion in a reactor, which can be either aerobic or anaerobic, and composting (Tchobanoglous *et al.*, 2014). Due to chemical stabilization processes resulting in an increase in sludge volume and the relatively large space and time requirements of composting processes, aerobic and anaerobic digestion are the preferred stabilization processes preceding sludge dewatering.

2.1.3.1 Aerobic digestion

Aerobic digestion processes operate similarly to the activated sludge process. The sludge is placed in an aerated reactor wherein microorganisms consume the organic material in the sludge breaking it down into simpler compounds. As the available organic matter is depleted, the microorganisms will begin to consume their own cellular tissue for energy. The digestion process as a whole oxidizes the organic matter and cellular tissue to form carbon dioxide (CO_2), water (H_2O), and ammonia (NH_3). The ammonia is then further oxidized to nitrate (NO_3^-), with a simplified digestion process shown in Equation 2.1 below, using $C_5H_7NO_2$ to represent the biomass in the sludge (Tchobanoglous *et al.*, 2014):

$$C_5H_7NO_2 + 7O_2 \rightarrow 5CO_2 + 3H_2O + HNO_3 \qquad \text{Equation 2.1}$$

Aerobic digestion is a much faster process compared with anaerobic digestion due to oxygen being an excellent electron acceptor. However, it carries a high energy demand, increasing cost, and is less efficient in that it generates higher quantities of sludge compared with anaerobic digestion (Tchobanoglous *et al.*, 2014). It is for this reason that it is used more often at smaller wastewater treatment facilities, with larger facilities often opting for anaerobic digestion for sludge stabilization. Aerobically digested sludge is also characterized as having poorer dewaterability for mechanical dewatering processes than anaerobically digested sludge. This is the result of the physical and chemical properties of the digested sludge product from the aerobic digestion process. As aerobic digestion processes are often based on the activated sludge process, aerobically digested sludge often has a flocculant appearance and a low TS content. This results in lower dewaterability as more water is trapped in the floc structures.

2.1.3.2 Anaerobic digestion

Anaerobic digestion processes are biological sludge stabilization processes which occur in the absence of oxygen. Organic matter is consumed and inorganic matter, primarily sulfate, is reduced by anaerobic microorganisms. This process occurs in three stages called hydrolysis, acidogenesis, and methanogenesis (Tchobanoglous *et al.*, 2014). In hydrolysis, complex organics such as carbohydrates, proteins, and lipids are hydrolyzed by extracellular enzymes to soluble organics such as glucose, amino acids, and fatty acids. In acidogenesis, microorganisms known as acid producers convert these compounds to short-chain organic acids. In methanogenesis, these organic acids are converted primarily into methane (CH_4) and carbon dioxide (CO_2) which off gas from the digestor. The methane

can be recaptured and used to produce energy, which can result in a net energy output from the digestion process.

Anaerobic digestion is an endothermic process, and as such requires a constant input of energy to function. Most reactors operate in the 30 °C to 38 °C range or the 50 °C to 57 °C range, known as mesophilic and thermophilic, respectively (Tchobanoglous *et al.*, 2014). This is done as the microorganisms present in sludge under anaerobic conditions operate most effectively within these temperature ranges, with the thermophilic microorganisms achieving stabilization of the sludge at a faster rate. Despite this energy requirement, anaerobic digestion can be a net energy producing process as a result of the aforementioned methane recapture.

Anaerobic digestion, though slower than aerobic digestion at achieving stabilization, consumes less energy and produces less sludge. It does, however, come with a high capital cost and is a more complex process to operate. It is for this reason that it is more common at larger wastewater treatment facilities, with smaller facilities often opting for lower complexity aerobic digesters for sludge stabilization.

Anaerobically digested sludges typically have higher TS contents than aerobically digested sludge and have a higher dewaterability. They are dark in colour and have a homogeneous appearance.

2.1.4 Sludge conditioning

In order to improve the dewaterability of the digested sludge, it is conditioned prior to dewatering. Conditioning can be the addition of a chemical conditioner (the most common method), heat treatment, or freeze-thaw conditioning (Dentel, 2001; Tchobanoglous *et al.*,

2014). In chemical conditioning, the addition of the chemical conditioner causes the sludge to flocculate, coagulating the solids and allowing solid-liquid separation. The most common chemical conditioners employed are iron and alum salts, lime, and organic polymers, with the latter being most widely employed to enhance mechanical sludge dewatering (Dentel *et al.*, 2000a; Tchobanoglous *et al.*, 2014). This is because polymers do not increase the total dry solids (DS) of the sludge, whereas the inorganic conditioners listed above can result in large increases in the total DS of the sludge (Tchobanoglous *et al.*, 2014). Another advantage of polymers is that the required dose of polymer conditioners is often quite lower than the required dose of inorganic conditioners for a given sludge. However, one drawback to the use of polymers as conditioners is their high cost relative to inorganic conditioners, which limits their usage in a wastewater treatment facility as a whole.

2.1.4.1 Conditioner mechanisms of action

Chemical conditioners work by flocculating the sludge in which they are dosed, thus coagulating the solids and releasing the water. Flocculation occurs when charged ions become attached to the surface of an oppositely charged particle. The solid particles in sludge are primarily negatively charged organics, and therefore attract positively charged ions to their surfaces. This forms what is referred to as a double layer, with a stern layer of positively charged ions at the surface of the negatively charged particle and a diffuse layer of ions above it. When the overall surface charge of the particle, known as the zeta potential, is sufficiently neutralized, the repulsive force between solid particles in the sludge is reduced, allowing coagulation of the particles.

There are two main mechanisms which cause this flocculation, known as charge neutralization and bridging (Bolto and Gregory, 2007; Dentel, 2001). In charge neutralization, the charged ions are adsorbed onto the surface of the oppositely charged particles, thus neutralizing the overall charge (Bolto and Gregory, 2007; Dentel, 2001). As described above, this reduces the net repulsive force between the particles, causing them to coagulate. A schematic of the charge neutralization model is shown in Figure 2.2a. In bridging, a section of a long-chain polymer is adsorbed onto a particle surface, leaving parts of the chain dangling in solution (Bolto and Gregory, 2007). These dangling portions of the polymer chain can adsorb onto the surface of another particle, thus bridging the particles to one another (Bolto and Gregory, 2007; Dentel, 2001). A schematic of the bridging model is shown in Figure 2.2b. Bridging of the polymer requires there be unoccupied, oppositely charged surface on the particles. Therefore, when the polymer is overdosed, the surfaces of the particles become saturated with adsorbed polymer, preventing bridging and thereby coagulation of the particles (Bolto and Gregory, 2007). This phenomenon, known as restabilization, is shown schematically in Figure 2.2c. At the same time, underdosing of the polymer results in insufficient bridging and therefore has the same result as overdosing (Bolto and Gregory, 2007). Accordingly, there exists an optimum dosage for polymer conditioning (Bolto and Gregory, 2007). In reality, the mechanism of flocculation for all conditioners is a combination of the two described above, but charge neutralization can be said to be the main mechanism for inorganic conditioners while bridging can be said to be the main mechanism for organic polymers.

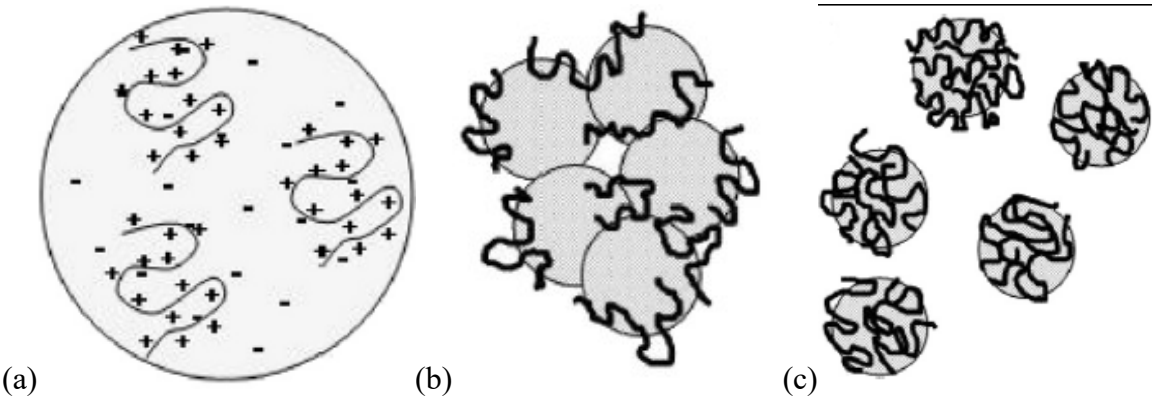

Figure 2.2: Schematic showing a) charge neutralization model of flocculation; b) bridging model of flocculation; c) restabilization of the solid particles as a result of a polymer overdose (Bolto and Gregory, 2007).

2.1.4.2 Polymer classification and characterization

Organic polymers are the most common form of chemical conditioners used for enhancing sludge dewatering processes. They are commonly referred to as organic polyelectrolytes as they dissociate into cationic and anionic species when added to water (Dentel, 2001). Their properties can be characterized by various physical and chemical characteristics, including the monomers present, molecular weight, charge, charge density, and physical appearance. Polymers are commercially available in liquid, emulsion, and solid forms (SNF Floerger, 2002). Each form has advantages, with liquid and emulsion forms being simpler to use and solid forms being easier to transport (SNF Floerger, 2002). Liquid products tend to only be 4% to 9% active matter, while emulsions are slightly higher at 60% active matter, with solids being the highest with 90% to 100% active matter (Dentel, 2001).

The charge and molecular weight of a polymer are controlled by the combination of monomers which make it up (Dentel, 2001). A higher molecular weight is generally the result of a longer polymer chain. A longer chain allows for more polymer bridging to occur,

thus improving flocculation of the particles. Charge can be controlled by combining a controlled percentage of charged monomers with a controlled percentage of neutral monomers (Dentel, 2001). However, because of the variability between polymers, the reported overall charge and molecular weight are averaged values (Dentel, 2001). Due to their size and thereby difficulty in precisely quantifying such values, the molecular weights and charge densities of polymers are often reported using terms such as "high" and "very-high" corresponding to quantifiable ranges as summarized in Table 2.1 below.

Table 2.1: Summary of polymer property characterization (Tchobanoglous *et al.*, 2014; WEF, 2012).

Characterization term	**Charge density (mol %)**	**Relative molecular weight**
Very-High	> 70 – 100	> 6,000,000 – 18,000,000
High	> 40 – 70	> 1,000,000 – 6,000,000
Medium	> 10 – 40	> 200,000 – 1,000,000
Low	< 10	< 200,000

As solids in sludge are primarily anionic, cationic charged polymers are most often used as chemical conditioners (Dentel, 2001). The most common monomer backbone of these polymers is polyacrylamide (PAM), the structure of which is shown in Figure 2.3 below (Dentel, 2001; WEF, 2012). Neither the acrylamide monomer nor its polymerized form is ionically charged (Dentel, 2001). As such, a cationic charge must be imparted onto the polyacrylamide backbone through one of two methods. These methods are to add cationic functional groups to the acrylamide monomers, or to bond neutral acrylamide monomers with modified acrylamide monomers to form an overall cationic copolymer (Dentel, 2001).

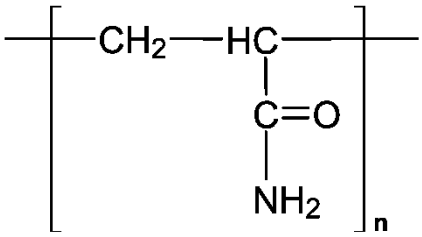

Figure 2.3: Chemical structure of polyacrylamide (Dentel, 2001).

The most common polymer employed through the first method is known as the Mannich polymer (Dentel, 2001). It is called such as it is based on polyacrylamide which has undergone the Mannich reaction, whereby formaldehyde (CH_2O) and dimethylamine ($(CH_3)_2NH$) are added to aminomethylate the acrylamide monomer (Dentel, 2001). The added amine group on the monomer structure carries a positive charge, causing the monomer to be overall cationic (Dentel, 2001).

The second method is to combine modified acrylamide monomers with unmodified monomers to form a copolymer through the process of copolymerization (Dentel, 2001). This allows for better control of physical and chemical properties of the polymer, such as the molecular weight and charge density (Dentel, 2001). This variation in properties is beneficial as it allows for polymers to be engineered to best condition specific sludges (Dentel, 2001). The ratio of modified monomers to the acrylamide monomers typically ranges from 20:80 to 55:45 mol % (Dentel, 2001). Different combinations of monomers can affect the polymerization reaction, enhancing it, and thus increasing the molecular weights of the polymer chains formed (Dentel, 2001). This is beneficial for wastewater sludge dewatering applications, as discussed above (Dentel, 2001). Other properties which can be controlled include the hydrophobicity and the conformation of the polymer (Dentel, 2001).

One important physical property that is controlled for is the overall structure of the polymer chain (Dentel, 2001). Three general structure types are possible, referred to as linear, branched, and cross-linked, as shown in Figure 2.4 below (Dentel, 2001; SNF Floerger, 2003). The choice of structure is dependent upon the intended application and the sludge properties. Linear polymers, the oldest type, require the lowest dosage but produce low strength flocs (SNF Floerger, 2003). Conversely, cross-linked polymers require the highest dosage due to their large molecular weights but produce high strength flocs (SNF Floerger, 2003). The dewatering properties of branched polymers lie somewhere in between those of linear and cross-linked polymers (SNF Floerger, 2003). As an example, a high shear process such as centrifugation would require high strength flocs, and therefore a cross-linked polymer would be optimal.

Figure 2.4: Schematic showing the structure of a a) linear polymer; b) branched polymer; c) cross-linked polymer (SNF Floerger, 2003)

2.1.4.3 Polymer make-down solution preparation and maturation

Prior to use, polymers must be prepared through mixing into a solution with water to a desired make-down concentration. Depending on the physical form of the polymer, there are a number of commercial systems described for preparation of the make-down solutions. Appropriate mixing of the make-down solution is required in order to maximize its homogeneity and the polymer activation (Owen *et al.*, 2002).

Post-mixing, the make-down solution undergoes an ageing process referred to as maturation. As the polymer make-down solution matures, the viscosity of the solution initially increases rapidly, followed by a rapid decrease (Gardner *et al.*, 1978; Owen *et al.*, 2002). At a certain point, the viscosity reduction will slow greatly, but continue slowly (Gardner *et al.*, 1978; Owen *et al.*, 2002). The existence of an optimum polymer solution maturation time for flocculation processes has been reported (Owen *et al.*, 2002; Owen *et al.*, 2007). Varying optimum maturation times have been reported for polymer dose optimization, ranging from 24 h (Novak and O'Brien, 1975) to 72 h (Owen *et al.*, 2002). Owen *et al.* (2002) proposed a mechanism for this optimization whereby polymers undergo a four-stage process during maturation, shown schematically in Figure 2.5 below. Initially, the polymer in solution form large gel lumps containing most of the polymer, though this is unavailable for flocculation (Figure 2.5a) (Owen *et al.*, 2002). After several hours, the gel lumps have dispersed, but several polymer chains will remain entangled, forming supramicron agglomerates (Figure 2.5b) (Owen *et al.*, 2002). These entanglements result in a reduction of polymer chains available to form particle bridging for flocculation (Owen *et al.*, 2002). After several days, most agglomerates will have dispersed and the concentration of free polymer chains is assumed to be at equilibrium (Figure 2.5c) (Owen *et al.*, 2002). This is the optimum maturation point, and thus the flocculant activity reaches a maximum (Owen *et al.*, 2002). If ageing continues past this point, the polymer chains begin to undergo conformational changes which result in decreased flocculant activity (Figure 2.5d) (Owen *et al.*, 2002). The most widely accepted mechanism for this is water breaking hydrogen bonds within the polymer chains, leading to a more compact coil

conformation of the polymer chains (Kulicke and Kniewske, 1981). This compaction reduces the ability of the polymers to form bridges between particles (Owen *et al.*, 2002).

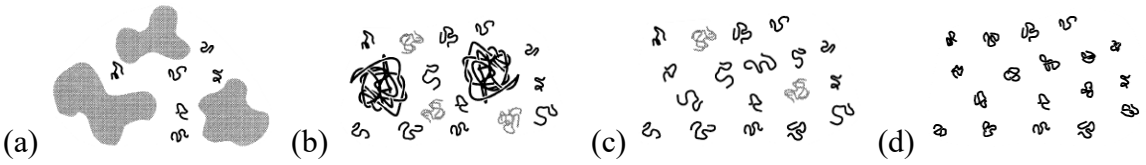

Figure 2.5: Schematic showing stages of polymer solution maturation: a) Initial showing polymer in gel lumps; b) After several hours showing polymer in agglomerates; c) After several days showing polymer in equilibrium; d) With longer-term ageing showing polymer conformation changes (Owen *et al.*, 2002).

2.1.5 Sludge dewatering

Sludge dewatering is a process defined by solid-liquid phase separation of the digested sludge resulting in a cake stream with a high solids content and a liquid stream with a relatively low solids content. The TS content of the cake is often in the range of 20% to 35% DS, compared to that of the digested sludge influent which is often in the range of 1% to 3% DS, resulting in a large volume reduction of the biosolids. This is done for a variety of reasons, including to make the biosolids in the cake more easily transported, handled, and reused (Tchobanoglous *et al.*, 2014). The liquid phase is either returned to the headworks of the wastewater treatment facility or undergoes additional treatment separately in a side stream process.

There are multiple sludge dewatering processes including gravity settling, mechanical dewatering, electro-dewatering, solar drying, and thermal drying (Tchobanoglous *et al.*, 2014). Due to space and energy requirements, the most common form of dewatering employed at large-scale wastewater treatment facilities is mechanical dewatering, often

with polymer conditioning preceding. Mechanical dewatering processes include centrifugation, belt filter presses, filter presses, rotary presses, and screw presses, with the first two being the most widespread (Tchobanoglous *et al.*, 2014).

In centrifuges, conditioned sludge is fed into a rotating bowl where it is subjected to a centrifugal force caused by this rotation. This causes the separation of the solid and liquid phases, which are recovered and referred to as cake and centrate, respectively (Tchobanoglous *et al.*, 2014). In belt filter presses, conditioned sludge is fed onto a belt filter where it first undergoes gravity drainage. Afterwards, a pressure is applied, usually though a system of opposing belts and rollers, which forces additional water from the sludge. Following this, the cake is recovered through scraping off the belts, and the liquid phase, referred to here as filtrate, is captured (Tchobanoglous *et al.*, 2014).

2.1.6 Side-stream treatment processes

Sludge thickening and dewatering processes result in solid and liquid product streams. The liquid streams, as shown in Figure 2.1, are often simply returned to the headworks of most wastewater treatment facilities. Alternatively, some facilities opt to perform additional treatment on these side-streams prior to returning them to the headworks. The composition of side-streams is highly variable as it is not only dependent upon the composition of the influent wastewater, but also upon the treatment, stabilization, and solid-liquid separation processes employed. Side-streams can have relatively high suspended solids (SS), biochemical oxygen demand (BOD), total Kjeldahl nitrogen (TKN), ammonium (NH_4), nitrogen oxide (NO_x), and phosphorus (P) concentrations compared with the influent

wastewater. As a result, and due to their relatively low flows, side-streams provide tempting points for treatment processes which target these components.

Due to the highly varied composition of side-streams, there exist a wide variety of side-stream treatment processes designed to achieve different goals. Broadly, these include the reduction of suspended solids and colloidal material, nutrient recovery, and nitrification and denitrification processes (Tchobanoglous *et al.*, 2014).

2.2 Laboratory-scale polymer dose optimization methods for sludge dewatering

As mentioned in Section 2.1.4.1, maintaining an optimum polymer dosage when conditioning sludge prior to dewatering is important for the flocculation and coagulation process. Underdosing results in insufficient polymer bridging while overdosing results in restabilization of the biosolid particles (Bolto and Gregory, 2007). There exist multiple lab-scale tests for measuring polymer concentration and sludge dewaterability, with either measurement type able to be used to optimize the polymer dosage. A few of the more commonly employed methods will be discussed in this section. Additional polymer characterization and quantification methods include gas chromatography, high-performance chromatography, mass spectrometry (Gibbons and Örmeci, 2013), the starch-triiodide method (Scoggings and Miller, 1979), viscosity (Jungreis, 1981), calorimetry (Hansen and Eatough, 1987), fluorescence spectrometry (Arryanto and Bark, 1992), radioactive labeling (Nadler *et al.*, 1994), flow injection analysis (Taylor *et al.*, 1998), nuclear magnetic resonance (NMR) spectroscopy (Chang *et al.*, 2002), florescence tagging (Becker *et al*., 2004), and spectrophotometric determination using cationic dyes

(Chmilenko *et al.*, 2004). These methods have been found to have reduced sensitivity and reproducibility in complex media due to interference from the presence of other compounds (Dentel *et al.*, 2000b; Lu and Wu, 2003).

2.2.1 Total solids analysis

The most basic method for optimization of polymer dosage is to measure the total solids (TS) content of the sludge prior to and of the cake after dewatering. TS is measured by placing 25 g to 50 g samples of sludge or cake into evaporating dishes and placing in an oven at 103 °C to 105 °C overnight (APHA *et al.*, 2005). The dishes are massed empty as well as with samples before and after the drying period in the oven (APHA *et al.*, 2005). The mass difference corresponds to the mass of water in the sample, and from this the TS content of the sample is determined through calculation (APHA *et al.*, 2005). By adjusting the polymer dosage and measuring the relative change in TS between the two streams, it is possible to maximize the cake TS and thus optimize the polymer dosage. This method and variations of it are time-consuming and are impractical on a large scale, however.

2.2.2 Capillary suction time test

The capillary suction time (CST) test is one of the most established methods of measuring sludge dewaterability. This empirical test measures the filterability of a sludge sample after chemical conditioning (Scholz, 2005). The test is performed by pouring the conditioned sludge into a funnel resting atop a Whatman No. 17 filter paper (APHA *et al.*, 2005). Sludge is filtered and the filtrate is pulled outwards from the funnel through the filter paper through capillary suction (Scholz, 2005). As this happens, a sludge cake is formed at the bottom of

the funnel, providing resistance to the capillary suction (Scholz, 2005). The time required for the filtrate to travel between two radii on the filter paper is measured, providing a measure of the cake resistance (APHA *et al.,* 2005; Scholz, 2005). The rate of the filtrate permeation through the filter paper is dependent upon the condition of the sludge and the filterability of the cake formed, with a lower CST corresponding to better filterability (Scholz, 2005). This allows for the optimum polymer conditioner dosage to be determined through a series of tests. In addition to being well established, the CST test is a highly popular test for measuring sludge dewaterability as it is simple, rapid, and inexpensive (Scholz, 2005).

2.2.3 Filtration tests

Two methods of filtration tests can be used to assess the dewaterability of a conditioned sludge sample. The first method, known as the time-to-filter (TTF) method, measures the time required to filter a standard volume of conditioned sludge. The second method, known as the filtrate volume method, conversely measures the volume of conditioned sludge filtered in a standard period of time. For both methods, maintaining a constant vacuum pressure and volume of conditioned sludge are necessary for test precision (APHA, 2005). A Whatman No. 1 or No. 2 filter should be used for all tests (APHA, 2005). A shorter time in the TTF method and a greater filtrate volume in the filtrate volume method both correspond to better solid-liquid phase separation in the conditioned sludge. Through a series of tests, therefore, an optimum polymer dosage can be determined for the sludge sample.

2.2.4 Turbidimetry

Turbidimetric methods employ a reagent which reacts with the polymer to produce an insoluble complex in the sample (Taylor and Nasr-El-Din, 1994). The result is that the polymer complex remains suspended in the solution, increasing the turbidity (Taylor and Nasr-El-Din, 1994). The polymer concentration is measured indirectly through the light scattered using a turbidimeter (Taylor and Nasr-El-Din, 1994). The usage of turbidimetric methods is limited by the number of variables which can affect the measurement, thus limiting its accuracy and precision (Taylor and Nasr-El-Din, 1994).

2.2.5 Colloid titration

Colloid titration is a method for the measurement of polymer concentration whereby a cationic polyelectrolyte is titrated with an anionic polyelectrolyte, or vice versa, using an endpoint indicator (Gehr and Kalluri, 1983; Taylor and Nasr-El-Din, 1994). This method is not very sensitive, and its accuracy is highly affected by the presence of other electrolytes in solution (Taylor and Nasr-El-Din, 1994). For this reason and the overall complexity of the method, it is not well suited for polymer dosage optimization for sludge treatment.

2.2.6 Size exclusion chromatography

Size exclusion chromatography (SEC) is a method by which the polymers in solution are separated from lower-molecular weight impurities (Keenan *et al*., 1998; Taylor and Nasr-El-Din, 1994). This is possible as the column packing pore size is selected based on the size of the polymer so that it is excluded without other impurities (Taylor and Nasr-El-Din, 1994). This allows for ultraviolet (UV) and refractive index (RI) detection methods to be

employed which would otherwise be unsuitable for the unpurified samples (Keenan *et al*., 1998; Taylor and Nasr-El-Din, 1994). An advantage of the SEC method for sludge dewatering applications is that contaminated samples can be analyzed due to the polymer being separated from other impurities (Keenan *et al*., 1998; Taylor and Nasr-El-Din, 1994). However, the method is slow, with a rate of only three to five samples per hour being reported (Taylor and Nasr-El-Din, 1994).

2.3 Real-time and in-line polymer dose optimization methods for sludge dewatering

The main limitations of the laboratory-scale polymer dose optimization methods discussed above are the complexities and time requirements of the methodologies. Accordingly, an optimal polymer dose optimization method would both operate in real-time and in-line on the sludge treatment process. The in-line nature of the optimization system allows for the measurement of the media without the need for grab samples, thus eliminating method complexity. Measurement in real-time further allows for automatic and real-time adjustment of the polymer dosage for the dewatering process.

There are two main real-time and in-line polymer dose optimization methods which will be explored here. These are torque rheology and ultraviolet/visible (UV-Vis) spectrophotometry.

2.3.1 Torque rheology

Rheology is a method for real-time monitoring of optimum polymer dosage in digested sludge conditioning. It describes the deformation of matter under stress and is often used

to analyze the behaviour of non-Newtonian fluids, such as wastewater sludge (Abu-Orf and Dentel, 1999; Örmeci and Abu-Orf, 2005; Chhabra and Richardson, 2008). As a result of this non-Newtonian behaviour, the shear rate (*dv/dy)* of a sludge sample is not linearly proportional to the shear stress (τ) (Abu-Orf and Dentel, 1999). Newton's equation for shear stress is shown in Equation 2.2 below, and the Herschel-Bulkley equation for shear stress of a non-Newtonian fluid in shown in Equation 2.3 (Abu-Orf and Dentel, 1999)

$$\tau = -\mu\left(\frac{dv}{dy}\right) \qquad \text{Equation 2.2}$$

$$\tau = \tau_o + \eta\left(\frac{dv}{dy}\right)^n \qquad \text{Equation 2.3}$$

where μ represents the dynamic viscosity of the fluid, τ_o represents the initial yield stress, η represents the plastic viscosity, and *n* is an empirical constant less than one. The initial yield stress seen in the Herschel-Bulkley equation (equation 2.3) is the result of the initial resistance to shear of the sludge solids until sufficient stress is applied (Abu-Orf and Dentel, 1999). The existence of a yield stress is an indicator of the non-Newtonian nature of fluids such as wastewater sludge (Hammadi *et al*., 2012).

The thixotropic nature of sludge has an impact on its rheological properties (Baudez, 2008; Hammadi *et al*., 2012). This is defined by a decrease in viscosity over time under an applied shear stress, with a slow recovery after the removal of the shear stress (Hammadi *et al*., 2012). Baudez *et al*. (2008) found that sludge deflocculates under an applied shear stress, with re-flocculation occurring when the shear stress was low. Following high shear stress, however, the structure of the fluid is broken, and re-flocculation does not occur (Baudez *et al*., 2008).

It has been shown that the yield stress of a conditioned sludge sample increases with polymer dosage up to the optimum dosage, with an optimum dosage observed at the polymer dose where a change in the shape of the rheogram is observed (Campbell and Cresculo, 1982). Campell and Cresculo (1982) measured the shear rate versus shear stress rheograms, in which the yield stress is indicated by initial peaks in the rheograms. The peaks correspond to the shear stress at which the flocs in solution break, with higher peaks indicating a higher shear stress requirement to break the flocs (Campbell and Cresculo, 1982; Abu-Orf and Dentel, 1999). The strength of the flocs in the sludge is thus used to characterize the dewaterability of the sludge (Örmeci and Abu-Orf, 2005).

The overall strength of a flocculated sludge network can be determined through rheological measurements (Örmeci and Abu-Orf, 2005). Örmeci *et al.* (2004) developed a method using a torque rheometer which showed an increase in the area under torque-time rheograms with increasing polymer dosage. The area under a torque-time rheogram, known as the totalized torque (TTQ), represents the total energy dissipation of the system under a shear stress (Örmeci *et al.*, 2004). This provides a measurement of the network strength of the flocculated sludge (Örmeci *et al.*, 2004). Abu-Orf and Örmeci (2005) applied this principle to develop a method for determining optimum polymer dosage using the TTQ values of torque-time rheograms for conditioned sludges. The optimum polymer dose using this TTQ method is determined by the rheogram with the maximum TTQ value (Abu-Orf and Örmeci, 2005).

Örmeci (2007) developed a second method for determining optimum polymer dose using torque-time rheograms wherein unconditioned sludge is dosed with polymer in the torque rheometer. Using this direct injection method, the optimum polymer dose is determined

from the maximum torque peak height measured after polymer dosing (Murray and Örmeci, 2008). Murray and Örmeci (2008) also observed that the rheograms produced for sludge overdosed with polymer conditioner showed erratic and inconsistent peaks following the initial peak after polymer dosing. They attributed this to large amounts of unmixed excess polymer in solution (Murray and Örmeci, 2008).

The TTQ and direct injection methods which utilize torque-time rheograms obtained using torque rheometers have been found to produce good rheogram replicability (Abu-Orf and Örmeci, 2005; Örmeci, 2007). In-line torque rheometers for full-scale sludge treatment processes are beneficial as they provide real-time measurements with low complexity, as opposed to the laboratory methods discussed in the previous section.

2.3.2 Ultraviolet/visible spectrophotometry

The interaction between matter and electromagnetic radiation has long been used as an effective tool for quantifying properties and components of the matter (Owen, 1996). This interaction can result in reflection, scattering, absorbance, fluorescence, and photochemical reactions (Owen, 1996). UV-Vis spectrophotometry typically measures the absorbance of the radiation passing through the matter (Owen, 1996).

The absorbance of a sample is defined as the difference between the incident radiation (I_O) and the transmitted radiation (I) (Owen, 1996). Conversely, the transmittance of a sample is defined as the fraction of the radiation which passes through the sample (Owen, 1996). Transmittance (T) and absorbance (A) are therefore defined by the following Equations 2.4 and 2.5, respectively (Owen, 1996).

$$T = \frac{I}{I_o} = 10^{-A} \qquad \text{Equation 2.4}$$

$$A = -\log\frac{I}{I_o} = -\log T \qquad \text{Equation 2.5}$$

As mentioned above, UV-Vis spectrophotometry is often employed for quantitative analysis of samples of matter. This is possible for most compounds which absorb radiation in the range of wavelengths from λ = 190 nm to λ = 800 nm (Owen, 1996). This is based on the Beer-Bourguer-Lambert Law, defined in Equations 2.6 and 2.7 for transmittance and absorbance, respectively (Owen, 1996). The Beer-Bourguer-Lambert Law is the basis of UV-Vis quantitative spectrophotometry as it relates the measured absorbance value to the concentration of a component provided a few known values (Owen, 1996). It is valid based on the assumptions that absorbance is linearly proportional to the concentration of the component of interest (*C*) and to the path length (*l*) of the sample through which UV-Vis radiation is transmitted (Owen, 1996).

$$T = e^{-klC} \qquad \text{Equation 2.6}$$

$$A = \varepsilon lC \qquad \text{Equation 2.7}$$

In the above Equation 2.6, k is a constant, while in Equation 2.7, ε is known as the extinction coefficient (Owen, 1996). The extinction coefficient is a parameter defined by the properties of the solution (solvent, temperature) and of the measurement technique (wavelength, instrument) (Owen, 1996). It is therefore only reliably obtained from a calibration curve for the substance being analyzed by a particular instrument (Owen, 1996). Polyacrylamide polymers used in sludge conditioning have been shown to strongly absorb UV radiation with peaks at wavelengths of λ = 190 nm to λ = 200 nm (Al Momani and Örmeci, 2014a, 2014b; Gibbons and Örmeci, 2013). Gibbons and Örmeci (2013) and Al Momani and Örmeci (2014a) developed calibration curves and determined detection limits

for different polymers dosed in water and sludge centrate samples. Using UV-Vis spectrophotometry, optimum polymer doses are detected in the sample with the lowest residual polymer concentration in the liquid product of a dewatering process, such as filtrate or centrate (Aghamir-Baha and Örmeci, 2014). This minimum residual polymer concentration is detected in the sample with the minimum absorbance value at $\lambda = 190$ nm (Aghamir-Baha and Örmeci, 2014; Al Momani and Örmeci, 2014b).

The above studies showed that UV-Vis spectrophotometry provided reliable and accurate measurements of residual polymer concentration in solution. In-line UV-Vis spectrophotometers such as the one employed by Al Momani and Örmeci (2014b) are beneficial as they provide real-time measurements with low complexity, as opposed to the laboratory methods discussed in the previous section.

2.4 Nutrient recovery in side-stream processes

As mentioned in Section 2.1.6, one of the most common types of treatment processes for side-streams is nutrient recovery. These processes are performed with the goal of removing either or both phosphorus and ammonia in a recoverable form, usually for reuse as a fertilizer or in industrial applications (Fattah *et al.*, 2008; Tchobanoglous *et al.*, 2014; Vaneeckhaute *et al*., 2018). This is desirable as phosphorus demand is expected to outstrip supply by the year 2035 (Cordell *et al*., 2009). Furthermore, removal of nutrients is often required by discharge regulations in order to minimize the potential for eutrophication of receiving water bodies (Abel-Denee *et al.*, 2018; Doyle and Parsons, 2002; Korchef *et al*., 2011). Performing nutrient recovery in side-stream processes aids this in reducing the nutrient loading to the wastewater treatment facility.

The most common methods for phosphorus and ammonia recovery are precipitation processes (Tchobanoglous *et al.*, 2014). For combined phosphorus and ammonia recovery, crystallization processes which form magnesium ammonium phosphate ($MgNH_4PO_4 \cdot 6H_2O$) are the most widespread precipitation processes (Doyle and Parsons, 2002; Tchobanoglous *et al.*, 2014). Jaffer *et al.* (2002) found that the liquid product stream from a centrifugation process was the most suitable location for struvite formation in a wastewater treatment facility based on an elemental mass balance approach.

2.4.1 Struvite characterization, formation, and recovery

Magnesium ammonium phosphate, commonly known as struvite, is a white crystalline compound (Doyle and Parsons, 2002). Struvite crystals have a distinct orthorhombic structure, as shown in Figure 2.6 below. The struvite compound forms via the simplified general reaction shown in Equation 2.8 below, though a number of intermediate steps occur in the actual crystallization process (Doyle and Parsons, 2002).

$$Mg^{2+} + NH_4^+ + PO_4^{3-} + 6H_2O \rightarrow MgNH_4PO_46(H_2O) \qquad \text{Equation 2.8}$$

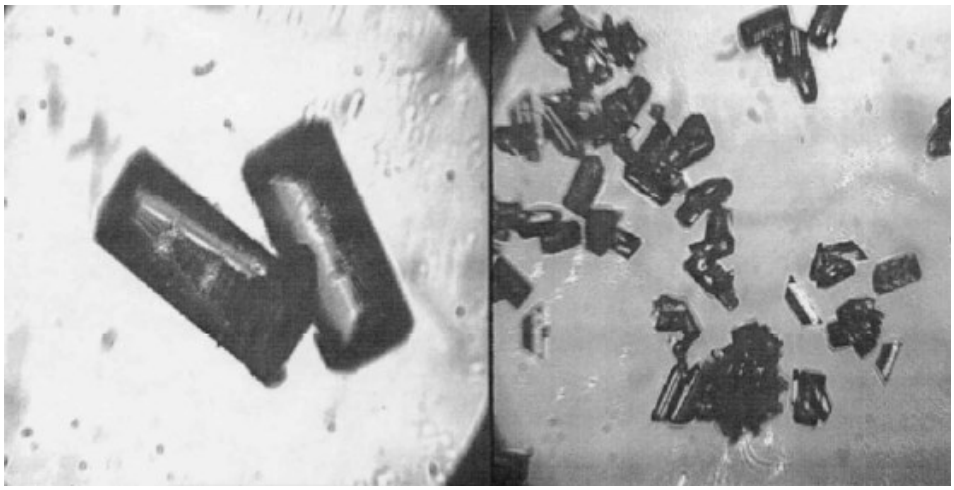

Figure 2.6: Struvite crystals precipitated from sludge liquors showing characteristic orthorhombic shape (Doyle *et al*., 2000).

In wastewater side-streams such as dewatering filtrate and centrate, ammonium and phosphorus are typically found in excess compared with magnesium, often by orders of magnitude (Abel-Denee *et al.*, 2018; Doyle and Parsons, 2002; Fattah *et al.*, 2008; Jaffer *et al*., 2002). Ammonium specifically is often in excess compared with both phosphorus and magnesium (Doyle and Parsons, 2002). The result of this is that magnesium is the limiting factor in struvite formation, which is why it is typically dosed to increase the Mg:P ratio (Doyle *et al*., 2000; Fattah *et al*., 2008). A Mg:P ratio slightly greater than 1.0 is desired, though higher Mg:P ratios have not been found to have a large effect on phosphorus recovery and high magnesium concentrations can be detrimental to treatment processes (Fattah *et al*., 2008).

In addition to the Mg:P ratio, struvite formation is dependent upon other parameters such as the N:P ratio, the concentration of other ions such as calcium, temperature, pH, the degree of supersaturation (S_a), and the conditional solubility product for struvite (K_{SO}) (Doyle and Parsons, 2002). The K_{SO} value is calculated based on the solubility product

(K_{SP}) for struvite, which itself is based on the total molar concentrations of the ions in solution taking account ionic strength and activity (Doyle and Parsons, 2002). Equation 2.9 below shows a generalized equation for calculating K_{SP} (Doyle and Parsons, 2002).

$$K_{SP} = M_x A_y = xM^{z+} yA^{z-} \qquad \text{Equation 2.9}$$

where *M* and *A* represent the cationic and anionic species in solution, respectively, *x* and *y* represent the number of cations and anions, respectively, and *z*+ and *z*– represent the valences (Doyle and Parsons, 2002). The K_{SO} value can then be estimated based on the calculated K_{SP} of struvite using the following Equation 2.10, where the α values are the fractions of Mg, N, and P which can go on to form struvite (Doyle and Parsons, 2002).

$$K_{SO} = \frac{K_{SP} MgNH_4PO_4}{\propto_{Mg} \propto_N \propto_P} \qquad \text{Equation 2.10}$$

K_{SO} values for struvite are highly affected by solution pH, and it has been shown that with increasing pH, the solubility of struvite decreases. Therefore, a higher pH is associated with greater struvite precipitation, and thus, greater phosphorus recovery (Doyle *et al*., 2000; Fattah *et al*., 2008; Moulessehoul *et al*., 2017).

Struvite precipitation occurs in two stages known as nucleation and growth (Doyle and Parsons, 2002). Nucleation, or the formation of crystals, can occur spontaneously in solution or can be aided by suitable nuclei, such as suspended solids (Doyle and Parsons, 2002). The time taken for nucleation to occur is known as the induction time (Doyle and Parsons, 2002). A lower induction time is desirable as the result is a greater amount of nucleation and thus struvite precipitation. Ohlinger *et al.* (1999) found that the induction time was inversely proportional to the supersaturation ratio (S_a). The supersaturation ratio

of struvite is based on its conditional solubility product and the activities of the component compounds of struvite, as shown in Equation 2.11 below (Ohlinger *et al*., 1999).

$$S_a = \left[\frac{[\{Mg^{2+}\}\{NH_4^+\}\{PO_4^{3-}\}]_{intial}}{K_{SO}}\right]^{1/3} \qquad \text{Equation 2.11}$$

As discussed above, K_{SO} is inversely proportional to the pH of the solution. Therefore, as per Equation 2.11, increasing the pH of the solution will increase the supersaturation of the struvite, thus increasing precipitation. Ohlinger *et al.* (1999) also found that the induction time of struvite decreased with increased mixing energy, meaning that as the mixing rate was increased, struvite crystal precipitation also increased. Based on these relationships, a higher pH and a more highly turbid mixing process will achieve higher struvite precipitation. Struvite crystallizers, such as the one described by Fattah *et al*. (2008), often both increase the pH and are designed for high mixing rates to take advantage of both of these relationships.

2.4.2 Potential monitors for struvite precipitation

Struvite formation can be measured directly through the use of X-ray Diffraction (XRD) (Doyle *et al.*, 2000; Kirinovic *et al*., 2017; Moulessehoul *et al*., 2017), Fourier transform infrared spectroscopy (FTIR) (Kirinovic *et al*., 2017; Moulessehoul *et al*., 2017), and Raman spectroscopy (Kirinovic *et al*., 2017). These methods are all time consuming and complex and are thus ill-suited for real-time monitoring of struvite formation in side-stream processes.

Struvite precipitation can also be monitored indirectly through the measurements of parameters such as phosphorus removal (Aguado *et al.*, 2016; Fattah *et al*., 2008;

Moulessehoul *et al*., 2017) and electrical conductivity (Bhuiyan *et al*., 2009; Moulessehoul *et al*., 2017). Monitoring through the measurement of electrical conductivity is limited as it is highly dependent upon the properties of the media being measured, such as temperature (Bhuiyan *et al*., 2009). Measuring phosphorus removal can be done through a variety of conventional colorimetric methods, but these cannot be performed in real-time to optimize other parameters such as magnesium dosage. Indirect measurements such as these are not very well-suited for monitoring struvite formation in wastewater side-streams with constantly changing characteristics.

There exist methods for measuring phosphorus concentrations in real-time, such as the one developed by Aguado *et al.* (2016). The researchers developed a voltammetric electronic tongue which was able to accurately and reliably quantify orthophosphate concentrations in real-time in a lab-scale struvite precipitation reactor treating synthetic urine (Aguado *et al.*, 2016). However, it is unknown how reliable this electronic tongue would perform in a more complex media such as a wastewater side-stream. There is therefore currently a lack of a low-complexity and reliable system for monitoring struvite formation and recovery in real-time. Such a system would allow for cost-effective and optimal nutrient recovery through struvite formation.

Chapter 3 – Materials and Methods

3.1 Experimental samples

3.1.1 Sludge samples

Three sludge samples were collected from different wastewater treatment plants (WWTP). Anaerobically digested sludge was collected from the Robert O. Pickard Environmental Centre (ROPEC), located in Ottawa, Ontario, and the Gatineau WWTP, located in Gatineau, Quebec. Aerobically digested sludge was collected from the Rockland WWTP, located in Clarence-Rockland, Ontario.

3.1.2 Full-scale sludge centrate samples

Anaerobically digested sludge centrate samples were collected from ROPEC. These samples were collected from the effluent of the bowl centrifuges operated by the facility.

3.1.3 Lab-scale sludge centrate samples

Anaerobically digested sludge samples were collected from ROPEC. The unconditioned sludge samples were centrifuged using a Sorvall Legend RT+ centrifuge (Thermo Fisher Scientific, Massachusetts, USA) at 10,000 G for ten minutes, shown in Figure 3.1. This was performed in 250 mL centrifuge sample bottles, and the total volume centrifuged at a time was either 500 mL, 1,000 mL, or 1,500 mL. Post-centrifugation, the centrate from each sample bottle was carefully removed from each bottle and placed into a common beaker for filtration as needed.

Figure 3.1: Sorvall Legend RT+ Centrifuge with centrifuge sample bottle (Thermo Fisher Scientific).

3.1.4 Sludge filtrate samples

Sludge samples were conditioned using polymer conditioners using a Phipps and Bird PB-700 Jar-tester (Richmond, VA), shown in Figure 3.2. The sludge sample to be conditioned was placed in a 500 mL beaker and placed in the Jar-tester with the paddle lowered. The polymer dose was then injected via pipette into the sludge sample, which was then mixed at 300 rpm for 30 seconds. This high mixing speed ensured polymer flocculation by being well mixed while the low mixing time reduced shear stress on the sludge, minimizing the effect of the thixotropic nature of the sludge.

Figure 3.2: Phipps and Bird PB-700 Jar-tester.

The conditioned sludge samples were filtered through either a Whatman No. 2 filter with a pore size of 8 µm (Whatman, UK) or a MF-Millipore Membrane 0.45 µm pore size filter (Millipore Sigma, USA), as needed. The samples were placed in a Buchner funnel which was placed above a 250 mL graduated cylinder with vacuum port (see Section 3.3.3 and Figure 3.6 for discussion and image of apparatus). A constant vacuum pressure of 20 in. Hg was applied using a vacuum pump (Welch, USA) and the filtrate was collected in a common beaker.

3.2 Chemicals employed

3.2.1 Polymers

Three polyacrylamide polymers with varying properties were employed. These were Zetag 8160 (manufactured by BASF Corporation), Flopolymer CA 4600 (manufactured by SNF Canada), and Flopolymer CB 4350 (manufactured by SNF Canada).

3.2.1.1 Made-down polymer stock solution preparation

Polymer stock solutions were made down to concentrations of 1.0% and 0.5% by preparing 10.0 g and 5.0 g of the polymer to be used, respectively, and mixing it into 1,000 mL of deionized water (Direct-Q UV Water Purification System, Millipore Sigma, USA). The mixing process was 5 minutes at 250 rpm followed by 55 minutes at 125 rpm. This mixing was accomplished using a Phipps and Bird PB-700 Jar-tester. After initial mixing, a hand blender was used to break up flocs which had formed. The hand blender was employed for 10 seconds. The made-down solution was then allowed to mature for 60 minutes prior to use in experiments. Polymer stock solutions were prepared daily.

3.2.2 Polymer dosing in samples

All relevant samples were dosed with polymer using the Phipps and Bird PB-700 Jar-tester (except the direct injection torque rheology method, see section 3.3.4.2). The sample to be conditioned was placed in a 500 mL beaker and placed in the Jar-tester with the paddle lowered. The polymer dose was then injected via pipette into the sludge sample, which was then mixed at 300 rpm for 30 seconds. This high mixing speed ensured polymer flocculation by being well mixed while the low mixing time reduced shear stress on the sludge, minimizing the effect of the thixotropic nature of the sludge.

3.2.3 Sodium nitrate dosing in deionized water

A stock solution of sodium nitrate ($NaNO_3$) was prepared by dissolving 1,000 mg $NaNO_3$ into 1,000 mL of deionized (DI) water. The dosed solution was mixed at 200 rpm for 3 minutes using a Phipps and Bird PB-700 Jar-tester. This mixing rate and time were found

to be sufficient to fully dissolve the anhydrous sodium nitrate powder in the deionized water.

A concentration series was prepared using this stock in order to produce a calibration curve for nitrate measured using ultraviolet/visible (UV-Vis) spectrophotometry. The concentration series was prepared in 250 mL samples of DI water. Sodium nitrate was dosed from the stock solution into the 250 mL DI water samples via pipette to the desired concentrations. The dosed sample was then mixed at 200 rpm for 2 minutes using a Phipps and Bird PB-700 Jar-tester. Each sample was then individually passed through an in-line UV-Vis spectrophotometer and their spectra were measured.

3.2.4 Magnesium sulfate and struvite formation in sludge filtrate and centrate

Struvite formation in the sludge filtrate and centrate samples was facilitated by the addition of magnesium. Magnesium sulfate ($MgSO_4$) was dosed incrementally into common samples of the sludge filtrate and centrate, with initial volumes of 1,000 mL. Following each addition of $MgSO_4$, the samples were mixed at 300 rpm for 3 minutes using a Phipps and Bird PB-700 Jar-tester. This constant mixing rate and time also ensured that the mixing turbulence applied to the dosed samples was kept constant so as to minimize the effect from that parameter in struvite formation. Between each addition of $MgSO_4$, the samples were mixed continuously at 100 rpm using the jar tester to ensure that the sample remained homogenous.

50 mL samples were taken after each dosing and mixing period for analysis. Prior to analysis, these samples were aerated using an air diffuser for 1 minute in order to oxidize

any remaining ammonium in solution. This had been tested and confirmed to be sufficient for reliable and consistent measurements.

3.3 Instruments and methodologies

3.3.1 Ultraviolet/visible spectrophotometry

Two UV-Vis spectrophotometers were employed. These were a desktop laboratory UV-Vis spectrophotometer (Cary 100 UV-Vis Spectrophotometer, Agilent Technologies, USA) and an in-line UV-Vis spectrophotometer (Real Spectrum PL Series, Real Tech Inc., Ontario, Canada). As the focus of this thesis was on real-time measurement methods, the in-line UV-Vis spectrophotometer was employed for most experiments. The Real Spectrum PL Series spectrophotometer measures absorbance at discreet wavelengths, meaning that absorbance measurements will be presented at the wavelengths measured by the instrument. For example, polyacrylamide polymers have a reported peak absorbance at a wavelength of approximately 190 nm (Al Momani and Örmeci, 2014a, 2014b), but results obtained using the Real Spectrum PL Series will present the peak absorbance at wavelength of 189.8 nm. The in-line UV-Vis spectrophotometer is shown in Figure 3.3 below. The desktop laboratory UV-Vis spectrophotometer used is shown in Figure 3.4 below.

Figure 3.3: Real Spectrum PL Series in-line UV-Vis spectrophotometer (Real Tech Inc.).

Figure 3.4: Cary 100 desktop laboratory UV-Vis spectrophotometer (Agilent Technologies).

All spectra using each instrument were measured between the wavelengths of 190 nm to 750 nm. This was because the two compounds of interest for this thesis, polyacrylamide polymers and nitrate, have their peak absorbances at wavelengths of 190 nm to 200 nm (Al Momani and Örmeci, 2014b) and 224 nm (Ferree and Shannon, 2001), respectively.

The Real Spectrum PL Series in-line UV-Vis spectrophotometer has four interchangeable quartz flow cells of different path lengths. These flow cells have path lengths of 1 mm, 2 mm, 4 mm, and 8 mm. The Cary 100 desktop laboratory UV-Vis spectrophotometer has the ability to change the path length of the cuvette employed, though only the 10 mm path length quartz cuvette was used.

3.3.2 Capillary suction time test

The capillary suction time (CST) test was used to measure the dewaterability of the sludge sample after polymer conditioning. Three 7 mL samples of the conditioned sludge sample were pipetted individually into the funnel of the CST tester placed above the Whatman No. 17 (Whatman, UK) filter paper. The CST tester (Triton Electronics Type 319 Multi-CST, England) measured the time required for filtrate to pass via capillary suction between two rings of sensors at a known separation. A shorter CST time corresponded to better dewaterability of the sludge, with the optimum polymer dose observed at the minimum CST time. The CST tester apparatus is shown in Figure 3.5.

Figure 3.5: Capillary suction time (CST) test apparatus (Triton Electronics).

3.3.3 Filtration test

The filtration test used was performed via the standard methods (APHA *et al.*, 2005). This test used a Whatman No. 2 filter (Whatman, UK) with a pore size of 8 μm in a Buchner funnel placed above a 250 mL graduated cylinder with vacuum port. Two 100 mL samples of conditioned sludge were individually poured into the Buchner funnel above individual filters to obtain duplicates. A constant vacuum pressure of 20 in. Hg was applied for a time of 10 minutes using a vacuum pump (Welch, USA), after which the volume of filtrate was measured. A larger filtrate volume corresponded to better filterability and thereby dewaterability, with the optimum polymer dose observed at the maximum filtrate volume. The filtration test apparatus is shown in Figure 3.6.

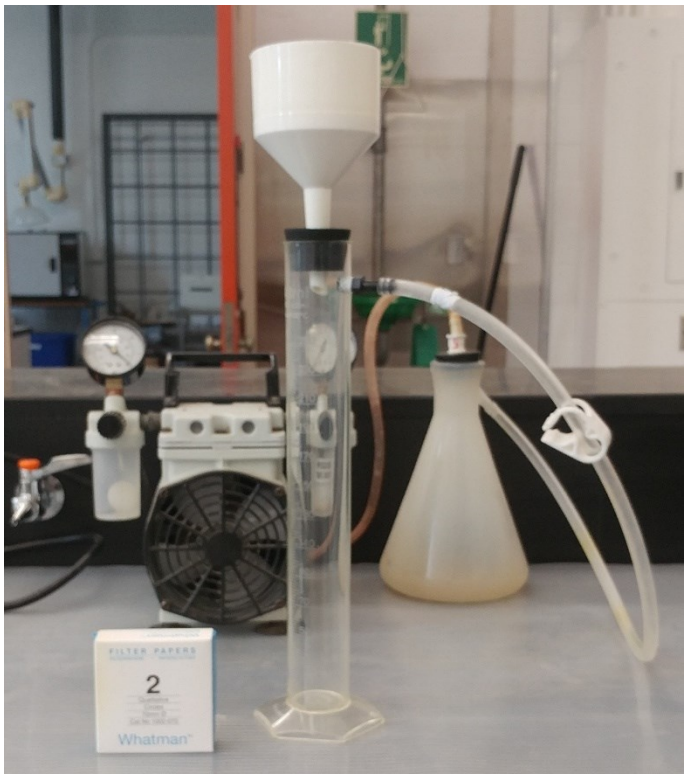

Figure 3.6: Filtration test apparatus.

3.3.4 Torque rheology

Torque rheology is a method for determining an optimum polymer dosage pre-dewatering. Using this method, torque rheograms are generated for sludge samples conditioned with increasing polymer dosages. A comparison of the torque rheograms generated was then used to determine the optimum polymer dosage. Two torque rheological methods were tested as the pre-dewatering in-line optimization methods using a Floccky Tester (Koei Industry Co., Ltd., Japan). The Floccky Tester measures the resistance to shear of a sample fluid over time by rotating its impeller at a constant velocity and measuring the torque required. These methods are known the totalized torque (TTQ) method and the direct injection method (Örmeci, 2007). A lab-scale torque rheometer was used in place of an in-

line full-scale torque rheometer, but the principles and methods are identical. The rheometer used is shown in Figure 3.7.

Figure 3.7: Floccky tester (Koei Industry Co., Ltd.).

3.3.4.1 Totalized torque method

The TTQ method utilized conditioned sludge and measured the area under the torque-time rheograms in order to determine the optimal polymer dosage. Two 200 mL samples of sludge were conditioned with polymer (as described in section 3.2.1.2) and individually placed in the vessel of the torque rheometer in order to obtain duplicates. The rheometer impeller was then rotated at a constant speed of 300 rpm for 120 seconds. This produced a torque-time rheogram from which the area under the curve (the TTQ) was determined. A larger area corresponded to better dewaterability, but an erratic rheogram with a high quantity of noise after the initial peak corresponded to an overdose.

3.3.4.2 Direct injection method

The direct injection method utilized unconditioned sludge and injected polymer directly into the sludge sample during mixing. The height of the peaks observed on the rheogram after polymer injection were measured. Two 200 mL samples of unconditioned sludge were individually placed in the vessel of the torque rheometer in order to obtain duplicates. The rheometer impeller was then rotated in three stages. The first stage was at a constant speed of 420 rpm for 10 seconds, and the second stage was at a constant speed of 300 rpm for 40 seconds. At the end of the second stage, the polymer was injected via pipette through a side port in the vessel, after which the third stage of mixing was performed at a speed of 300 rpm for 120 seconds. A peak was observed immediately after polymer injection and its peak high was determined. A higher peak corresponded to higher dewaterability, but an erratic rheogram with a high quantity of noise and additional peaks after the initial peak corresponded to an overdose.

3.3.5 Turbidity

Turbidity measurements were performed for sludge centrate and filtrate samples using a HACH 2100AN Turbidimeter (Hach, Colorado, USA), shown in Figure 3.8. Individual 30 mL samples were individually placed in sample vials which were placed in in the turbidimeter. The turbidity of each sample was then measured in triplicates using a common vial and different grab samples.

Figure 3.8: HACH 2100AN Turbidimeter.

3.3.6 Particle analysis

For struvite formation experiments, a particle analysis of sludge centrate and filtrate samples was conducted. This was performed using a particle counter (Dynamic Particle Analyzer DPA 4100, Brightwell Technologies Inc., Ontario, Canada), shown in Figure 3.9. This particle counter functions by drawing a sample out of a reservoir placed above an optical detector. The sample fluid is passed through a flow cell where it is optically analyzed by the instrument.

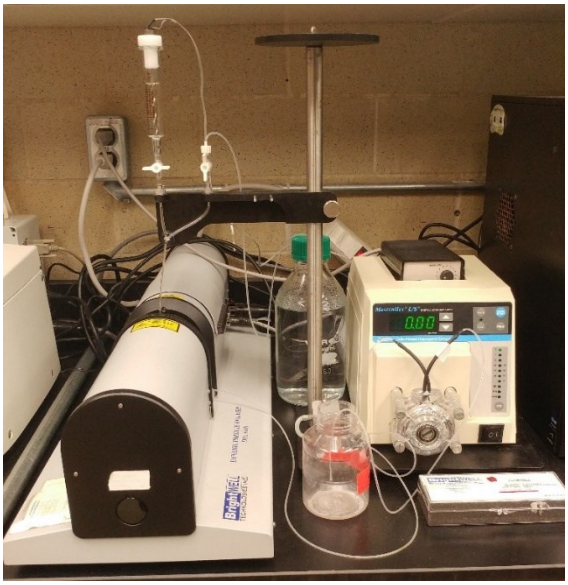

Figure 3.9: Dynamic Particle Analyzer DPA 4100 (Brightwell Technologies Inc.).

A 10 mL sample reservoir was filled with the sample to be analyzed and a stir screw was placed in the reservoir to ensure that the sample remained homogenous during testing. The sample was then pumped at a rate of 0.22 mL/min for 2 minutes through a 400 µm flow cell. The instrument then measured the particle size distribution and the concentration of particles greater than the detection limit of the instrument. The detection limit was a particle diameter of 2.00 µm, and the bin size for the particle size distribution was 0.25 µm. This means that the smallest bin size for the particle size distribution contained particles between the sizes of 2.00 µm to 2.25 µm.

3.3.7 Microscopy

Visual confirmation of struvite formation for all relevant samples was achieved through the use of microscopy. A Nikon Eclipse Ti (Nikon, Montreal) inverted microscope was employed for this purpose, shown in Figure 3.10. For each analysis, a 10 µL sample was

placed on a 25 x 75 x 1 mm microscope slide, and a 22 x 22 mm No. 1.5 glass cover was placed on top. The prepared slide was placed on the microscope stage. Each sample was focused at the magnification in use, and multiple fields of view were analyzed to get a sense of the visual makeup of the sample. Once this was achieved, photos of the sample were taken as a record.

Figure 3.10: Nikon Eclipse Ti inverted microscope.

Chapter 4 – Investigation into the impact of path length and solids concentration on the sensitivity of polymer measurement using UV-Vis spectrophotometry

Abstract

Most methods for the measurement of polymers in water and wastewater are often highly complex or have low reproducibility in complex media such as dewatered sludge water. Using UV-Vis spectrophotometry for the detection of polymers has relatively low complexity and high reliability. The sensitivity of the method is dependent upon a number of factors including the polymer employed, the path length, and impurities in the sample, such as the solid particles. This study investigated the impact of path length and solids concentration on the detection of polymer in anaerobically digested sludge centrate using UV-Vis spectrophotometry. Absorbance spectra of deionized water and sludge centrate were measured in the wavelength range of 189.8 nm to 747.5 nm using an in-line UV-Vis spectrophotometer, and 190 nm to 800 nm using a desktop UV-Vis spectrophotometer. Maximum absorbance values were measured at 189.8 nm and 190 nm for the in-line and desktop spectrophotometers, respectively, for each sample. Path lengths of 1 mm, 2 mm, 4 mm, and 8 mm were analyzed using the in-line spectrophotometer, and a path length of 10 mm was analyzed using the desktop spectrophotometer. The 4 mm path length was found to be the most sensitive to polymer detection as smaller path lengths resulted in high flow turbulence through the flow cells, while interference from impurities in the centrate lowered the sensitivity of the larger path lengths. The use of this smaller path length reduced the need for dilution of the centrate prior to measurement. Increased filtration and

dilution were found to decrease the sensitivity of the method to the detection of residual polymer. It was therefore determined that increased solids concentration in centrate was not a significant factor in polymer detection using UV-Vis spectrophotometry.

Keywords: Ultraviolet/visible spectrophotometry, polymer, sludge, measurement, detection, monitoring.

4.1 Introduction

Digested sludge is often conditioned prior to dewatering processes in order to improve its dewaterability. In chemical conditioning, the addition of a chemical conditioner causes the sludge to flocculate, coagulating the solids and allowing solid-liquid separation. Polyacrylamide polymers are the most common type of chemical conditioners employed for sludge conditioning (Mortimer, 1991). This is because polymers do not increase the total dry solids (DS) of the sludge, whereas the use of inorganic conditioners can result in large increases in the total DS of the sludge. Another advantage of polymers is that the required dose of polymer conditioners is often quite lower than the required dose of inorganic conditioners for a given sludge. However, one drawback to the use of polymers as conditioners is their high cost relative to inorganic conditioners. Through measuring the concentration of residual polymer in the liquid product of the dewatered sludge, real-time monitoring of the dewaterability of the sludge can be achieved.

There exist multiple methods for polymer measurement and quantification. These include gas chromatography, high-performance chromatography, mass spectrometry (Gibbons and Örmeci, 2013), the starch-triiodide method (Scoggings and Miller, 1979), viscosity (Jungreis, 1981), calorimetry (Hansen and Eatough, 1987), turbidimetry (Taylor and Nasr-El-Din, 1994), fluorescence spectrometry (Arryanto and Bark, 1992), colloid titration (Gehr and Kalluri, 1983), radioactive labeling (Nadler *et al.*, 1994), flow injection analysis (Taylor *et al.*, 1998), size exclusion chromatography (SEC) (Keenan *et al*., 1998), nuclear magnetic resonance (NMR) spectroscopy (Chang *et al.*, 2002), florescence tagging (Becker *et al*., 2004), and spectrophotometric determination using cationic dyes (Chmilenko *et al.*, 2004).

These methods have been found to have reduced sensitivity and reproducibility in complex media due to interference from the presence of other compounds (Dentel *et al.*, 2000b; Lu and Wu, 2003). Keenan *et al.* (1998) reported a detection limit of 20 μg/L in nanopure water and 66 μg/L in alum sludge supernatant using SEC. Becker *et al*. (2004) reported a detection limit of 10 μg/L in purified water and 100 μg/L in water samples collected from a drinking water reservoir using fluorescence tagging. In addition, the various methods do not necessarily yield the same concentrations for common samples. Gehr and Kalluri (1983) measured polymer concentrations of 0.6 mg/L and 0.1 mg/L using colloid titration and test suspension methods, respectively, for the same sludge filtrate sample. Chang *et al.* (2002) measured polymer concentrations of 8 mg/L, 1.18 mg/L, and 0.11 mg/L using NMR, viscosity, and colloid titration methods, respectively, for the same sludge filtrate sample.

Ultraviolet/visible (UV-Vis) spectrophotometry has been used to measure residual polymer concentration in dewatered sludge water, and polyacrylamide polymers have been reported to have a peak absorbance at a wavelength of 190 nm (Gibbons and Örmeci, 2013; Aghamir-Baha and Örmeci, 2014; Al Momani and Örmeci, 2014a). The method detection limit for the spectrophotometric method is dependent upon the polymer employed and the wavelength measured (Gibbons and Örmeci, 2013). Gibbons and Örmeci (2013) reported a detection limit of 0.55 mg/L for polymer in deionized (DI) water at a wavelength of 200 nm. Al Momani and Örmeci (2014a, 2014b) reported detection limits ranging from 0.05 mg/L to 0.13 mg/L for different polymers in distilled water at a wavelength of 191.5 nm. They also reported detection limits ranging from 0.25 mg/L to 1.35 mg/L for different polymers in sludge centrate samples at a wavelength of 191.5 nm (Al Momani and Örmeci,

2014a, 2014b). UV-Vis spectrophotometry is a relatively simple method for polymer measurement compared to more complex and sophisticated methods such as NMR and SEC, but it is much more sensitive and reliable than simpler methods such as colorimetric and turbidimetric methods (Gibbons and Örmeci, 2013). One drawback however is that more complex samples, such as sludge centrate, often require large dilutions (Al Momani and Örmeci, 2014a, 2014b).

As noted by Gibbons and Örmeci (2013) and confirmed by Al Momani and Örmeci (2014a, 2014b), the sensitivity of the UV-Vis spectrophotometric method is dependent upon the polymer employed. As this is a variable independent of the method, it is desirable to improve the sensitivity through other parameters. One such parameter is the path length of the spectrophotometer sample cell. The path length is defined as the distance which light travels through the sample and is absorbed. According to the Beer-Lambert Law, the path length is related proportionally to the absorbance value. As such, the magnitude of the absorbance value increases with increased path length as the radiation must travel further through the sample. Accordingly, when using larger path lengths, samples may require dilution in order to reduce their absorbance magnitude into the measurement range of the instrument. A smaller path length reduces the need for sample dilution, which is desired in full-scale and in-line applications where dilution increases the complexity of the system.

When using larger path lengths, more polymer is present to absorb the light, improving detection capabilities of the method. However, other parameters such as the presence of impurities may interfere with reliable polymer detection in larger path lengths. These impurities include anything which absorb or scatter light, such as other cationic or anionic species, dissolved organic substances, and solid particles. Improved sensitivity of the UV-

Vis spectrophotometric method would be beneficial for all applications, improving optimum polymer dose accuracy in sludge dewatering applications and detection capabilities in applications with relatively low polymer doses and concentrations, such as drinking water treatment and certain research applications.

The goal of this study was to investigate the impact of path length and total solids (TS) concentration on residual polymer detection using UV-Vis spectrophotometry. This was done both in order to improve the sensitivity of the method and to reduce the need for dilution of the samples. The effect of path length was analyzed using two spectrophotometers, one in-line unit and one desktop unit, with path lengths of 1 mm, 2 mm, 4 mm, and 8 mm in the in-line spectrophotometer, and of 10 mm in the desktop spectrophotometer. The effect of particle size and TS concentration on residual polymer detection was assessed through varied filtration and dilution of samples.

4.2 Materials and Methods

The experiments in this study were conducted to develop an improved method with higher sensitivity for polymer detection using in-line UV-Vis spectrophotometry. For this, polymer was initially dosed directly into deionized water (Direct-Q UV Water Purification System, Millipore Sigma, USA) and later into sludge centrate samples with selected concentrations and analyzed using UV-Vis spectrophotometry.

4.2.1 Ultraviolet/visible spectrophotometers

The deionized water sample tests were conducted to establish calibration curves for the in-line UV-Vis spectrophotometer instrument (Real Spectrum PL Series, Real Tech Inc.,

Ontario, Canada). The absorbance spectra for the centrate samples were measured using both the Real Spectrum in-line UV-Vis spectrophotometer and a desktop laboratory UV-Vis spectrophotometer (Cary 100 UV-Vis Spectrophotometer, Agilent Technologies, USA) for comparison. The Real Spectrum in-line UV-Vis spectrophotometer employs a quartz flow cell through which a sample is pumped at a constant rate. The flow cell can be interchanged for variable path lengths of 1 mm, 2 mm, 4 mm, and 8 mm. Each flow cell itself has a constant width, and the smaller path lengths are therefore achieved through smaller slit sizes in flow cells.

The Real Spectrum in-line spectrophotometer measures the absorbance of the sample between the wavelengths of 189.8 nm and 747.5 nm at intervals of approximately 1 nm using deuterium and tungsten lamps. Each flow cell path length can measure absorbances between zero and a different maximum value. For the 1 mm, 2 mm, 4 mm, and 8 mm path lengths, the maximum absorbance values are 13 abs, 6.5 abs, 3.25 abs, and 1.6 abs, respectively. All samples were analyzed in the in-line UV-Vis Spectrophotometer at a sample flow rate of approximately 70 mL/min using a Real Pump Clean System I, Version 1.3 (Real Tech Inc., Ontario, Canada).

The Cary 100 desktop spectrophotometer employs a 10 mm quartz cuvette which is filled with a single grab sample and placed in the instrument for measurement. It measures the absorbance of the sample between the wavelengths of 190 nm and 800 nm at intervals of 1 nm using deuterium and tungsten lamps.

4.2.2 Sludge centrate samples

Anaerobically digested sludge samples were collected from the Robert O. Pickard Environmental Centre (ROPEC), located in Ottawa, Ontario. The unconditioned sludge samples were centrifuged using a Sorvall Legend RT+ centrifuge (Thermo Fisher Scientific, Massachusetts, USA) at 10,000 G for ten minutes. This was performed in the 250 mL centrifuge sample bottles, and the total volume centrifuged at a time was either 500 mL, 1,000 mL, or 1,500 mL. Post-centrifugation, the centrate from each sample bottle was carefully removed from each bottle and placed into a common beaker for filtration as needed.

4.2.3 Polymer

The polyacrylamide polymer Zetag 8160 (manufactured by BASF Corporation) was used and is characterized as having a medium-high cationic charge density and a high molecular weight. It comes in the form of a granular solid.

Polymer stock solutions were made-down to a concentration of 1.0% by preparing 10.0 g of the polymer and mixing it into 1,000 mL of deionized water. The mixing process was 5 minutes at 250 rpm followed by 55 minutes at 125 rpm. This mixing was completed using the Phipps and Bird PB-700 Jar-tester (Richmond, VA). After initial mixing, a hand blender was used to break up flocs which had formed. The hand blender was employed for 10 seconds. The made-down solution was then allowed to mature for 60 minutes prior to use in experiments. Polymer stock solutions were prepared daily.

4.2.4 Variation of flow cell and cuvette path length

The first phase of experiments involved the variation of the in-line spectrophotometer flow cell path length. The spectra of the deionized water samples were measured using the 1 mm, 2 mm, 4 mm, and 8 mm in-line flow cell path lengths. The spectra of the sludge centrate samples were measured using the 4 mm and 8 mm in-line flow cell path lengths. All centrate samples were also analyzed using the 10 mm path length quartz cuvette of the desktop laboratory spectrophotometer for comparison. For these tests, all sludge centrate samples were filtered through a Whatman No. 2 filter with a pore size of 8 μm (Whatman, UK) using a vacuum pump (Welch, USA) and diluted by a factor of 1:50 using deionized water prior to polymer dosing. This was done in order to bring the absorbance of the samples within the optimal ranges of the spectrophotometers used. Each sample for these experiments had its spectrum analyzed in triplicates. The average values are reported, and all error bars show the standard deviation of the triplicates.

4.2.5 Variation of sludge centrate TS content

The second phase of experiments involved the variation of the TS content of the sludge centrate to investigate the effect of TS on method sensitivity. Individual sludge centrate samples were analyzed in three forms: unfiltered, filtered through a Whatman No. 2 filter with a pore size of 8 μm, and filtered through a MF-Millipore Membrane 0.45 μm pore size filter (Millipore Sigma, USA). Each sludge centrate sample was diluted individually by a factor of 1:25 and a factor of 1:50 using deionized water, for a total of six samples. Higher levels of filtration reduced the mean particle size as well as the particle concentration, while higher dilution factors reduced only the particle concentration. All sludge centrate samples

were analyzed in triplicates using the 4 mm flow cell path length of the in-line spectrophotometer. The average values are reported, and all error bars show the standard deviation of the triplicates.

4.2.6 Polymer dosing of samples

All samples were dosed to selected concentrations of polymer via pipette. This was performed directly into 400 mL samples of deionized water and directly into 400 mL samples of sludge centrate post-filtration and post-dilution, as needed. Post-dosing, all samples were mixed at 250 rpm for 30 seconds using a Phipps and Bird PB-700 Jar-tester (Richmond, VA). This ensured homogeneity and complete conditioning of the samples.

4.2.7 Ultraviolet/visible spectroscopy polymer detection method

Polyacrylamide polymers have their peak absorbance at a wavelength of 190 nm to 200 nm (Al Momani and Örmeci, 2014b), so the spectra of the samples were measured from 190 nm to 350 nm. The low end of this range (190 nm) is limited by the capability of the instrument, but this does not impact polymer detection sensitivity. A higher polymer concentration in the media was correlated to a higher absorbance at 190 nm.

4.3 Results and Discussion

4.3.1 The effect of flow cell path length on the detection of polymer in deionized water

The absorbance spectra of deionized water conditioned with Zetag 8160 polymer were analyzed to examine the effect of flow cell path length on polymer detection using the in-

line UV-Vis spectrophotometer. The flow cell path lengths analyzed were 1 mm, 2 mm, 4 mm, and 8 mm. Polymer was dosed to concentrations of 1.0, 2.0, 3.0, 4.0, 5.0, 10.0, 15.0, and 20.0 mg/L by pipette. As polyacrylamide polymers do not greatly absorb light above 240 nm, the spectra were taken in the range of 190 nm to 350 nm (Al Momani and Örmeci, 2014a). The spectra obtained using the 1 mm path length flow cell is shown in Figure 4.1a below. Likewise, the spectra obtained using the 2 mm, 4 mm, and 8 mm path length flow cells are shown in Figures 4.1b, 4.1c, and 4.1d, respectively. The same samples were tested for each subsequent flow cell for consistency.

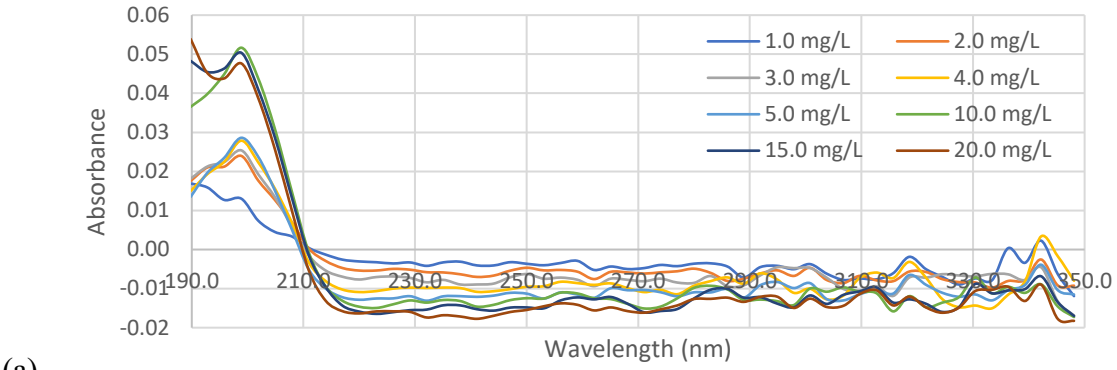

(a)

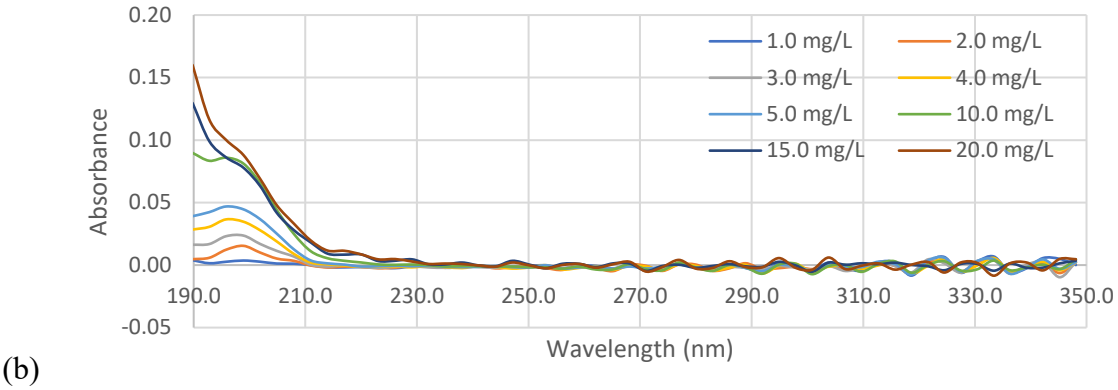

(b)

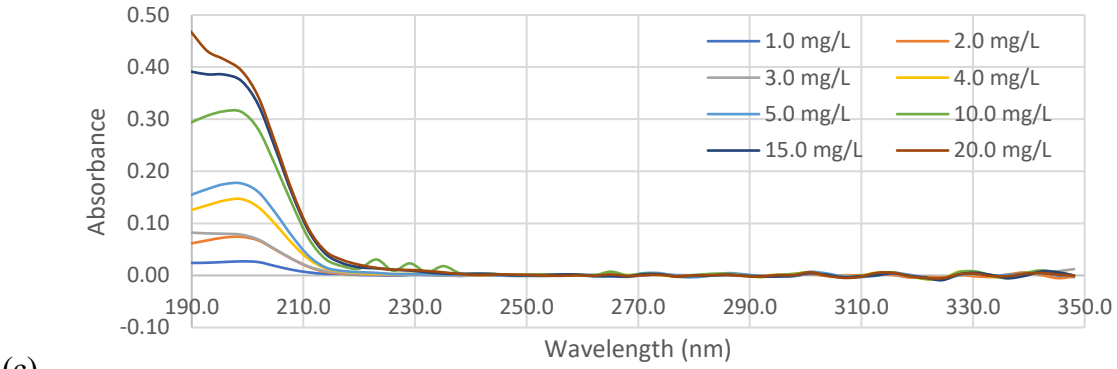

(c)

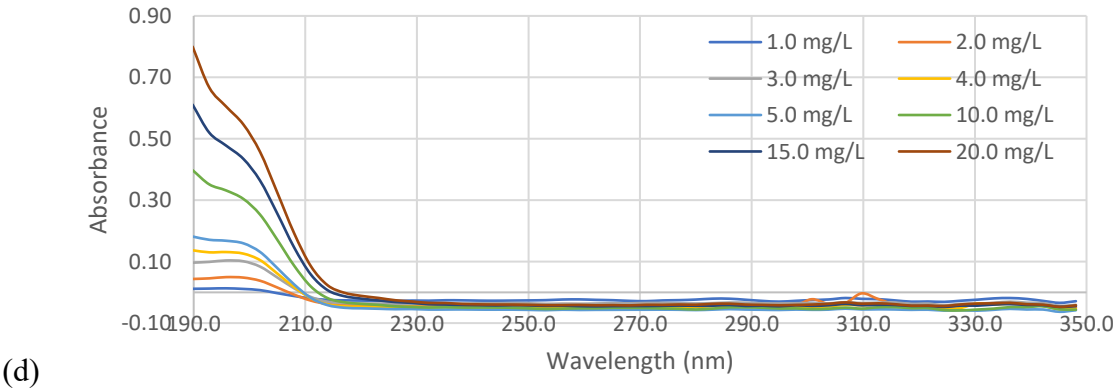

(d)

Figure 4.1: Absorbance spectra of Zetag 8160 polymer in deionized water using an in-line spectrophotometer with a flow cell path length of a) 1 mm; b) 2 mm; c) 4 mm; d) 8 mm.

As shown in Figure 4.1, as the concentration of Zetag 8160 polymer increased, a corresponding increase in the absorbance of the deionized water samples was observed. The peak absorbance value was observed at a wavelength of 190 nm for all samples, with the exception of a few of the 1 mm path length samples. No significant absorbance was measured above a wavelength of 240 nm for any of the samples. This was expected and was in accordance with Al Momani and Örmeci (2014a), who measured a peak absorbance of polyacrylamide polymers at a wavelength of 191.5 nm.

Through preliminary visual analysis of the spectra shown above in Figure 4.1, it was evident that the tests conducted using the 1 mm path length flow cell yielded highly erratic absorbance spectra. This high variability in the measurements appeared to decrease as the path length of the flow cell was increased, as evident when comparing the visual appearances of each spectra in Figure 4.1. The shorter path length flow cells were possibly insufficiently sensitive for reliable measurements of polymer concentration due to their smaller openings. These smaller openings possibly caused turbulent currents and air bubbles in the flow cells, resulting in the erratic absorbance spectra measured.

The relationship between Zetag 8160 polymer concentration and the magnitude of the absorbance of each sample at wavelengths of 189.8 nm, 201.9 nm, and 211.0 nm is shown below in Figure 4.2. These relationships are shown by Figures 4.2a, 4.2b, 4.2c, and 4.2d for the 1 mm, 2 mm, 4 mm, and 8 mm path length flow cells, respectively. Error bars are present on all data points, even if they are not visible. A summary of a linear regression analysis for the data shown in Figure 4.2 follows in Table 4.1.

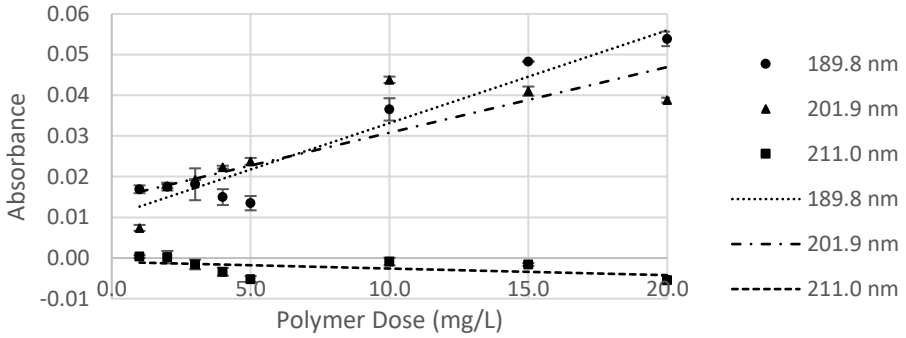

(a)

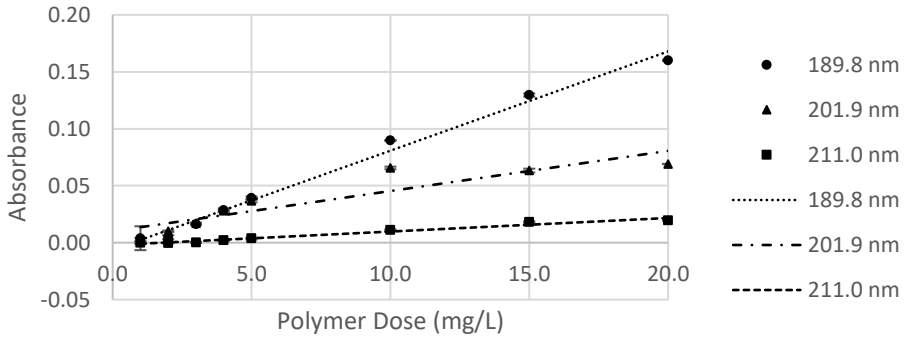

(b)

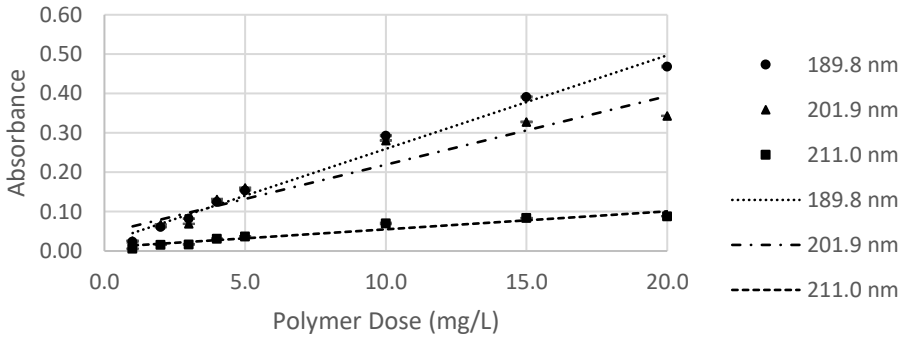

(c)

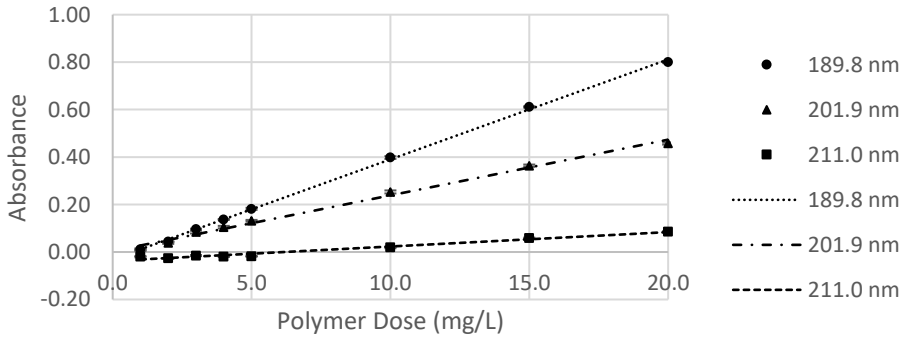

(d)

Figure 4.2: Relationship between Zetag 8160 polymer concentration in deionized water and absorbance at 189.8 nm, 201.9 nm, and 211.0 nm using flow cell path lengths of a) 1 mm; b) 2 mm; c) 4 mm; d) 8 mm.

Table 4.1: Summary of linear regression analysis of relationship between Zetag 8160 polymer concentration in deionized water and absorbance at 189.8 nm, 201.9, and 211.0 nm using flow cell path lengths of 1 mm, 2 mm, 4 mm, and 8 mm.

	1 mm path length			**2 mm path length**		
	189.8 nm	201.9 nm	211.0 nm	189.8 nm	201.9 nm	211.0 nm
Coefficient of Determination (R^2)	0.922	0.728	0.244	0.991	0.833	0.970
Residual Sum of Squares (RSS)	$1.44*10^{-4}$	$3.21*10^{-4}$	$2.71*10^{-5}$	$2.29*10^{-4}$	$8.22*10^{-4}$	$1.43*10^{-5}$
Total Sum of Squares (TSS)	$1.86*10^{-3}$	$1.18*10^{-3}$	$3.58*10^{-5}$	$2.53*10^{-2}$	$4.93*10^{-3}$	$4.82*10^{-4}$
F statistic	71.42	16.04	1.93	657.8	29.93	196.7
F statistic P-value	$1.50*10^{-4}$	$7.08*10^{-3}$	$2.14*10^{-1}$	$2.32*10^{-7}$	$1.56*10^{-3}$	$8.19*10^{-6}$
Intercept	0.0104	0.0147	-0.0010	-0.0064	0.0101	-0.0022
Slope	0.0023	0.0016	-0.0002	0.0087	0.0035	0.0012
	4 mm path length			**8 mm path length**		
	189.8 nm	201.9 nm	211.0 nm	189.8 nm	201.9 nm	211.0 nm
Coefficient of Determination (R^2)	0.984	0.908	0.925	0.999	0.993	0.972
Residual Sum of Squares (RSS)	$3.03*10^{-3}$	$1.01*10^{-2}$	$5.61*10^{-4}$	$3.96*10^{-4}$	$1.35*10^{-3}$	$3.47*10^{-4}$
Total Sum of Squares (TSS)	$1.89*10^{-1}$	$1.10*10^{-1}$	$7.44*10^{-3}$	$5.85*10^{-1}$	$1.83*10^{-1}$	$1.25*10^{-2}$
F statistic	368.5	59.20	73.57	8,875	808.4	211.0
F statistic P-value	$1.29*10^{-6}$	$2.52*10^{-4}$	$1.38*10^{-4}$	$9.64*10^{-11}$	$1.25*10^{-7}$	$6.68*10^{-6}$
Intercept	0.0218	0.0452	0.0094	-0.0308	0.0039	-0.0376
Slope	0.0238	0.0174	0.00457	0.0421	0.0235	0.0061

Analysis of Figure 4.2 and Table 4.1 shows that the magnitude of the absorbances at each of the three wavelengths increased as a factor of the increased path lengths, as expected. Using linear regression, the slope of the regression lines was seen to have increased with increasing path length at a rate lessening with each increase in path length. A higher slope was indicative of a greater sensitivity to changes in polymer concentration, as would be expected with higher path lengths.

The best correlation between Zetag 8160 polymer concentration and absorbance occurs at a wavelength of 189.8 nm for all flow cell path lengths. This was expected as this is the

peak absorbance for polyacrylamide polymers (Al Momani and Örmeci, 2014a). Furthermore, this correlation is strongest for the 8 mm path length ($R^2 = 0.999$) and weakest for the 1 mm path length ($R^2 = 0.922$), consistent with the visual analysis discussed above. The magnitude of the residual sum of squares (RSS) compared to that of the total sum of squares (TSS) was also the lowest for the 8 mm path length, and highest for the 1 mm path length, further indicating that the data for 8 mm path length had the strongest relationship. The P-value for all linear regressions showed that each regressed model was statistically significant (P-value < 0.05), with the strongest significance being seen with the 8 mm path length.

Considering the lower correlation and significance seen in the 1 mm path length data and the high variability seen in the 1 mm and 2 mm path length spectra in Figure 4.1, subsequent experiments focussed on the 4 mm and 8 mm path length flow cells when using the in-line UV-Vis spectrophotometer.

4.3.2 The effect of flow cell path length on the detection of polymer in sludge centrate

The absorbance spectra of sludge centrate conditioned with Zetag 8160 polymer were analyzed to examine the effect of flow cell path length on polymer detection in sludge centrate samples. This test was completed using the in-line UV-Vis spectrophotometer and the desktop spectrophotometer to compare the performance of the two instruments, the sensitivities of the 4 mm and 8 mm path lengths to the standard 10 mm path length, and the sensitivity of the continuous measurement of the in-line spectrophotometer. The flow cell path lengths analyzed using the in-line spectrophotometer were 4 mm and 8 mm. These

were compared to the desktop spectrophotometer using a quartz cuvette with a path length of 10 mm. All sludge centrate samples were filtered through an 8 μm pore size filter and diluted by a factor of 1:50 prior to polymer conditioning. Polymer was dosed to concentrations of 1.0, 2.0, 3.0, 4.0, 5.0, 10.0, 15.0, and 20.0 mg/L by pipette. The spectra obtained using the 4 mm path length flow cell, 8 mm path length flow cell, and the 10 mm path length cuvette are shown in Figure 4.3a, 4.3b, and 4.3c, respectively. The same samples were tested for each subsequent flow cell and the cuvette for consistency.

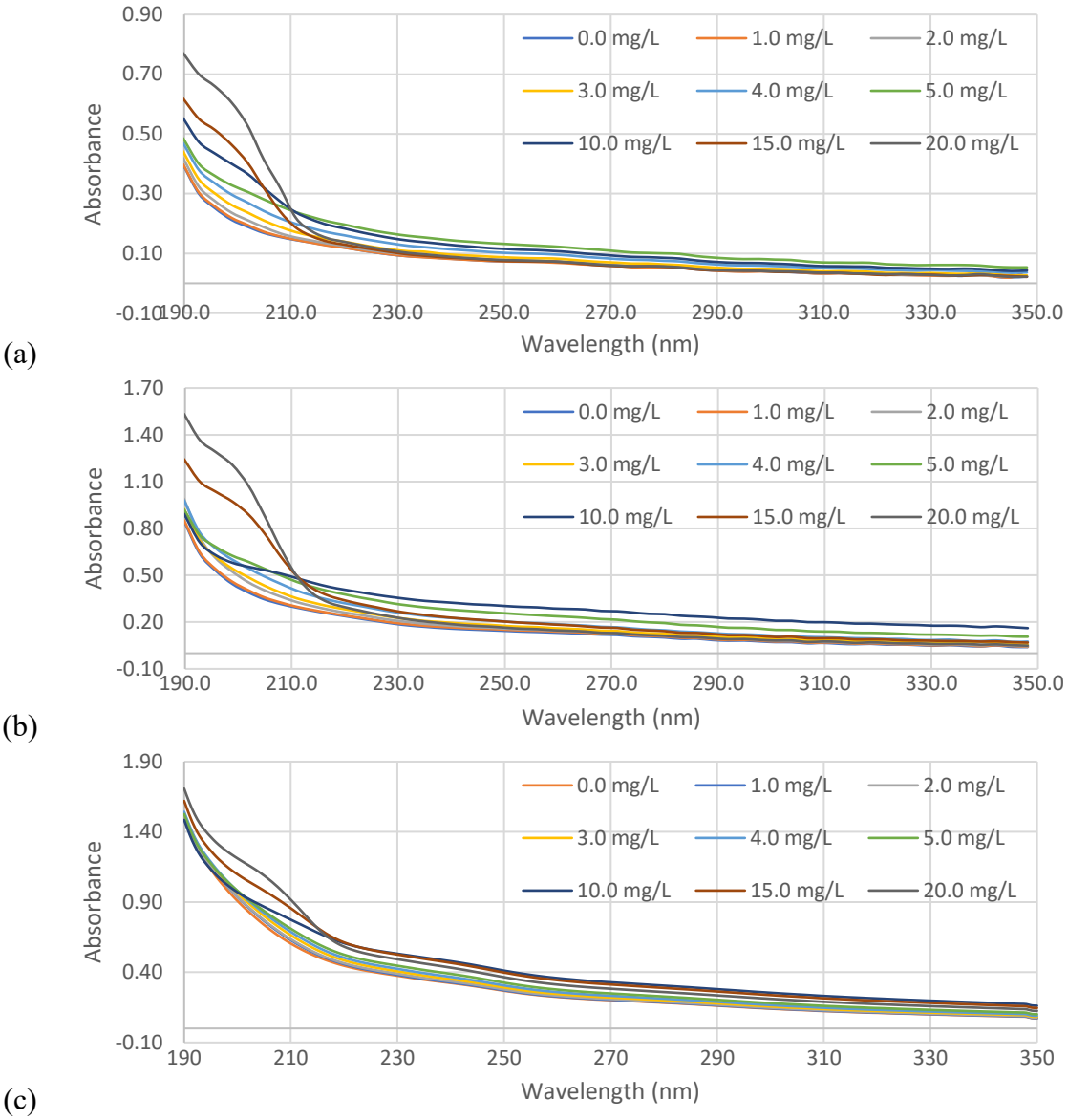

Figure 4.3: Absorbance spectra of Zetag 8160 polymer in filtered sludge centrate diluted by a factor of 1:50 using a) an in-line spectrophotometer with a flow cell path length of 4 mm; b) an in-line spectrophotometer with a flow cell path length of 8 mm; c) a desktop spectrophotometer with a cuvette path length of 10 mm.

As shown in Figure 4.3, as the concentration of Zetag 8160 polymer increases, a corresponding increase in the absorbance of the sludge centrate samples was observed. The peak absorbance value was observed at a wavelength of 190 nm for all samples, with no

significant absorbance being measured above a wavelength of 240 nm. This was consistent with the tests conducted in deionized water discussed in the above section.

The relationship between Zetag 8160 polymer concentration and the magnitude of the absorbance of each sample at wavelengths of 189.8 nm, 201.9 nm, and 211.0 nm is shown below in Figure 4.4. These relationships are shown by Figures 4.4a, 4.4b, and 4.4c for the 4 mm, 8 mm, and 10 mm path lengths, respectively. Error bars are present on all data points, even if they are not visible. A summary of a linear regression analysis for the data shown in Figure 4.4 follows in Table 4.2.

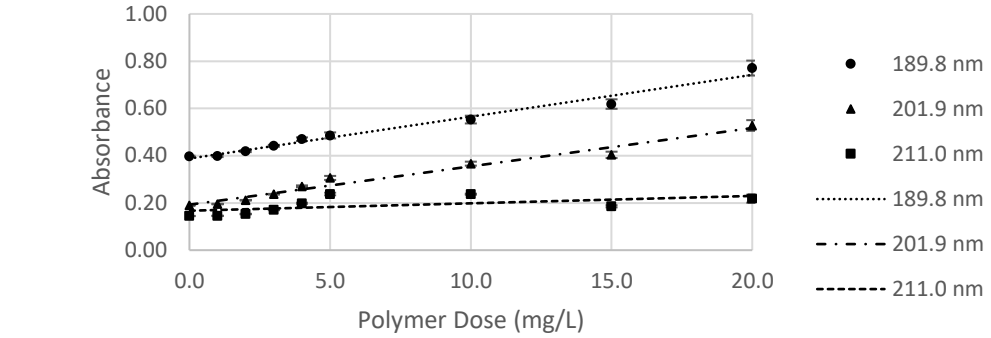

(a)

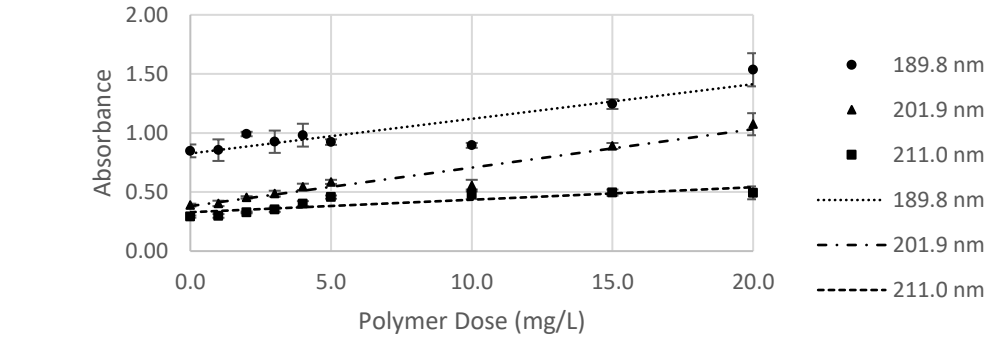

(b)

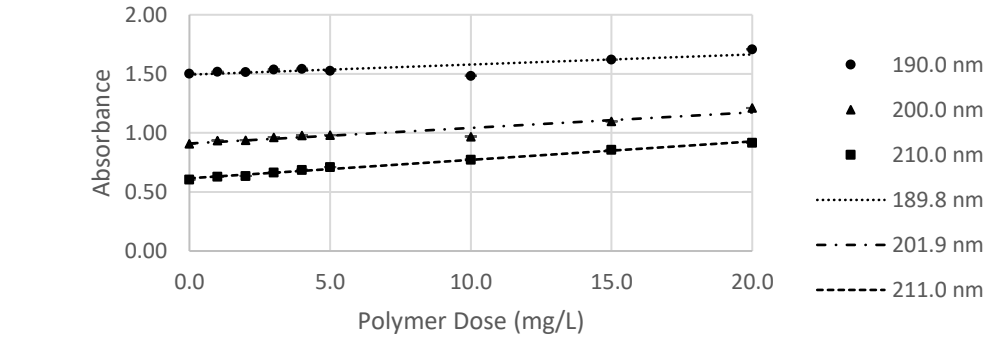

(c)

Figure 4.4: Relationship between Zetag 8160 polymer concentration in filtered sludge centrate and absorbance at 189.8 nm, 201.9 nm, and 211.0 nm using flow cell path lengths of a) 4 mm; b) 8 mm; and at 190 nm, 200 nm, and 210 nm using cuvette path length of c) 10 mm.

Table 4.2: Summary of linear regression analysis of relationship between Zetag 8160 polymer concentration in sludge centrate and absorbance at 189.8 nm, 201.9, and 211.0 nm using flow cell path lengths of 4 mm and 8 mm and at 190 nm, 200 nm, and 210 nm using cuvette path length of 10 mm.

	4 mm path length			**8 mm path length**		
	189.8 nm	201.9 nm	211.0 nm	189.8 nm	201.9 nm	211.0 nm
Coefficient of Determination (R^2)	0.979	0.972	0.336	0.800	0.934	0.743
Standard Error	0.019	0.020	0.032	0.108	0.064	0.046
Residual Sum of Squares (RSS)	$2.56*10^{-3}$	$2.90*10^{-3}$	$7.37*10^{-3}$	$8.16*10^{-2}$	$2.85*10^{-2}$	$1.47*10^{-2}$
Total Sum of Squares (TSS)	$1.22*10^{-1}$	$1.03*10^{-1}$	$1.11*10^{-2}$	$4.09*10^{-1}$	$4.31*10^{-1}$	$5.72*10^{-2}$
F statistic	326.3	241.4	3.536	28.04	99.04	20.28
P-value of F	$3.94*10^{-7}$	$1.11*10^{-6}$	$1.02*10^{-1}$	$1.13*10^{-3}$	$2.21*10^{-5}$	$2.79*10^{-3}$
Intercept	0.388	0.193	0.167	0.826	0.381	0.329
Slope	0.0177	0.0162	0.0031	0.0293	0.0326	0.0106

	10 mm path length		
	190.0 nm	200.0 nm	210.0 nm
Coefficient of Determination (R^2)	0.703	0.900	0.992
Standard Error	0.041	0.032	0.011
Residual Sum of Squares (RSS)	$1.18*10^{-2}$	$7.36*10^{-3}$	$7.82*10^{-4}$
Total Sum of Squares (TSS)	$3.96*10^{-2}$	$7.33*10^{-2}$	$9.31*10^{-2}$
F statistic	16.58	62.77	826.0
P-value of F	$4.74*10^{-3}$	$9.70*10^{-5}$	$1.59*10^{-8}$
Intercept	1.49	0.910	0.616
Slope	0.0086	0.0131	0.0156

Analysis of Figure 4.4 showed a deviation in the linearity of the relationship between absorbance and polymer concentration. This deviation was most visible at a polymer concentration of 10 mg/L, where the absorbance is lower than predicted by the regressed model, but closer inspection showed that the same is true for the 5.0 mg/L and 15.0 mg/L concentrations. Comparing the relationships from the 4 mm and 8 mm path lengths of the in-line spectrophotometer, the 8 mm flow cell appeared to be more sensitive to this deviation than the 4 mm flow cell.

This deviation was hypothesized to be attributable to the effect of particles in the sludge centrate. Particles present in the filtered sludge centrate would be flocculated and coagulated by the addition of the polymer, thus reducing the residual polymer in the sludge centrate solution. This would result in a reduction in the measured absorbance by the spectrophotometer. At higher polymer doses, there is excess polymer, and its residual concentration begins to rise. Furthermore, settling out of the flocculated particles is a possibility in the desktop spectrophotometer but not in the in-line unit due to continuous mixing. The deviation caused by this particle effect is visible both in Figure 4.4 and in the regression analyses summary in Table 4.2.

As a result of the hypothesized particle effect described above, the linearity of the relationship between absorbance and polymer concentration decreased as a result of increased path length. This was seen in each subsequent increase in path length, from 4 mm ($R^2 = 0.979$ at 189.8 nm) to 8 mm ($R^2 = 0.800$ at 189.8 nm) to 10 mm using the desktop spectrophotometer ($R^2 = 0.703$ at 190.0 nm). This was further indicated by the magnitude of the RSS compared to that of the TSS for each model, showing that the relative magnitudes were lowest for the 4 mm path length and increases for each subsequent path length increase. The P-value for all linear regressions showed that each regressed model was statistically significant, with the 4 mm path length showing the most significant correlation. It should be noted that since these data are obtained from two different spectrophotometers, the differences in the statistical data between the 4 mm and 8 mm flow cells and the 10 mm cuvette can partially be attributed to differences between the instruments.

The regressions for the trends at λ = 201.9 nm for the 8 mm and λ = 200.0 nm and λ = 210.0 nm for the 10 mm path lengths show an increase in correlation between the absorbance and polymer concentration through higher R^2 values. However, as evidenced by the low relative RSS to TSS magnitudes, the regressed models were weak fits of the data. This seemingly stronger correlation at higher wavelengths is explained by the particle effect discussed above. At the higher wavelengths where the polymer does not absorb light as effectively, the effect of polymer removal through adsorption on particles was less detectable, leading to more linear relationships. Using the 4 mm path length, the same trend was less pronounced, though it was still present.

Comparison of the results obtained at 190.0 nm using the desktop spectrophotometer to those obtained at 189.8 nm using the in-line spectrophotometer showed that the desktop spectrophotometer was less sensitive to polymer concentration measurement in sludge centrate. This was seen in the lower coefficient of determination, higher RSS compared to TSS magnitude, and higher P-value for the relationship between polymer concentration and absorbance, compared to those for the in-line spectrophotometer flow cells. This was also seen in the slopes of the regression curves for the different path lengths, with a smaller magnitude slope predicted for the 10 mm path length regression curve (0.0086 at 190.0 nm) than for those of the 4 mm (0.017 at 189.8 nm) and 8 mm (0.029 at 189.8 nm) path lengths. A greater magnitude slope was indicative of a greater difference in absorbance between different polymer concentrations and was indicative of a greater sensitivity. It was therefore determined in this case that the desktop spectrophotometer was not as sensitive to detection of different polymer concentrations as was the in-line spectrophotometer.

Further, this was true despite the smaller path length of the in-line flow cells than that of the cuvette used in the desktop spectrophotometer.

A comparison of the regression analyses of the 4 mm and 8 mm path length flow cells shows an overall greater sensitivity when using the 8 mm path length. However, the hypothesized particle effect discussed above was expected to also cause a degree of turbulence in the flow through the flow cells. This was evidenced by the high standard errors seen in the regression of the 8 mm flow cell data (0.108 at 189.8 nm) compared to those seen in the regression of the 4 mm flow cell data (0.019 at 189.8 nm). As a result, the 4 mm path length flow cell was found to be the optimum flow cell path length for polymer detection in sludge centrate and was thus used exclusively in further experiments.

4.3.3 The effect of particle size and solids concentration on the detection of polymer in sludge centrate

The absorbance spectra of sludge centrate conditioned with Zetag 8160 polymer were analyzed to examine the effect of particle concentration on polymer detection in sludge centrate samples. This test was completed using the 4 mm path length flow cell in the in-line UV-Vis spectrophotometer. Individual sludge centrate samples were left unfiltered, filtered through an 8 µm pore size filter, and filtered through a 0.45 µm pore size filter prior to polymer conditioning. Each filtered sludge centrate sample was then individually diluted by a factor of 1:25 and 1:50, for a total of six samples with varying relative particle sizes and concentrations. Higher levels of filtration reduced the mean particle size as well as the particle concentration, while higher dilution factors reduced only the particle concentration.

Polymer was dosed to concentrations of 1.0, 2.5, 5.0, 10.0, 15.0, 20.0, 25.0, and 30.0 mg/L by pipette. For the sludge centrate samples diluted by a factor of 1:25, the spectra for the unfiltered, 8 μm pore size filtered, and 0.45 μm pore size filtered samples are shown in Figures 4.5a, 4.5b, and 4.5c, respectively. For the sludge centrate samples diluted by a factor of 1:50, the spectra of the unfiltered, 8 μm pore size filtered, and 0.45 μm pore size filtered samples are shown in Figures 4.6a, 4.6b, and 4.6c, respectively.

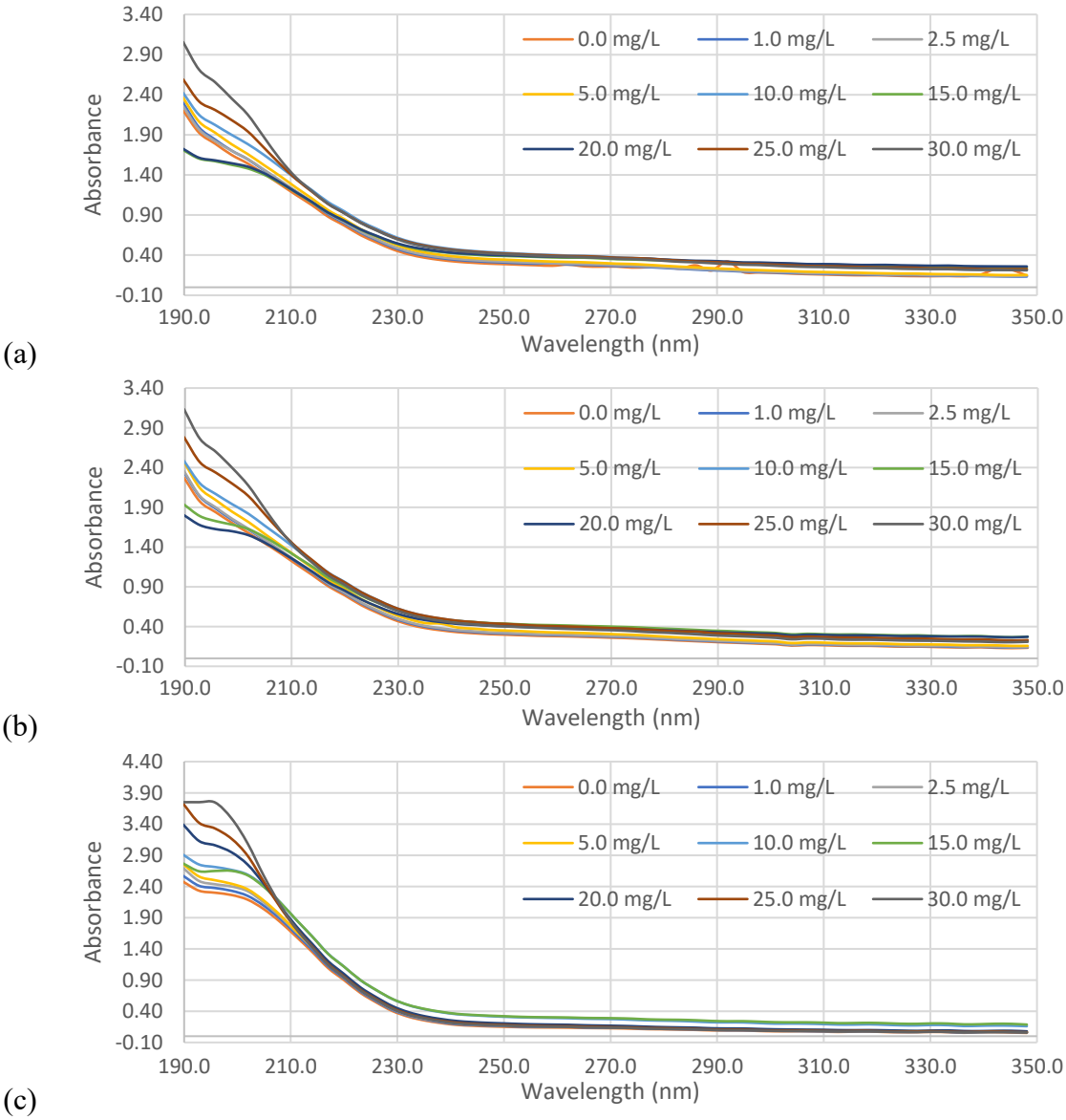

Figure 4.5: Absorbance spectra of Zetag 8160 polymer in sludge centrate using a 4 mm flow cell, diluted by a factor of 1:25, and a) unfiltered; b) filtered through an 8 µm pore size filter; c) filtered through a 0.45 µm pore size filter.

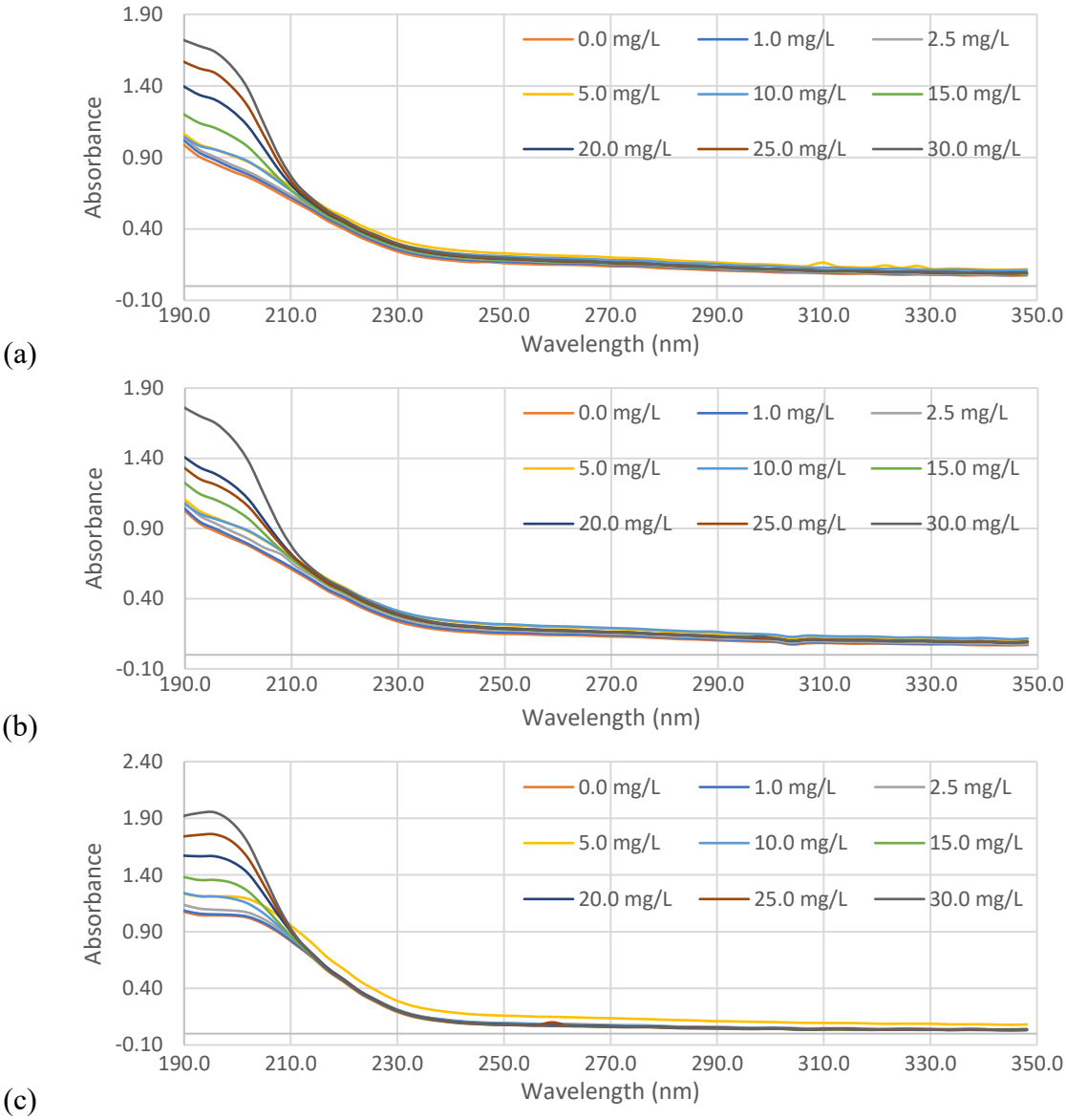

Figure 4.6: Absorbance spectra of Zetag 8160 polymer in sludge centrate using a 4 mm flow cell, diluted by a factor of 1:50, and a) unfiltered; b) filtered through an 8 µm pore size filter; c) filtered through a 0.45 µm pore size filter.

As shown in Figures 4.5 and 4.6, as the concentration of Zetag 8160 polymer increases, a corresponding increase in absorbance of the sludge centrate samples was observed. The peak absorbance value was observed at a wavelength of 190 nm for all samples, with no significant absorbance measured above 240 nm.

Through preliminary visual analysis of the spectra shown above in Figures 4.5 and 4.6, it was evident that as the level of filtration was increased (from unfiltered to the 8 μm pore size to the 0.45 μm pore size), the peak absorbance of the sample also increased. This provided preliminary evidence for the particle effect hypothesis discussed above. A lower particle concentration in the more highly filtered samples was predicted to result in decreased polymer flocculation and coagulation, thus increasing the residual suspended polymer concentration in solution. A higher polymer concentration in solution would result in a higher absorbance, as observed in the above Figures 4.5 and 4.6.

Another observation made when comparing the spectra of the 1:50 dilution series and the 1:25 dilution series was the overall higher absorbance of the samples diluted by the lower factor. This was hypothesized to be the effect of the 1:25 dilution series having a higher overall particle concentration as well as a higher background soluble species concentration. Particles in suspension and soluble species present were expected to scatter or absorb UV radiation, resulting in higher absorbance measurements.

The relationship between Zetag 8160 polymer concentration and the magnitude of the absorbance of each sample at wavelengths of 189.8 nm, 201.9 nm, and 211.0 nm is shown below in Figure 4.7. Figures 4.7a/b, 4.7c/d, and 4.7e/f show these relationships for samples that are unfiltered, filtered through an 8 μm pore size filter, and filtered through a 0.45 μm pore size filter, respectively. Figures 4.7a/c/e show the relationships of the samples which were diluted by a factor of 1:25, while Figures 4.7b/d/f show the relationships of the samples which were diluted by a factor of 1:50. Error bars are present on all data points, even if they are not visible. A summary of a linear regression analysis for the data shown in Figure 4.7 follows in Table 4.3.

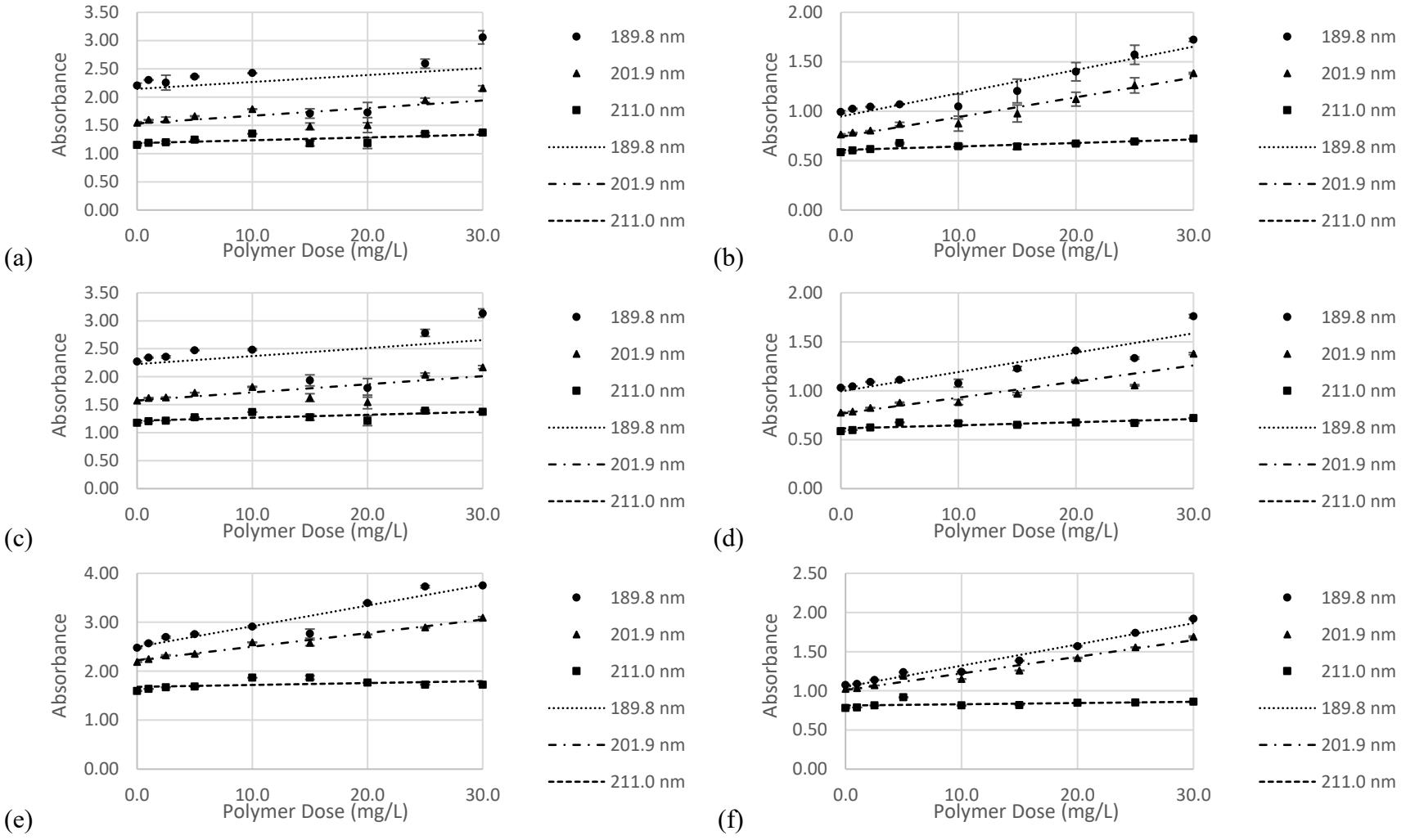

Figure 4.7: Relationship between Zetag 8160 polymer concentration in sludge centrate and absorbance at 189.8 nm, 201.9 nm, and 211.0 nm using a 4 mm flow cell with filtration and dilution factors of: a) Unfilt./1:25; b) Unfilt./1:50; c) 8 µm/1:25; d) 8 µm/1:50; e) 0.45 µm/1:25; f) 0.45 µm/1:50.

Table 4.3: Summary of linear regression analysis of relationship between Zetag 8160 polymer concentration in sludge centrate and absorbance at 189.8 nm, 201.9, and 211.0 nm using flow cell path length of 4 mm, dilution factors of 1:25 and 1:50, and unfiltered samples, samples filtered through an 8 µm pore size filter, and samples filtered through a 0.45 µm filter.

	Unfiltered/1:25 Dilution			**8 µm Filter/1:25 Dilution**			**0.45 µm Filter/1:25 Dilution**		
	189.8 nm	201.9 nm	211.0 nm	189.8 nm	201.9 nm	211.0 nm	189.8 nm	201.9 nm	211.0 nm
Coefficient of Determination (R^2)	0.107	0.440	0.413	0.154	0.532	0.500	0.907	0.978	0.207
Standard Error	0.418	0.180	0.0703	0.396	0.160	0.062	0.159	0.0483	0.0898
Residual Sum of Squares (RSS)	1.22	0.227	0.0346	1.10	0.180	0.0267	0.178	0.0164	0.0565
Total Sum of Squares (TSS)	1.37	0.406	0.0590	1.30	0.385	0.054	1.92	0.763	0.0713
F statistic	0.837	5.51	4.93	1.28	7.95	7.01	68.6	319	1.83
F statistic P-value	0.391	0.0513	0.0618	0.296	0.0258	0.0330	$7.30*10^{-5}$	$4.25*10^{-7}$	0.219
Intercept	2.14	1.53	1.19	2.26	1.58	1.21	2.50	2.22	1.68
Slope	0.0122	0.0136	0.0050	0.0143	0.0145	0.0052	0.0423	0.0277	0.0039
	Unfiltered/1:50 Dilution			**8 µm Filter/1:50 Dilution**			**0.45 µm Filter/1:50 Dilution**		
	189.8 nm	201.9 nm	211.0 nm	189.8 nm	201.9 nm	211.0 nm	189.8 nm	201.9 nm	211.0 nm
Coefficient of Determination (R^2)	0.931	0.967	0.767	0.913	0.932	0.800	0.974	0.960	0.170
Standard Error	0.0757	0.0433	0.0231	0.105	0.0693	0.0224	0.0526	0.0509	0.0410
Residual Sum of Squares (RSS)	0.0402	0.0131	0.0037	0.0997	0.0432	0.0045	0.0194	0.0181	0.0117
Total Sum of Squares (TSS)	0.581	0.402	0.0160	1.14	0.632	0.0226	0.734	0.457	0.141
F statistic	94.2	208	23.1	94.1	122	35.9	258	170	1.43
F statistic P-value	$2.61*10^{-5}$	$1.84*10^{-6}$	$1.95*10^{-3}$	$4.61*10^{-6}$	$1.53*10^{-6}$	$2.05*10^{-4}$	$8.78*10^{-7}$	$3.64*10^{-6}$	0.271
Intercept	0.946	0.741	0.607	0.970	0.749	0.616	1.05	1.01	0.812
Slope	0.0236	0.0200	0.0036	0.0223	0.0170	0.0030	0.0271	0.0212	0.0016

Analysis of the polymer dose – absorbance relationships in Figure 4.7 confirmed the hypothesized particle effect discussed above. The effect was visible as the negative deviations from linearity seen at the 15 to 20 mg/L and at the 10 to 15 mg/L concentrations in Figures 4.7a/c/e (1:25 dilution) and Figures 4.7b/d/f (1:50 dilution), respectively. This particle effect was most pronounced in samples with a higher concentration of particles. These samples were the ones with a lower dilution factor (1:25 compared with 1:50) and a lower level of filtration. This was expected as more adsorption of polymer onto particles would occur in samples with a higher particle concentration, thus reducing the residual polymer concentration measured in these samples. Furthermore, the 189.8 nm wavelength appears to be the most sensitive of the three wavelengths tested, as expected as this is the wavelength corresponding to the peak absorbance of the polyacrylamide polymer.

The particle effect and deviation of linearity can also be seen in the results of the linear regression analyses summarized in Table 4.2. As the linear relationship between absorbance and polymer concentration was previously established in previous sections, a deviation from linearity was an indication of interference, and in this experiment, namely the aforementioned particle effect. As would be expected, the samples with higher particle concentrations had weaker linear correlations, namely the unfiltered and 8 μm pore size filtered samples diluted by a factor of 1:25. In addition to low R^2 values and relative RSS to TSS magnitudes, the regressions for these two sample series were found to be statistically insignificant based on the P-values.

Based on the results summarized in Figure 4.7 and Table 4.3, the particle effect is present in all samples regardless of level of filtration or dilution factor. It is most prominent in the unfiltered samples with lower dilution factors. This indicates that in full-scale operations

which require the measurement of residual polymer, filtration of the sample prior to measurement is not necessary. Furthermore, at the higher dilution factor of 1:50, the impact of the particle effect was reduced as the particle concentration was lower. This lowered the sensitivity of the method to the impact of the particles on residual polymer concentration.

4.4 Conclusion

This study was conducted to investigate the sensitivity for measuring residual polymer concentration in sludge centrate using different path lengths (1 mm, 2 mm, 4 mm, and 8 mm) in an in-line UV-Vis spectrophotometer. It also investigated the effect of particle size and TS concentration on residual polymer detection using this method through varying levels of filtration and dilution.

Calibration curves were generated for polymer dosed in deionized water and in sludge centrate samples, and their data was linearly regressed. These showed that the 4 mm path length flow cell was the optimal path length for residual polymer detection using the in-line UV-Vis spectrophotometer for sludge dewatering applications. Smaller path lengths were shown to result in too much variability in the absorbance measurements for reliable polymer concentration quantification, while interference from other parameters such as solids was shown to reduce the sensitivity of larger path lengths. It was also shown that the in-line UV-Vis spectrophotometer was superior to the desktop UV-Vis spectrophotometer due to a higher sensitivity for residual polymer detection in sludge centrate.

It was shown that the UV-Vis spectrophotometry method was sensitive to particle concentration through tests varying dilution factor and filter size. This was seen through the lower relative linearity in the regressed data of the samples with higher TS content (no

or lower filtration and less dilution) compared with those of lower TS content. Filtration through smaller pore sized filters was observed to reduce the sensitivity of residual polymer detection using the UV-Vis spectrophotometer due to the reduced particle size and concentration. Likewise, increased dilution reduced the impact of particles and again resulted in a lower sensitivity for residual polymer detection. This combined with the increased sensitivity of the smaller 4 mm path length reduces the need for filtration and lowers the amount of dilution required for sludge centrate in full-scale applications.

Chapter 5 – Investigation into torque rheology and ultraviolet/visible spectrophotometry as a feed-forward and feed-back control sludge dewatering optimization system

Abstract

Polyacrylamide polymer conditioners are often employed to enhance mechanical sludge dewatering processes, though they are expensive and both overdosing and underdosing have detrimental impacts on the efficacy of the process. This study investigated the use of a feed-forward and feed-back control system for polymer dosage optimization in sludge dewatering. Two torque rheological methods, totalized torque and direct injection, were analyzed as feed-forward controls, while UV-Vis spectrophotometry was analyzed as a feed-back control. The optimum polymer dosages measured by these methods were compared with established laboratory methods, capillary suction time and a filtration test. A feed-forward and feed-back control system using the TTQ torque rheological method and UV-Vis spectrophotometry was found to accurately and consistently measure optimum polymer dose when compared with the established laboratory methods. It was shown that this system was reliable when varying polymer types were employed and was thus unimpacted by this change. Different sludge types, two anaerobically digested and one aerobically digested, were analyzed for optimum polymer dosages using the system. These experiments showed that an optimum polymer dose could be reliably measured by the feed-forward and feed-back control system even in sludge samples where optimum dosages could not be measured through the established laboratory methods. The use of a feed-

forward and feed-back control system was also shown to provide redundancy when one control method was unable to measure an optimum polymer dose.

Keywords: Torque rheology, ultraviolet/visible spectrophotometry, polymer, sludge, dewatering, optimization.

5.1 Introduction

Mechanical sludge dewatering processes often employ polyacrylamide polymer conditioners to enhance the flocculation of the solids and separation of the water phase in the sludge (Dentel, 2001). Many wastewater treatment plants add more than the optimal polymer dosage in their dewatering processes in order to avoid an underdose. However, both underdosing and overdosing of polymer conditioners decreases the solids recovery of the dewatering process, and therefore maintaining an optimum polymer dose is necessary to maximize the efficacy of the process (Bolto and Gregory, 2007). Additionally, polymer conditioners can account for over 50% of the biosolids handling process (US EPA, 1987). Therefore, the optimization of polymer dosage can result in significant cost savings for a dewatering facility.

There are a number of laboratory methodologies which can be used to optimize the polymer dosage of a dewatering process. Many wastewater treatment facilities rely on methods such as capillary suction time (CST) and time to filter tests for maintaining an optimum polymer dosage. However, due to the variable nature of the sludge influent, these must be repeated often to be effective. Laboratory methods are also time-consuming, and can often times be complex, making them ill-suited for continuous real-time monitoring of optimum polymer dose.

Using in-line and real-time methodologies for polymer dose optimization is the solution to these problems. In-line and real-time polymer dose optimization methods by definition do not require grab samples to be taken and analyzed in a laboratory. They can also be used in tandem with an automatic system to adjust the made-down polymer flowrate in real-

time. Consequently, an optimum polymer dose can be maintained in real-time considering variable sludge inflow conditions.

A real-time polymer dose optimization system can be improved upon by using a feed-forward and feed-back control (two-stage) polymer dose optimization system. In such a system, one in-line optimization method is employed upstream of the dewatering process and another is employed downstream. This allows for a two-stage verification of the optimum polymer dose, thus ensuring the accuracy and reliability of the system as a whole. Figure 5.1 below shows a flow chart of a sludge dewatering process with such an in-line and real-time polymer dose optimization system with feed-forward and feed-back control.

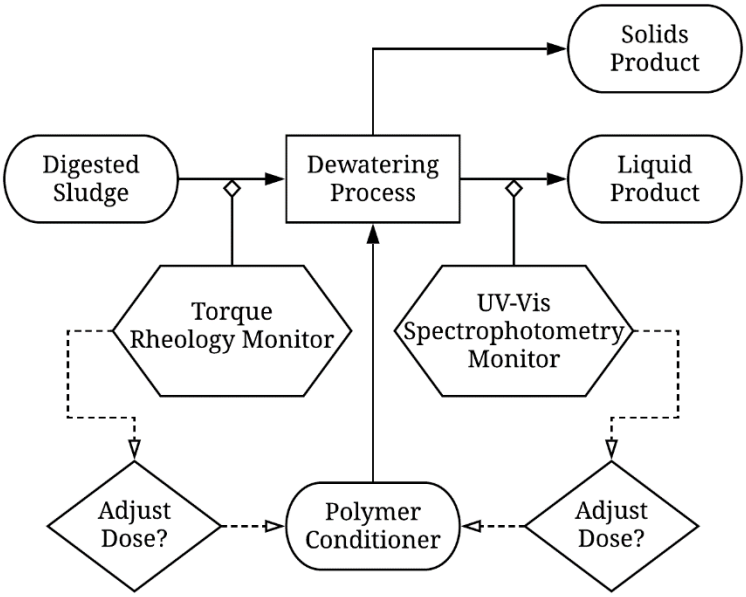

Figure 5.1: Sludge dewatering process flow chart showing pre-dewatering torque rheology monitor and post-dewatering UV-Vis spectrophotometry monitor for maintaining optimum polymer dosage.

Upstream from the dewatering process, in the unconditioned digested sludge, a rheological method has the potential for real-time monitoring of the optimum polymer dosage. Rheology is defined as the study of the flow and deformation of materials and is an effective tool for the characterization of sludge (Örmeci, 2007). A torque rheometer is a device which measures the rheological properties of a fluid through measuring its resistance to shear. It does this by spinning an impeller at a constant rate and measuring its torque. Using this, torque rheograms can be generated and the resistance to shear of the sludge over time can be determined. There are two torque rheological methods reported in literature which can be used to determine the rheological properties of the sludge. These are known as the totalized torque (TTQ) method and the direct injection method (Örmeci, 2007). These methods use the area under the rheogram and the peak heights of the rheograms, respectively, to determine an optimum polymer dosage (Örmeci, 2007). Both of these methods have been successfully tested for polymer dose optimization at lab-scale and at full-scale dewatering facilities (Abu-Orf and Örmeci, 2005; Örmeci and Abu-Orf, 2005; Örmeci, 2007).

Downstream from the dewatering process, in its liquid product, an ultraviolet/visible (UV-Vis) spectrophotometry method has the potential for real-time monitoring of the optimum polymer dosage. Polyacrylamide polymers have a peak absorbance at a wavelength of 190 nm, and the concentration of residual polymer can be determined by measuring the absorbance of the liquid product at this wavelength (Al Momani and Örmeci, 2014b). An optimum polymer dose for a sludge dewatering process can be determined through monitoring the changes in absorbance over time of its liquid product. Finding and maintaining a minimum absorbance value at λ = 190 nm maintains a minimum residual

polymer concentration, and therefore an optimum polymer dosage in the dewatering process upstream. This method was analyzed previously for use in drinking water treatment coagulation processes (Cormier, 2019). The novelty of this research in comparison is the testing of the UV-Vis spectrophotometric method in wastewater sludges and in the concurrent testing of the torque rheological methods to test the feasibility of the proposed two-stage polymer dose optimization system.

The purpose of this study was to investigate the feasibility and reliability of a two-stage system using torque rheology and UV-Vis spectrophotometry for polymer dose optimization. The goal was to confirm that these methods predict the same optimum polymer dose for the same sludge sample and polymer conditioner at the lab-scale and to compare these results with established laboratory methods for determining an optimum polymer dosage. The study first investigated the consistency of the system using a single polymer and sludge source. The use of different polymer types with variable chemistry, molecular weight, charge, and structure were then investigated. The final phase of the study investigated different sludge sources with variable sludge characteristics to further analyze the consistency of the system. The use of this system has the potential to reduce costs and increase dewatering process efficacy and efficiency.

5.2 Materials and Methods

The experiments conducted for each sample consisted of the two pre-dewatering torque rheology methods and the post-dewatering UV-Vis spectroscopy method, further discussed below. These were conducted in parallel with established laboratory methods over the course of two days to minimize variation of the samples. The dewatering experiments

performed are summarized in the flow chart seen in Figure 5.2 and are described in further detail in the following sections.

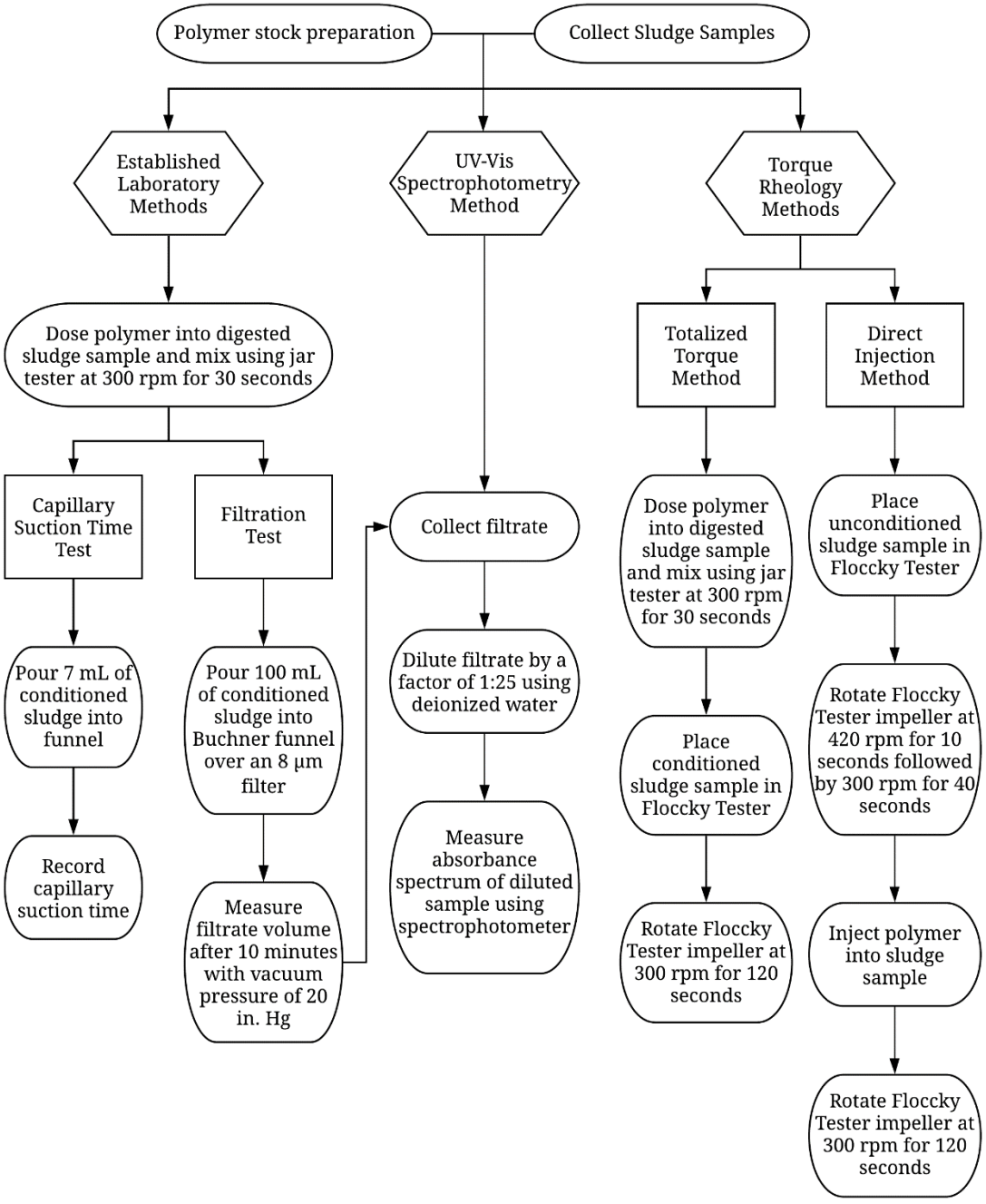

Figure 5.2: Flow chart of the experimental processes for polymer dose optimization experiments.

5.2.1 Variation of polymer conditioners

Three polyacrylamide polymers with varying properties were employed. These were Zetag 8160 (manufactured by BASF Corporation), Flopolymer CA 4600 (manufactured by SNF Canada), and Flopolymer CB 4350 (manufactured by SNF Canada). The characteristics of these polymers are summarized in Table 5.1 below:

Table 5.1: Summary of characteristics for polymers employed.

Polymer	Charge Density	Ionic Character	Molecular Weight	Physical Form
Zetag 8160	Medium-High	Cationic	High	Granular Solid
Flopolymer CA 4600	High	Cationic	Ultra-High	Granular Solid
Flopolymer CB 4350	Low	Cationic	Very-High	Granular Solid

Flopolymer CA 4600 was being employed by the Robert O. Pickard Environmental Centre (ROPEC) at the time of the study. Flopolymer CB 4350 was being employed by the Gatineau Wastewater Treatment Plant (WWTP) at the time of the study. These polymers were selected due to their use at the facilities from which sludge samples were obtained and for their variable characteristics.

5.2.2 Made-down polymer stock solution preparation

Polymer stock solutions were made-down to a concentration of 0.50% by mixing 5.0 g of the polymer to be used into 1,000 mL of deionized water (Direct-Q UV Water Purification System, Millipore Sigma, USA). The mixing process was 5 minutes at 250 rpm followed by 55 minutes at 125 rpm. This mixing was completed using a Phipps and Bird PB-700 Jar-tester (Richmond, VA). After the initial mixing, a hand blender was used to break up

flocs which had formed. The hand blender was employed for 10 seconds. The made-down solution was then allowed to mature for 60 minutes prior to use in experiments. Polymer stock solutions were prepared daily to minimize variations caused by increased maturation times.

5.2.3 Variation of sludge samples

Three sludge samples were collected and tested from different wastewater treatment facilities. Anaerobically digested sludge was collected from both ROPEC, located in Ottawa, Ontario, and the Gatineau WWTP, located in Gatineau, Quebec. Aerobically digested sludge was collected from the Rockland WWTP, located in Clarence-Rockland, Ontario. Both ROPEC and the Gatineau WWTP presently employ mechanical dewatering using bowl centrifuges and Flopolymer CA 4600 and Flopolymer CB 4350, respectively. The Rockland WWTP does not presently employ any form of mechanical dewatering, and thus polymers are not employed.

The anaerobically digested sludge samples were stored at room temperature and kept for a maximum of three weeks. The aerobically digested sludge samples were stored at room temperature with constant aeration performed using air diffusers and were kept for a maximum of three days. Each set of experiments conducted on a single sample were performed in a single day to minimize the effects of the ageing of the samples.

5.2.4 Sludge conditioning

All sludge samples to be used in experiments were conditioned using the Phipps and Bird PB-700 Jar-tester, except the direct injection torque rheology method, discussed further in

section 5.2.6.2. The sludge sample to be conditioned was placed in a 500 mL beaker and placed in the jar-tester with the paddle lowered. The polymer dose was then injected via pipette into the sludge sample, which was then mixed at 300 rpm for 30 seconds. This high mixing speed ensured polymer flocculation by being well mixed while the low mixing time reduced shear stress on the sludge, minimizing the effect of the thixotropic nature of the sludge.

5.2.5 Determination of optimum polymer dose using established laboratory methods

Two established laboratory methods were conducted to determine optimum polymer dosages for the sludge samples. These were the capillary suction time (CST) test and a filtration test. The results of these methods were compared with the results from the methods employed by the proposed two-stage polymer dose optimization system.

5.2.5.1 Capillary suction time test

The CST test was used to measure the dewaterability of the sludge sample after polymer conditioning. The following process was performed as per the manufacturer's (Triton Electronics, England) recommended procedure. Three 7 mL samples of the conditioned sludge sample were pipetted individually into the funnel of the CST tester placed above the Whatman No. 17 filter paper (Whatman, UK). The CST tester (Triton Electronics Type 319 Multi-CST, England) measured the time required for filtrate to pass via capillary suction between two rings of sensors at a known separation. A shorter CST time

corresponded to better dewaterability of the sludge, with the optimum polymer dose observed at the minimum CST time.

5.2.5.2 Filtration test

The filtration test used was performed via the standard methods (APHA *et al.*, 2005). This test used a Whatman No. 2 filter with a pore size of 8 μm (Whatman, UK) in a Buchner funnel placed above a 250 mL graduated cylinder with vacuum port. Two 100 mL samples of the conditioned sludge sample were individually poured into the Buchner funnel above individual filters to obtain duplicates. A constant vacuum pressure of 20 in. Hg was applied for a time of 10 minutes using a vacuum pump (Welch, USA), after which the volume of filtrate was measured. A larger filtrate volume corresponded to better filterability and thereby dewaterability, with the optimum polymer dose observed at the maximum filtrate volume.

5.2.6 Determination of optimum polymer dose using torque rheology pre-dewatering

Torque rheology was analyzed for measuring optimum polymer dose pre-dewatering as a feed-forward control. Using this method, torque rheograms were generated for sludge samples conditioned with increasing polymer dosages. A comparison of the torque rheograms generated was then used to determine the optimum polymer dosage. Two torque rheological methods were tested as the pre-dewatering in-line optimization methods using a Floccky Tester (Koei Industry Co., Ltd., Japan). These methods are known the totalized torque (TTQ) method and the direct injection method (Örmeci, 2007). A lab-scale torque

rheometer was used in place of an in-line full-scale torque rheometer, but the principles and methods are identical.

5.2.6.1 Totalized torque method

The TTQ method utilized conditioned sludge and measured the area under the torque-time rheograms in order to determine the optimal polymer dosage. Two 200 mL samples of sludge were independently conditioned with polymer, as described in section 5.2.4, and individually placed in the vessel of the torque rheometer in order to obtain duplicates. The rheometer impeller was then rotated at a constant speed of 300 rpm for 120 seconds. This produced a torque-time rheogram from which the area under the curve (the TTQ) was determined. A larger area corresponded to better dewaterability, but an erratic rheogram with a high quantity of noise after the initial peak corresponded to an overdose.

5.2.6.2 Direct injection method

The direct injection method utilized unconditioned sludge and injected polymer directly into the sludge sample during mixing. The height of the peaks observed on the rheogram after polymer injection were measured. Two different 200 mL samples of unconditioned sludge were individually placed in the vessel of the torque rheometer in order to obtain duplicates. The rheometer impeller was then rotated in three stages. The first stage was at a constant speed of 420 rpm for 10 seconds, and the second stage was at a constant speed of 300 rpm for 40 seconds. At the end of the second stage, the polymer was injected via pipette through a side port in the vessel, after which the third stage of mixing was performed at a speed of 300 rpm for 120 seconds. A peak was observed immediately post

polymer injection and its peak high was determined. A higher peak corresponded to higher dewaterability, but an erratic rheogram with a high quantity of noise and additional peaks after the initial peak corresponded to an overdose.

5.2.7 Determination of optimum polymer dose using ultraviolet/visible spectrophotometry post-dewatering

An UV-Vis spectrophotometric method was tested as a post-dewatering feed-back polymer dose optimization control. This method utilized an in-line and real-time UV-Vis spectrophotometer (Real Spectrum PL Series, Real Tech Inc., Ontario, Canada). Filtrate obtained from the conditioned sludge samples in the filtration tests was diluted by a factor of 1:25 using deionized water. The resulting solution was passed through the spectrophotometer and its spectrum was analyzed in triplicates using the 4 mm path length flow cell. Polyacrylamide polymers have their peak absorbance at a wavelength of 190 nm (Al Momani and Örmeci, 2014b), so the spectra of the samples were measured from 190 nm to 350 nm. The low end of this range is limited by the range of the instrument, but this does not impact performance. The optimum polymer dose was observed in the sample with the lowest absorbance value at a wavelength of 189.8 nm.

5.3 Results and Discussion

5.3.1 Dewatering optimization tests

In order to assess the replicability of the polymer dose optimization methodology, three sets of experiments were conducted utilizing one polymer (Flopolymer CA 4600) and digested sludge from a single facility, ROPEC, collected on different days. For the

following section, these experiments will be referred to as ROPEC 1, ROPEC 2, and ROPEC 3, indicating different sample collection dates. In these experiments, the results of the established laboratory CST and filtration methods were compared with the in-line UV-Vis spectroscopy and torque rheology methods. A summary of the total solids content of the digested sludge samples tested is provided in Table 5.2 below.

Table 5.2: Summary of total solids content of digested sludge samples.

Digested Sludge Sample	Total Solids (TS)	Standard Deviation of TS
ROPEC 1	1.56%	0.11%
ROPEC 2	1.88%	0.10%
ROPEC 3	1.76%	0.06%

The digested sludge samples tested had some TS content variability between them despite being taken from the same facility. As the samples were collected individually during different months of the year, this was attributable to day to day variation in facility operating conditions, wastewater influent conditions, and seasonal variability.

Figures 5.3, 5.4, and 5.5 below show the results of the dewatering optimization experiments conducted for the ROPEC 1, 2, and 3 samples, respectively. Figures 5.3a, 5.4a, and 5.5a show the absorbance spectra of the samples tested. Figures 5.3b, 5.4b, and 5.5b show the rheograms of the TTQ rheological method. Figures 5.3c, 5.4c, and 5.5c show the rheograms of the direct injection rheological method. Figures 5.3d, 5.4d, and 5.5d show the results of the UV-Vis absorbance and laboratory methods tests. Figures 5.3e, 5.4e, and 5.5e show the results of the TTQ values of the TTQ rheological method and the peak heights of the direct injection rheological method.

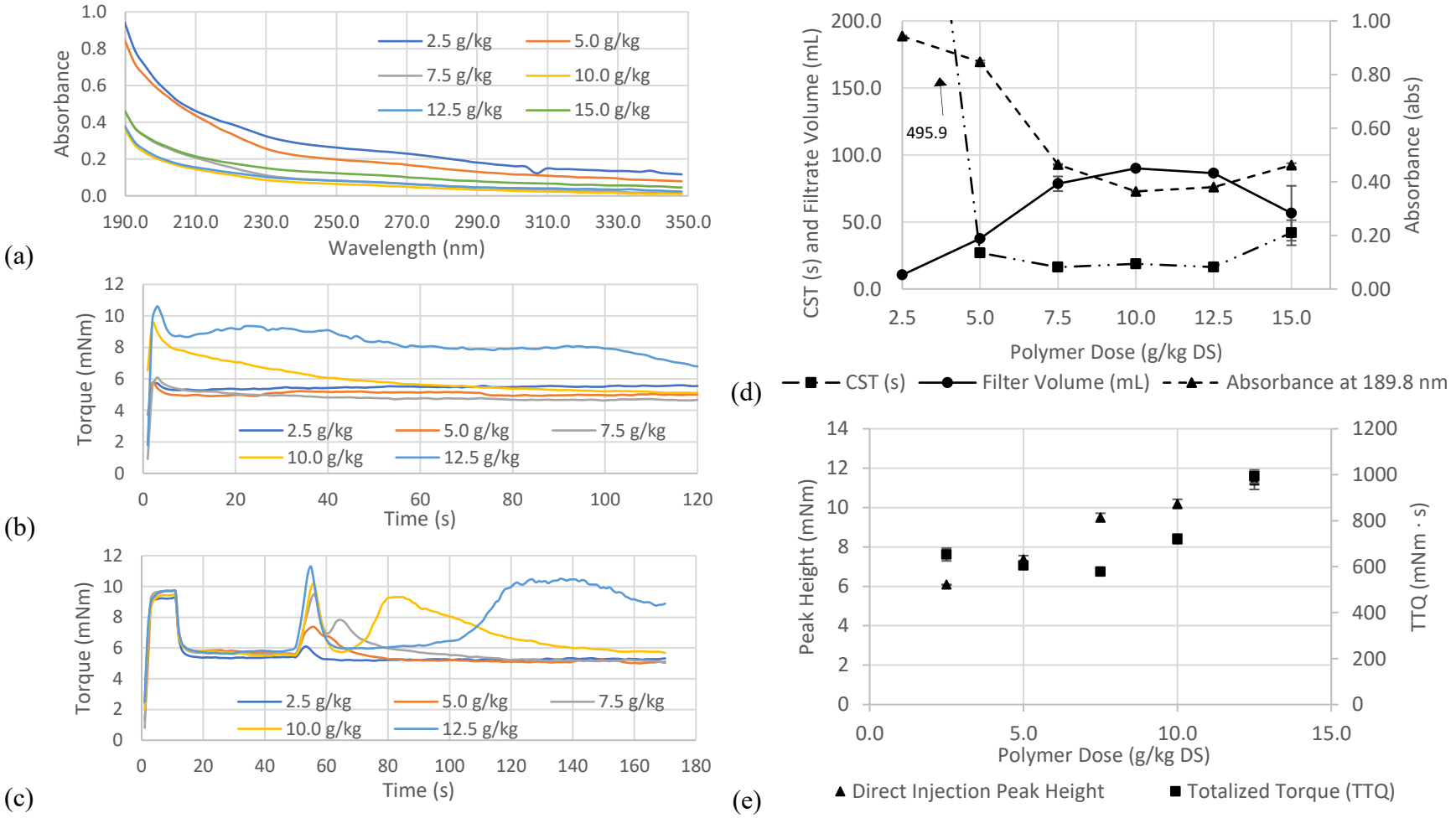

Figure 5.3: Results of ROPEC 1 sludge dewatering optimization tests a) Absorbance spectra of sludge filtrate; b) Torque rheograms of TTQ rheological method; c) Torque rheograms of direct injection torque rheological method; d) Peak absorbance of filtrate samples at 189.8 nm and mean CST times and filtration test volumes; e) Direct injection peak heights and totalized torque values.

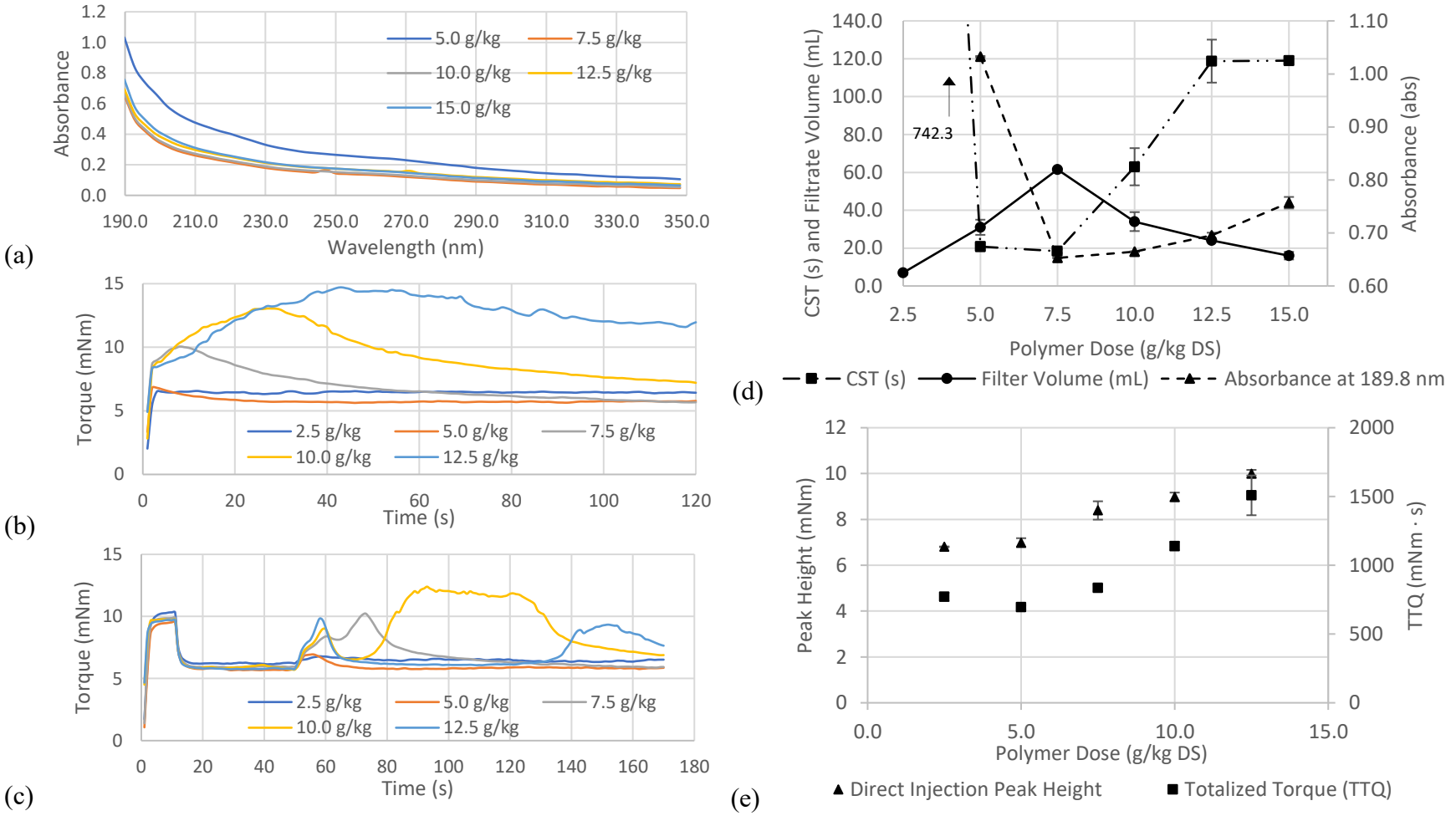

Figure 5.4: Results of ROPEC 2 sludge dewatering optimization tests a) Absorbance spectra of sludge filtrate; b) Torque rheograms of TTQ rheological method; c) Torque rheograms of direct injection torque rheological method; d) Peak absorbance of filtrate samples at 189.8 nm and mean CST times and filtration test volumes; e) Direct injection peak heights and totalized torque values.

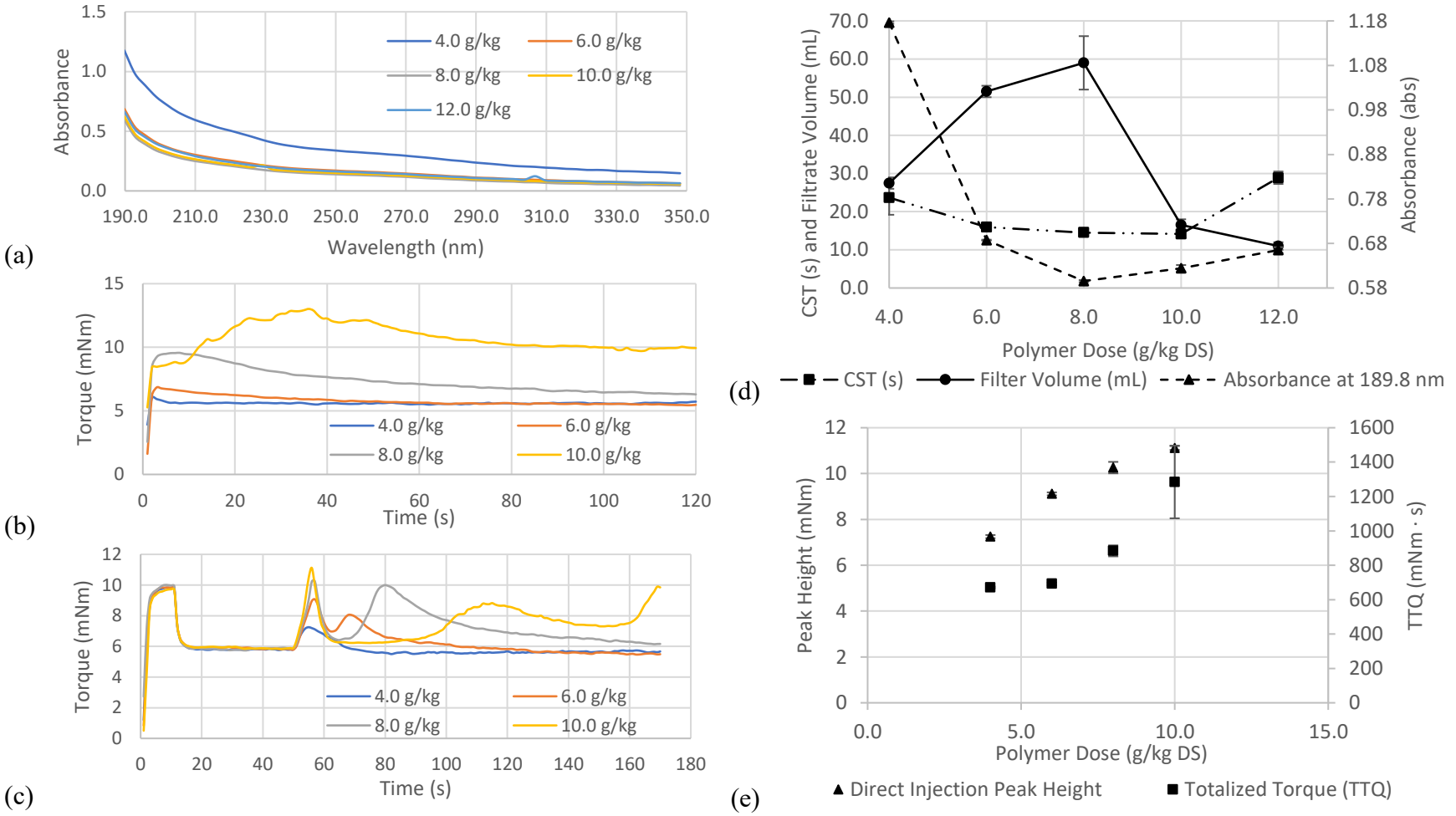

Figure 5.5: Results of ROPEC 3 sludge dewatering optimization tests a) Absorbance spectra of sludge filtrate; b) Torque rheograms of TTQ rheological method; c) Torque rheograms of direct injection torque rheological method; d) Peak absorbance of filtrate samples at 189.8 nm and mean CST times and filtration test volumes; e) Direct injection peak heights and totalized torque values.

The peak absorbances in the spectra of all the samples tested were observed at a wavelength of 189.8 nm, as shown in Figures 5.3a, 5.4a, and 5.5a, with no significant absorbance observed above 240 nm.

For the ROPEC 1 sludge samples, the results of the UV-Vis method and the laboratory methods are shown in Figure 5.3d. A minimum absorbance value was observed at a polymer dosage of 10.0 g/kg DS, corresponding to the optimum dosage. The laboratory methods tested for comparison support this prediction. The maximum filtrate volume was obtained at the same polymer dosage of 10.0 g/kg, and while the CST time results did not produce a distinct minimum, the lowest CST times were obtained in the polymer dosage range of 7.5 g/kg DS to 12.5 g/kg. The rheograms obtained using the TTQ method, shown in Figure 5.3b, showed that the 12.5 g/kg dosage was overdosed. This was indicated by the rough curve of the rheogram after the initial peak, compared with the smooth curves of the rheograms for the other dosages. The optimum polymer dosage was thus observed at the maximum TTQ value prior to this overdose, at a dosage of 10.0 g/kg as shown in Figure 5.3e. The rheograms obtained using the direct injection method, shown in Figure 5.3c, showed that the 10.0 g/kg and 12.5 g/kg dosages were overdosed. This was shown by the large spikes in the rheograms after the initial peak, which were indicative of re-flocculation by excess polymer in solution. The optimum polymer dosage was thus observed at the maximum peak prior to this overdose, at a dosage of 7.5 g/kg as shown in Figure 5.3e. These results are summarized in Table 5.3 below.

For the ROPEC 2 sludge samples, the results of the UV-Vis method and the laboratory methods are shown in Figure 5.4d. A minimum absorbance value was observed at a polymer dosage of 7.5 g/kg DS, corresponding to the optimum dosage. The laboratory

methods tested for comparison support this prediction. The maximum filtrate volume and minimum CST time were observed at the same polymer dosage of 7.5 g/kg. The rheograms obtained using the TTQ method, shown in Figure 5.4b, showed that the 10.0 g/kg and 12.5 g/kg dosages were overdosed. This was indicated by the rough curves of the rheograms after the initial peak, compared with the smooth curves of the rheograms for the other dosages. The optimum polymer dosage was thus observed at the maximum TTQ value prior to this overdose, at a dosage of 7.5 g/kg as shown in Figure 5.4e. The rheograms obtained using the direct injection method, shown in Figure 5.4c, showed that the 10.0 g/kg and 12.5 g/kg dosages were overdosed. This was indicated by the large spikes in the rheograms after the initial peak, which were indicative of re-flocculation by excess polymer in solution. A small dip was also seen in the 7.5 g/kg dose rheogram after the initial peak, followed by a larger distinct peak. This was indicative that the 7.5 g/kg dose may be slightly overdosed, though not as visibly as in the rheograms of the higher dosages. The optimum polymer dosage was thus concluded to be in the dose range of 5.0 g/kg to 7.5 g/kg. These results are summarized in Table 5.3 below.

For the ROPEC 3 sludge samples, the polymer dose interval was changed from 2.5 g/kg to 2.0 g/kg in order to test the accuracy of the methodologies using the smaller interval. The results of the UV-Vis method and the laboratory methods are shown in Figure 5.5d. A minimum absorbance value was observed at a polymer dosage of 8.0 g/kg DS, corresponding to the optimum dosage. The laboratory methods tested for comparison support this prediction. The maximum filtrate volume was obtained at a polymer dosage of 8.0 g/kg, while the minimum CST time was obtained in the dose range of 8.0 to 10.0 g/kg. The difference between these CST times was 0.3 seconds, within the standard deviations

of the tests for both dosages. The rheograms obtained using the TTQ method, shown in Figure 5.5b, showed that the 10.0 g/kg dosage was overdosed. This was indicated by the rough curve of the rheogram after the initial peak, compared with the smooth curves of the rheograms for the other dosages. The optimum polymer dosage was thus observed at the maximum TTQ value prior to this overdose, at a dosage of 8.0 g/kg as shown in Figure 5.5e. The rheograms obtained using the direct injection method, shown in Figure 5.5c, showed that the 8.0 g/kg and 10.0 g/kg dosages were overdosed. This was indicated by the large spikes in the rheograms after the initial peak, which were indicative of re-flocculation by excess polymer in solution. The optimum polymer dosage was thus observed at the maximum peak prior to this overdose, at a dosage of 6.0 g/kg as shown in Figure 5.5e. These results are summarized in Table 5.3 below.

Table 5.3: Summary of optimum polymer dosage predictions by method for three tested ROPEC digested sludge samples.

Digested sludge sample	**Optimum polymer dose measurement by method (g/kg DS)**				
	CST	Filtration	UV-Vis Spectroscopy	TTQ	Direction Injection
ROPEC 1	7.5 – 12.5	10.0	10.0	10.0	7.5
ROPEC 2	7.5	7.5	7.5	7.5	5.0 – 7.5
ROPEC 3	8.0 – 10.0	8.0	8.0	8.0	6.0

As can be seen in Table 5.3, the UV-Vis spectrophotometry method and the torque rheological methods were not only generally consistent with one another, they were also consistent with the established laboratory methods. That is to say that the optimum polymer dosages predicted by each of the methods were consistent with one another within one sludge sample. However, there were two exceptions to this overall consistency. Firstly, the

CST method was twice unable to identify a distinct optimum polymer dosage and instead provided an optimum dosage range. Secondly, the direct injection torque rheology method consistently predicted a lower optimum dosage than the consensus of the other tests. These inconsistencies were indications that these methods may be less reliable than the other methods tested here. These tests confirmed the reliability of a two-stage in-line and real-time process for polymer dose optimization using torque rheology (the TTQ method specifically) pre-dewatering and UV-Vis spectrophotometry (absorbance at $\lambda = 189.8$ nm) post-dewatering.

In-spite of all experimental variables being controlled apart from the date on which the sludge sample was collected, different optimum polymer dosages were predicted for every sludge sample. As the experiments above were conducted independently during different months with variable sludge characteristics, the optimum polymer dosages predicted by each were also variable. This was evidence that a real-time and in-line polymer dose optimization method is required to consistently achieve optimum dewaterability of the sludge.

5.3.2 The effect of polymer type

The second phase of dewatering optimization experiments undertaken was performed to assess the optimization methodology for usage with different polymer conditioners. For these tests, Zetag 8160, Flopolymer CA 4600, and Flopolymer CB 4350 were employed to independently condition digested sludge from ROPEC. These experiments were performed back-to-back on samples from the same sludge to minimize changes in the sludge

characteristics. The sludge has a total solids content of 1.88% with a standard deviation of 0.10%. The characteristics of these polymers were summarized in Table 5.1.

Figures 5.6, 5.7, and 5.8 below show the results of the dewatering optimization experiments conducted for the ROPEC sludge conditioned using the Zetag 8160, Flopolymer CA 4600, and Flopolymer CB 4650 polymers, respectively. Figures 5.6a, 5.7a, and 5.8a show the absorbance spectra of the samples tested. Figures 5.6b, 5.7b, and 5.7b show the rheograms of the TTQ rheological method. Figures 5.6c, 5.7c, and 5.8c show the rheograms of the direct injection rheological method. Figures 5.6d, 5.7d, and 5.8d show the results of the UV-Vis absorbance and laboratory methods tests. Figures 5.6e, 5.7e, and 5.8e show the results of the TTQ values of the TTQ rheological method and the peak heights of the direct injection rheological method.

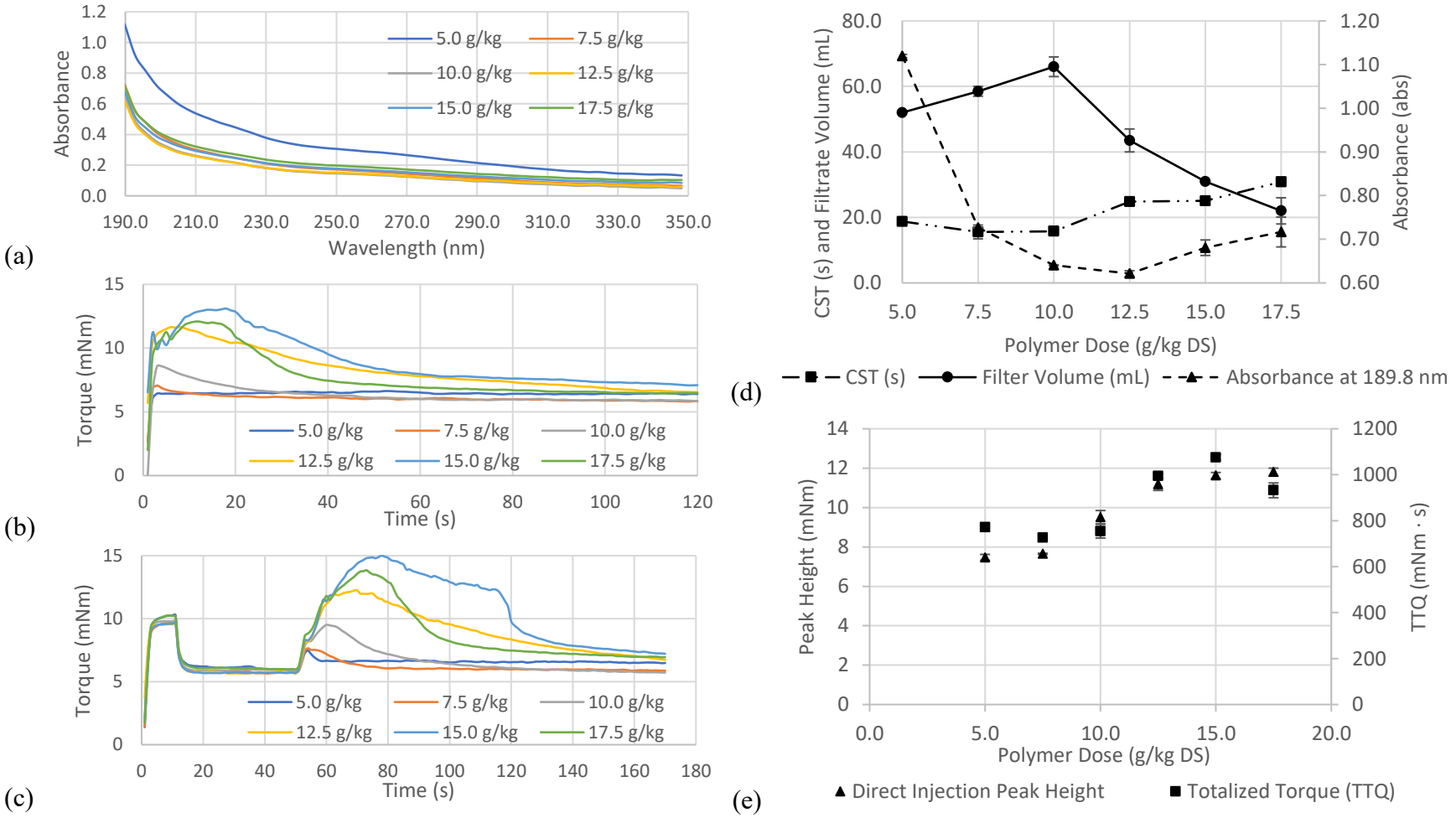

Figure 5.6: Results of dewatering optimization tests for ROPEC sludge conditioned using Zetag 8160 a) Absorbance spectra of sludge filtrate; b) Torque rheograms of TTQ rheological method; c) Torque rheograms of direct injection torque rheological method; d) Peak absorbance of filtrate samples at 189.8 nm and mean CST times and filtration test volumes; e) Direct injection peak heights and totalized torque values.

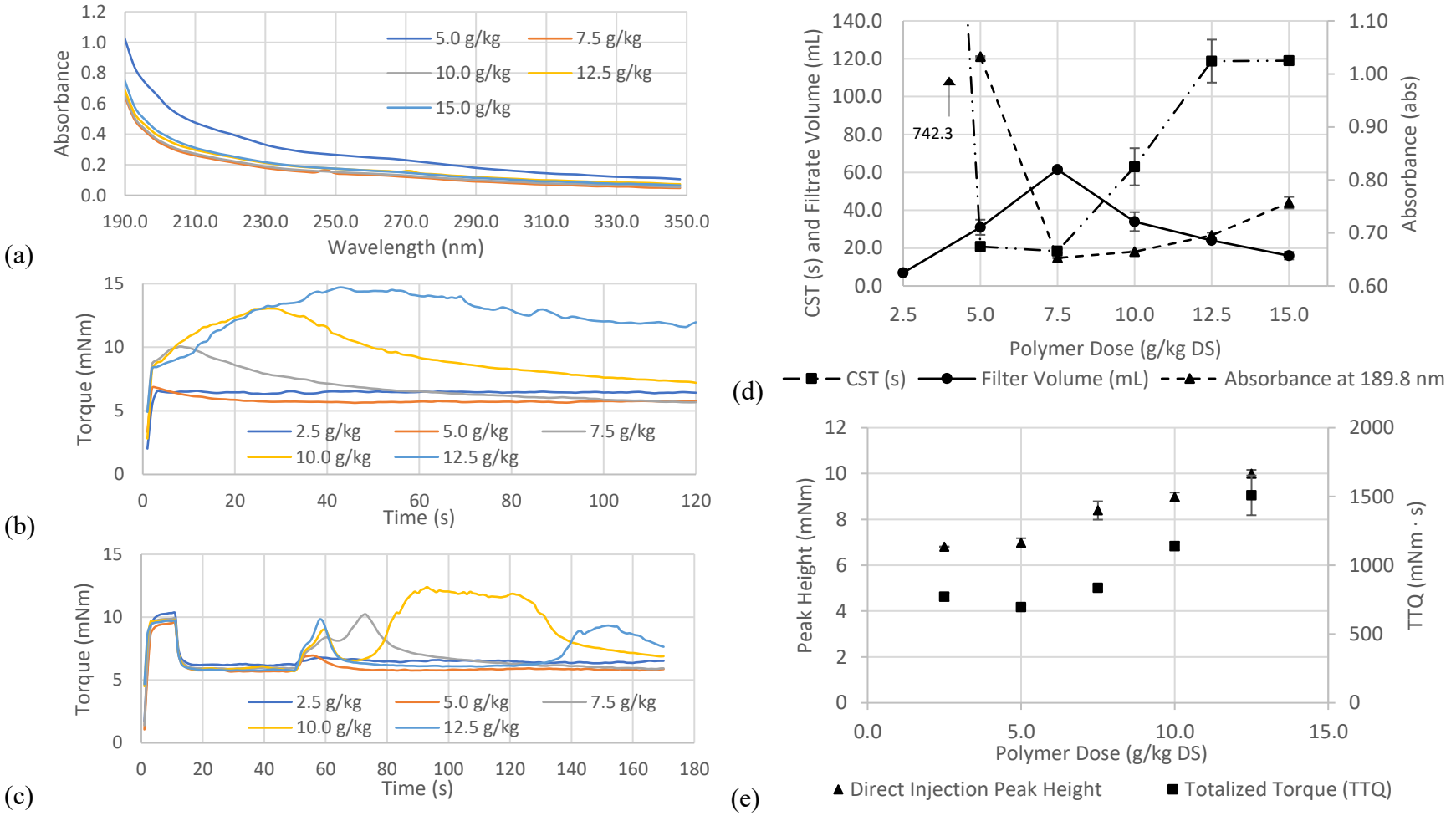

Figure 5.7: Results of dewatering optimization tests for ROPEC sludge conditioned using Flopolymer CA 4600 a) Absorbance spectra of sludge filtrate; b) Torque rheograms of TTQ rheological method; c) Torque rheograms of direct injection torque rheological method; d) Peak absorbance of filtrate samples at 189.8 nm and mean CST times and filtration test volumes; e) Direct injection peak heights and totalized torque values.

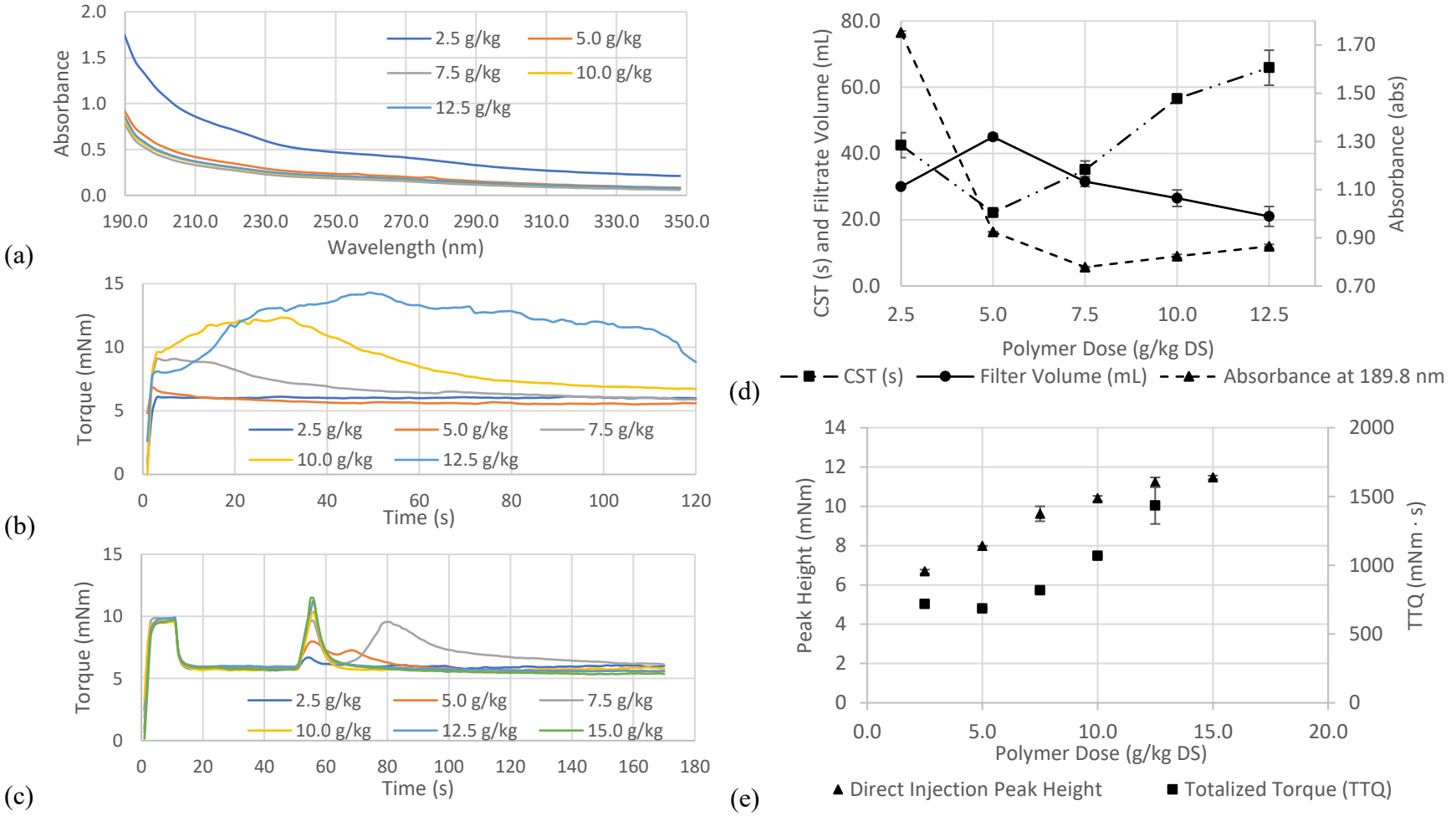

Figure 5.8: Results of dewatering optimization tests for ROPEC sludge conditioned using Flopolymer CB 4350 a) Absorbance spectra of sludge filtrate; b) Torque rheograms of TTQ rheological method; c) Torque rheograms of direct injection torque rheological method; d) Peak absorbance of filtrate samples at 189.8 nm and mean CST times and filtration test volumes; e) Direct injection peak heights and totalized torque values.

The peak absorbances in the spectra of all the samples tested were observed at a wavelength of 189.8 nm, as shown in Figures 5.6a, 5.7a, and 5.8a, with no significant absorbance observed above 240 nm.

For the sludge sample conditioned using Zetag 8160, the results of the UV-Vis method and the laboratory methods are shown in Figure 5.6d. A minimum absorbance value was observed at a polymer dosage of 12.5 g/kg DS, corresponding to the optimum dosage. The laboratory methods tested for comparison deviate slightly from this prediction. The maximum filtrate volume was obtained at a polymer dosage of 10.0 g/kg, while the minimum CST time was obtained in the dose range of 7.5 g/kg DS to 10.0 g/kg. The difference between these CST times was only 0.3 seconds, within the standard deviations of the tests for both dosages. The rheograms obtained using the TTQ method, shown in Figure 5.6b, showed that the 15.0 g/kg and 17.5 g/kg dosages were overdosed. This was indicated by the indistinct initial peaks and rough curves of the rheograms after the initial peak, compared with the smooth curves and distinct peaks of the rheograms for the other dosages. The optimum polymer dosage was thus observed at the maximum TTQ value prior to this overdose, at a dosage of 12.5 g/kg as shown in Figure 5.6e. The rheograms obtained using the direct injection method, shown in Figure 5.6c, showed that the 12.5 g/kg, 15.0 g/kg, and 17.5 g/kg dosages were overdosed. This was indicated by the rough curves in the rheograms after the initial peak, which were indicative of re-flocculation by excess polymer in solution. The optimum polymer dosage was thus at the maximum peak prior to this overdose, at a dosage of 10.0 g/kg as shown in Figure 5.6e. These results are summarized in Table 5.4 below.

For the sludge samples conditioned using Flopolymer CA 4600, the results of the UV-Vis method and the laboratory methods are shown in Figure 5.7d. A minimum absorbance value was observed at a polymer dosage of 7.5 g/kg DS, corresponding to the optimum dosage. The laboratory methods tested for comparison support this prediction. The maximum filtrate volume and minimum CST time were obtained at the same polymer dosage of 7.5 g/kg. The rheograms obtained using the TTQ method, shown in Figure 5.7b, showed that the 10.0 g/kg and 12.5 g/kg dosages were overdosed. This was indicated by the rough curves of the rheograms after the initial peak, compared with the smooth curves of the rheograms for the other dosages. The optimum polymer dosage was thus observed at the maximum TTQ value prior to this overdose, at a dosage of 7.5 g/kg as shown in Figure 5.7e. The rheograms obtained using the direct injection method, shown in Figure 5.7c, showed that the 10.0 g/kg and 12.5 g/kg dosages were overdosed. This was indicated by the large spikes in the rheograms after the initial peak, which were indicative of re-flocculation by excess polymer in solution. A small dip was also seen in the 7.5 g/kg dose rheogram after the initial peak, followed by a larger distinct peak. This was indicative that the 7.5 g/kg dose may be slightly overdosed, though not as visibly as in the rheograms of the higher dosages. The optimum polymer dosage was thus observed in the dose range of 5.0 g/kg to 7.5 g/kg. These results are summarized in Table 5.4 below.

For the sludge sample conditioned using Flopolymer CB 4350, the results of the UV-Vis method and the laboratory methods are shown in Figure 5.8d. A minimum absorbance value was observed at a polymer dosage of 7.5 g/kg DS, corresponding to the optimum dosage. The laboratory methods tested for comparison deviate slightly from this prediction. The maximum filtrate volume and minimum CST time were obtained at a polymer dosage

of 5.0 g/kg. The rheograms obtained using the TTQ method, shown in Figure 5.8b, showed that the 10.0 g/kg and 12.5 g/kg dosages were overdosed. This was indicated by the rough curves of the rheograms after the initial peak, compared with the smooth curves of the rheograms for the other dosages. The optimum polymer dosage was thus observed at the maximum TTQ value prior to this overdose, at a dosage of 7.5 g/kg as shown in Figure 5.8e. The rheograms obtained using the direct injection method, shown in Figure 5.8c, were less conclusive in their optimum dose measurement. A clear overdose curve was seen for the sample dosed at 7.5 g/kg, indicated by the large spike after the initial peak resulting from re-flocculation caused by excess polymer in solution. Based on this, the optimum polymer dosage was observed at the maximum peak prior to this overdose, at a dosage of 5.0 g/kg as shown in Figure 5.8e. However, at the higher doses of 10.0 g/kg, 12.5 g/kg, and 15.0 g/kg, the expected overdose curves were not present, replaced instead by distinct peaks. The result was a degree of uncertainty regarding the optimum polymer dosage measurement by this method. This can be seen as a limitation of the direct injection method. These results are summarized in Table 5.4 below.

Table 5.4: Summary of optimum polymer dosage predictions by method for a ROPEC digested sludge sample using three different polyacrylamide conditioners.

Polymer conditioner	**Optimum polymer dose measurement by method (g/kg DS)**				
	CST	Filtration	UV-Vis Spectroscopy	TTQ	Direction Injection
Zetag 8160	7.5 – 10.0	10.0	12.5	12.5	10.0
Flopolymer CA 4600	7.5	7.5	7.5	7.5	5.0 – 7.5
Flopolymer CB 4350	5.0	5.0	7.5	7.5	5.0*

*****_indicates a degree of uncertainty regarding optimum dose, see above explanation._

The first thing of note from these results was the consistency between the UV-Vis spectrophotometry and TTQ torque rheological methods. For each of the three polymer conditioners tested, both of these methods measured the same optimum polymer dose as the other. This provided evidence that a two-stage in-line polymer dose optimization system using the TTQ method pre-dewatering and the UV-Vis method post-dewatering would be consistent within itself.

It was also noteworthy that the direct injection torque rheology method predicted that the optimum dosage was lower than the UV-Vis and TTQ methods. This was consistent with what was found in the previous section. Based on this, it was observed that the direction injection method consistently undermeasured the optimum polymer dosage.

For the sludge samples conditioned using Zetag 8160 and Flopolymer CB 4350, the optimum polymer doses measured by the CST and filtration methods were also lower than those measured by the UV-Vis and TTQ methods. These laboratory methods measure and use the filterability of the conditioned sludge samples as a measure of their dewaterability. The lower optimum dosages measured were likely the result of the lower molecular weights of the Zetag 8160 and Flopolymer CB 4350 polymers. A higher molecular weight is known to enhance polymer bridging, and thus improve flocculation.

5.3.3 The effect of sludge type

The third phase of dewatering optimization experiments undertaken was performed to assess the optimization methodology for usage with different sludge types. For these tests, anaerobically digested sludge from ROPEC, anaerobically digested sludge from Gatineau WWTP, and aerobically digested sludge from Rockland WWTP were each individually

conditioned using the Flopolymer CA 4600 and Flopolymer CB 4350 polymers. The characteristics of these polymers were summarized in Table 5.1. A summary of the total solids content of the digested sludge samples is provided in Table 5.5 below.

Table 5.5: Summary of total solids content of digested sludge samples.

Digested Sludge Sample	Total Solids (TS)	Standard Deviation of TS
ROPEC	1.88%	0.10%
Gatineau	0.99%	0.03%
Rockland	1.12%	0.02%

As shown in Table 5.5, the TS content of the three sludge samples were highly varied, with the anaerobically digested Gatineau and the aerobically digested Rockland samples having much lower TS contents than the anaerobically digested ROPEC sample. This was most likely attributable to the different inflow conditions and treatment processes of the three facilities.

The results of the dewatering optimization experiments conducted for the anaerobically digested ROPEC sludge conditioned using Flopolymer CA 4600 and Flopolymer CB 4350 are discussed in the above Section 5.3.2 and shown in Figures 5.7 and 5.8, respectively. The results of these tests are summarized in Table 5.6.

Figures 5.9 and 5.10 below show the results of the dewatering experiments conducted for the anaerobically digested Gatineau sludge conditioned using the Flopolymer CA 4600 and Flopolymer CB 4650 polymers, respectively. Figures 5.9a and 5.10a show the absorbance spectra of the samples tested. Figures 5.9b and 5.10b show the rheograms of the TTQ rheological method. Figures 5.9c and 5.10c show the rheograms of the direct injection rheological method. Figures 5.9d and 5.10d show the results of the UV-Vis absorbance and

laboratory methods tests. Figures 5.9e and 5.10e show the results of the TTQ values of the TTQ rheological method and the peak heights of the direct injection rheological method.

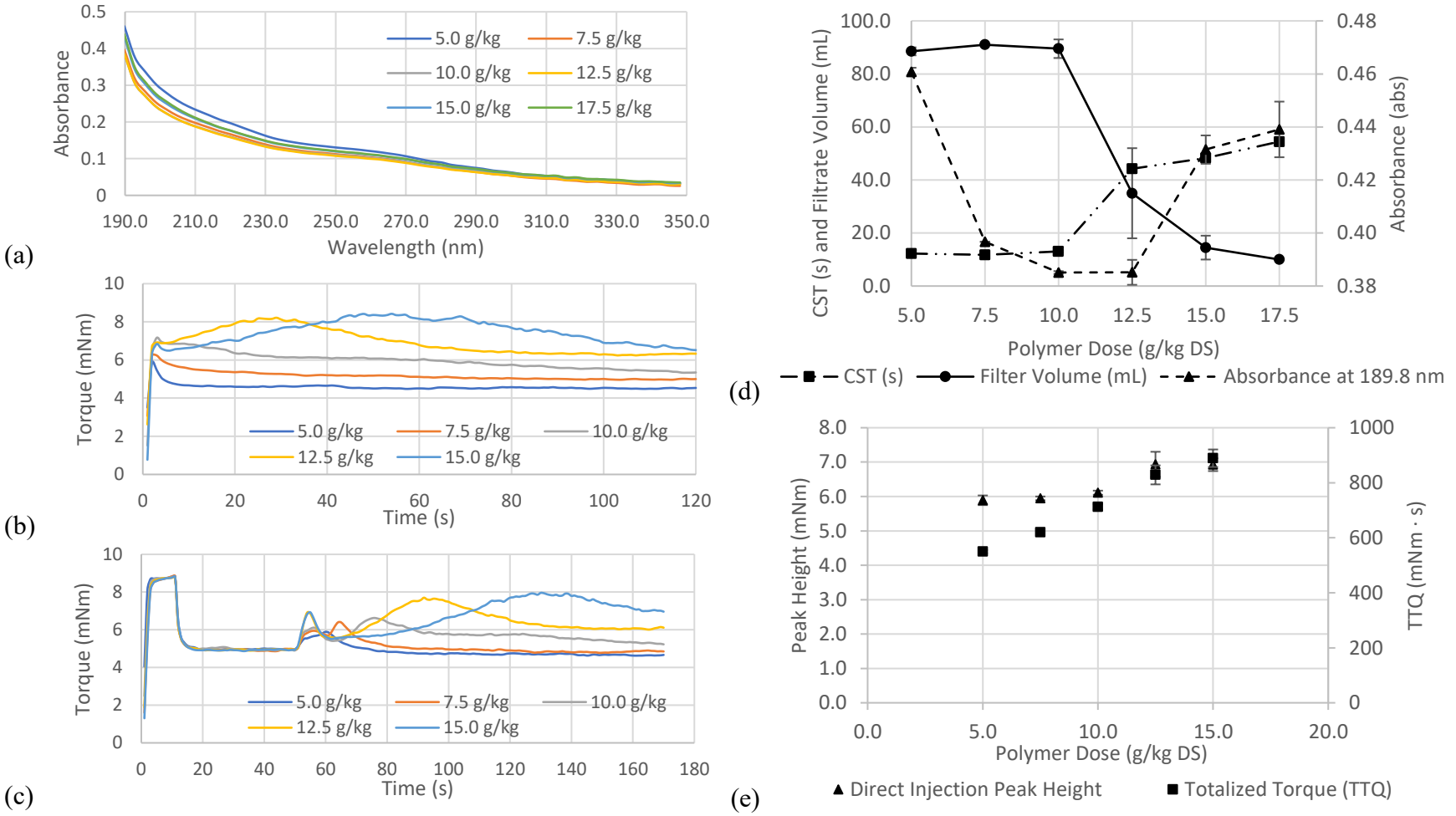

Figure 5.9: Results of dewatering optimization tests for Gatineau sludge conditioned using Flopolymer CA 4600 a) Absorbance spectra of sludge filtrate; b) Torque rheograms of TTQ rheological method; c) Torque rheograms of direct injection torque rheological method; d) Peak absorbance of filtrate samples at 189.8 nm and mean CST times and filtration test volumes; e) Direct injection peak heights and totalized torque values.

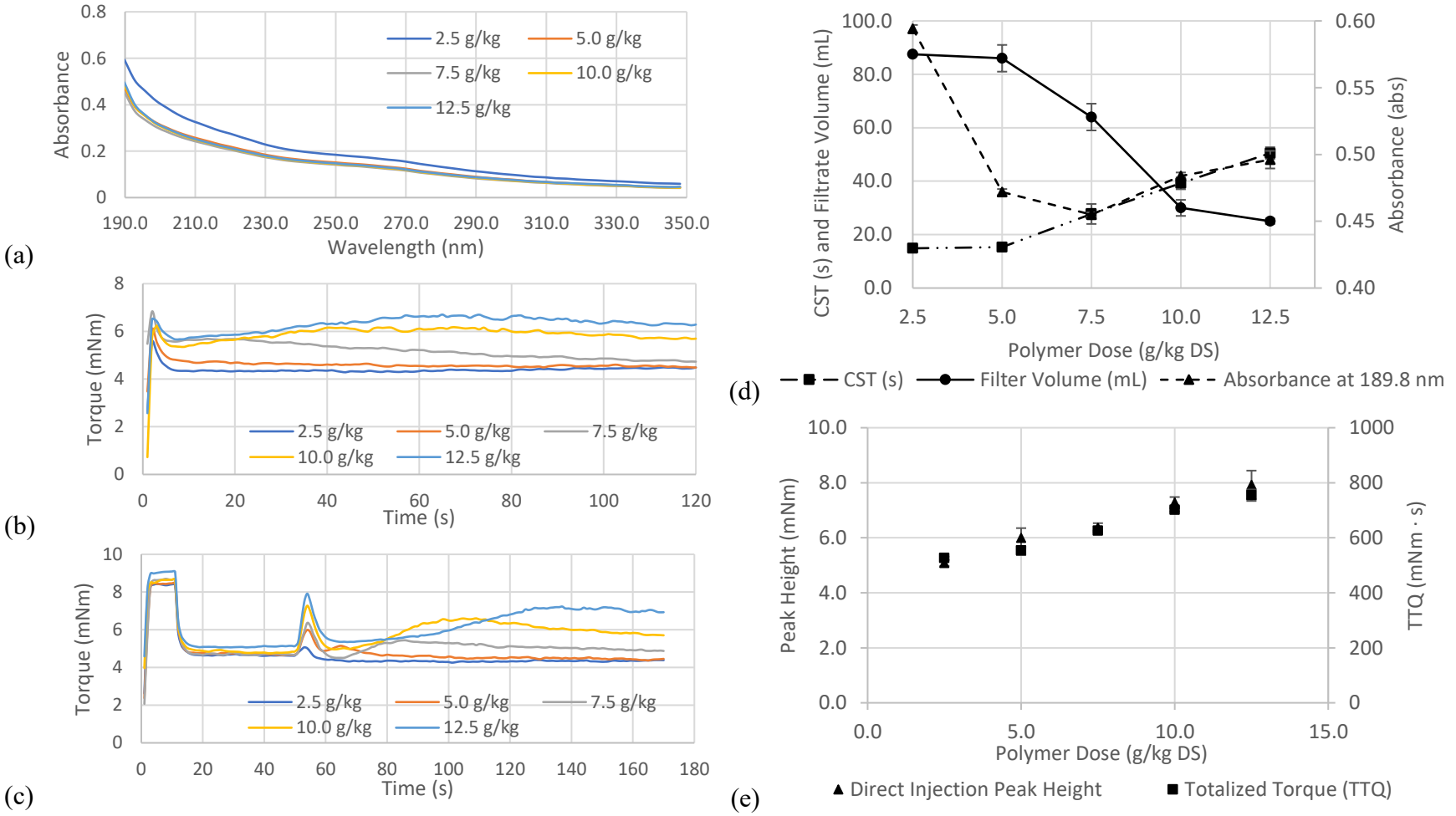

Figure 5.10: Results of dewatering optimization tests for Gatineau sludge conditioned using Flopolymer CB 4350 a) Absorbance spectra of sludge filtrate; b) Torque rheograms of TTQ rheological method; c) Torque rheograms of direct injection torque rheological method; d) Peak absorbance of filtrate samples at 189.8 nm and mean CST times and filtration test volumes; e) Direct injection peak heights and totalized torque values.

The peak absorbances in the spectra of the Gatineau samples tested were observed at a wavelength of 189.8 nm, as shown in Figures 5.9a and 5.10a, with no significant absorbance observed above 240 nm.

For the anaerobically digested Gatineau sludge sample conditioned using Flopolymer CA 4600, the results of the UV-Vis method and the laboratory methods are shown in Figure 5.9d. A minimum absorbance value of 0.385 was observed at polymer dosages of both 10.0 g/kg to 12.5 g/kg DS, corresponding to the optimum dose range. The laboratory methods tested did not produce the expected trends seen in the previous experiments above. Instead, a positive 'S' curve was seen for the CST test times, and a negative 'S' curve was seen for the filtration test volumes. These 'S' curves were centered on the optimum polymer dose range predicted by the UV-Vis method, but optimum dosages cannot be determined from the CST times and filtrate volumes due to the lack of minimum and maximum values, respectively. This was an indication of the limitations of these laboratory methods. The rheograms obtained using the TTQ method, shown in Figure 5.9b, showed that the 12.5 g/kg and 15.0 g/kg dosages were overdosed. This was indicated by the rough curves of the rheograms after the initial peak, compared with the smooth curves of the rheograms for the other dosages. The optimum polymer dosage was thus observed at the maximum TTQ value prior to this overdose, at a dosage of 10.0 g/kg as shown in Figure 5.9e. The rheograms obtained using the direct injection method, shown in Figure 5.9c, showed that the 10.0 g/kg, 12.5 g/kg, and 15.0 g/kg dosages were overdosed. This was indicated by the large spikes in the rheograms after the initial peak, which were indicative of re-flocculation by excess polymer in solution. A small dip was also seen in the 7.5 g/kg dose rheogram after the initial peak, followed by a larger distinct peak. This is indicative that the 7.5 g/kg

dose may be slightly overdosed, though not as visibly as in the rheograms of the higher dosages. The optimum polymer dosage was thus observed in the dose range of 5.0 g/kg to 7.5 g/kg. These results are summarized in Table 5.6 and further discussed below.

For the anaerobically digested Gatineau sludge sample conditioned using Flopolymer CB 4350, the results of the UV-Vis method and the laboratory methods are shown in Figure 5.10d. A minimum absorbance value was observed at polymer dosage of 7.5 g/kg DS, corresponding to the optimum dosage. The laboratory methods tested again did not produce the expected trends. Instead, a positive 'S' curve was seen for the CST test times, and a negative 'S' curve was seen for the filtration test volumes. These 'S' curves were centered on the optimum polymer dose range predicted by the UV-Vis method, but optimum dosages cannot be determined from the CST times and filtrate volumes due to the lack of minimum and maximum values, respectively. This was an indication of the limitations of these laboratory methods. The rheograms obtained using the TTQ method, shown in Figure 5.10b, showed that the 10.0 g/kg and 12.5 g/kg dosages were overdosed. This was indicated by the rough curves of the rheograms after the initial peak, compared with the smooth curves of the rheograms for the other dosages. The optimum polymer dosage was thus observed at the maximum TTQ value prior to this overdose, at a dosage of 7.5 g/kg as shown in Figure 5.10e. The rheograms obtained using the direct injection method, shown in Figure 5.10c, showed that the 7.5 g/kg, 10.0 g/kg, and 12.5 g/kg dosages were overdosed. This was indicated by the large spikes and rough curves in the rheograms after the initial peak, which were indicative of re-flocculation by excess polymer in solution. The optimum polymer dosage was thus observed at the maximum peak prior to this overdose, at a dosage

of 5.0 g/kg as shown in Figure 5.10e. These results are summarized in Table 5.6 and further discussed below.

Figures 5.11 and 5.12 below show the results of the dewatering experiments conducted for the aerobically digested Rockland sludge conditioned using the Flopolymer CA 4600 and Flopolymer CB 4650 polymers, respectively. Figures 5.11a and 5.12a show the absorbance spectra of the samples tested. Figures 5.11b and 5.12b show the rheograms of the TTQ rheological method. Figures 5.11c and 5.12c show the rheograms of the direct injection rheological method. Figures 5.11d and 5.12d show the results of the UV-Vis absorbance and laboratory methods tests. Figures 5.11e and 5.12e show the results of the TTQ values of the TTQ rheological method and the peak heights of the direct injection rheological method.

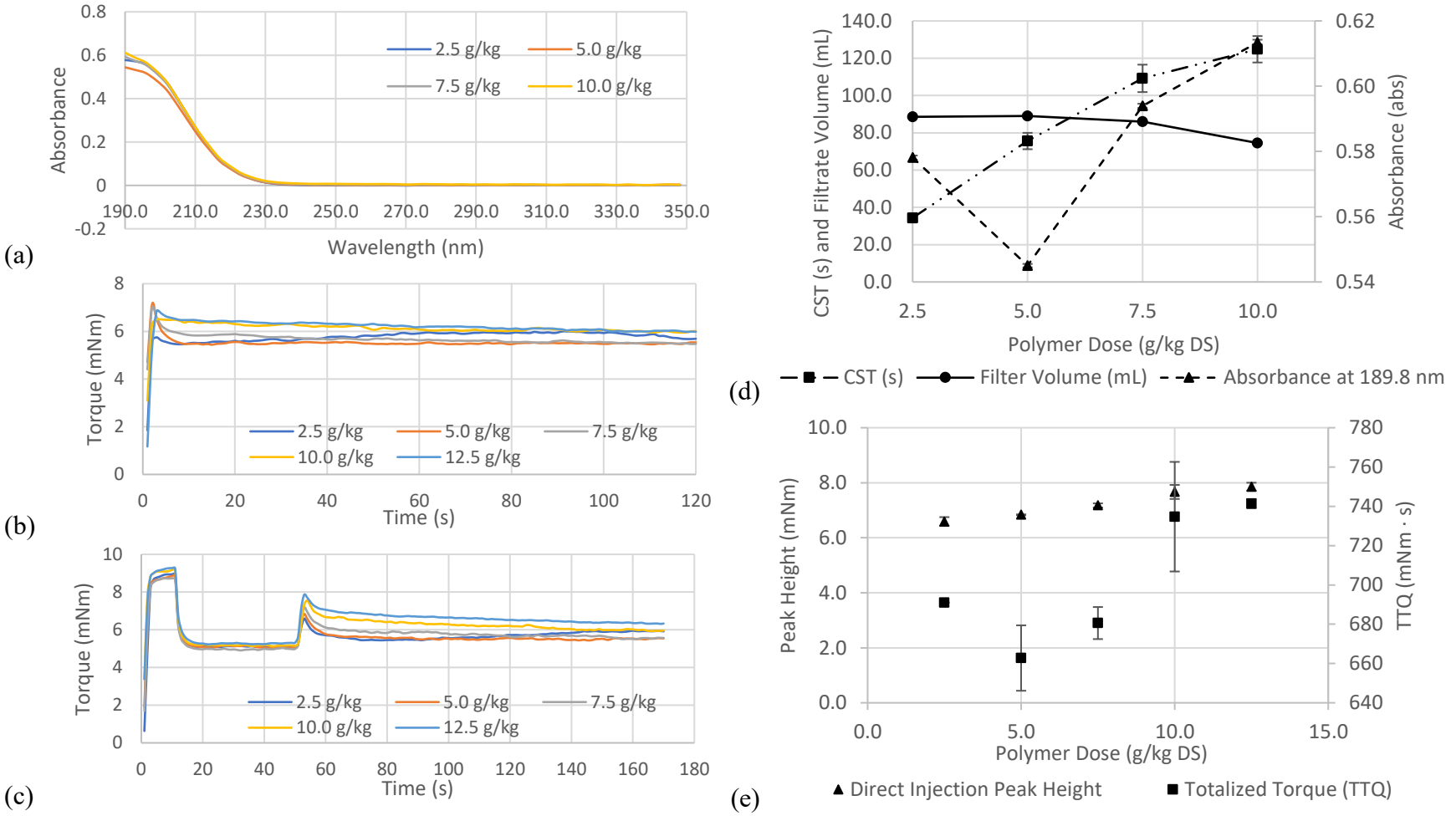

Figure 5.11: Results of dewatering optimization tests for Rockland sludge conditioned using Flopolymer CA 4600 a) Absorbance spectra of sludge filtrate; b) Torque rheograms of TTQ rheological method; c) Torque rheograms of direct injection torque rheological method; d) Peak absorbance of filtrate samples at 189.8 nm and mean CST times and filtration test volumes; e) Direct injection peak heights and totalized torque values.

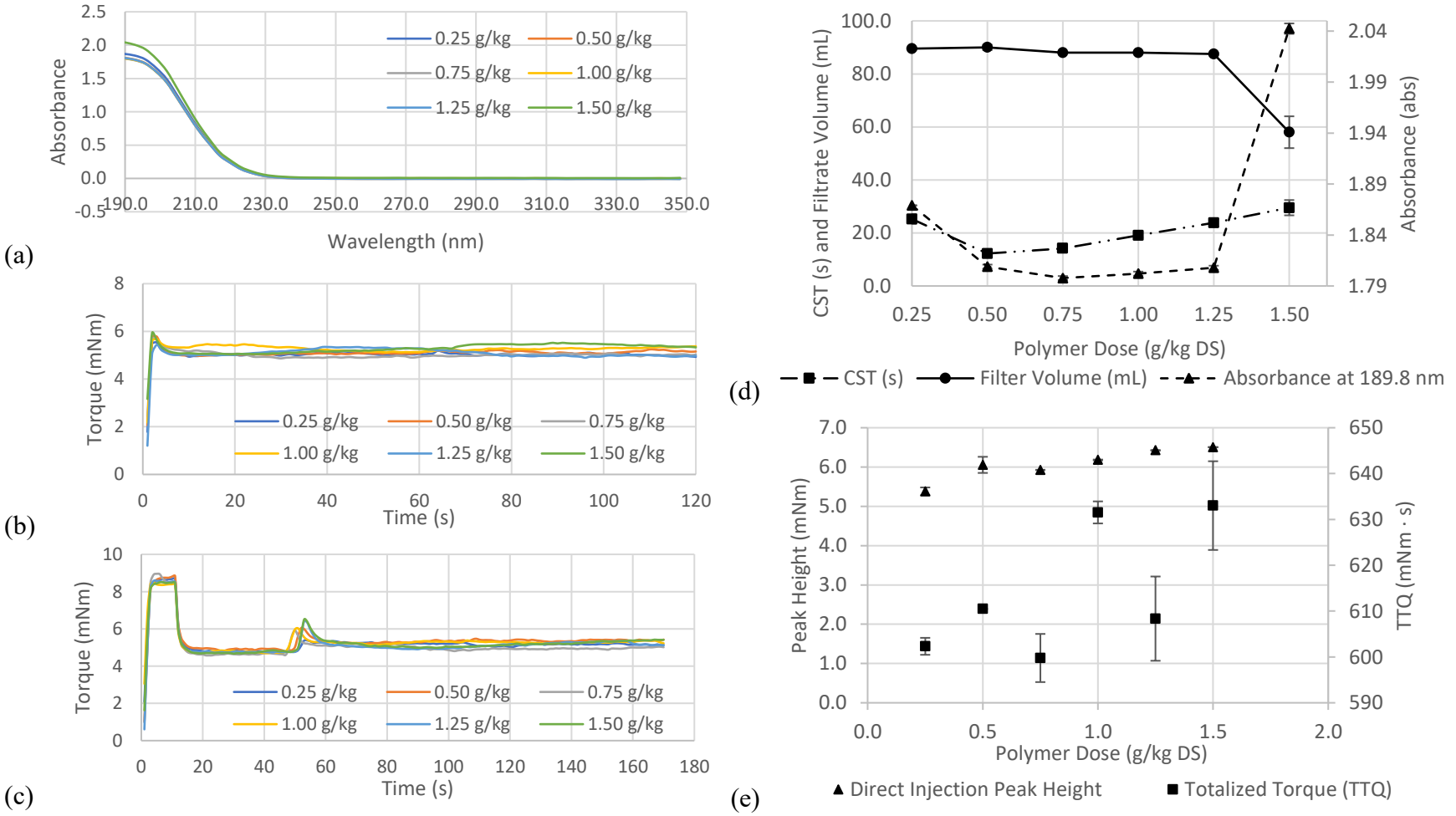

Figure 5.12: Results of dewatering optimization tests for Rockland sludge conditioned using Flopolymer CB 4350 a) Absorbance spectra of sludge filtrate; b) Torque rheograms of TTQ rheological method; c) Torque rheograms of direct injection torque rheological method; d) Peak absorbance of filtrate samples at 189.8 nm and mean CST times and filtration test volumes; e) Direct injection peak heights and totalized torque values.

The peak absorbances in the spectra of the Rockland samples tested were observed at a wavelength of 189.8 nm, as shown in Figures 5.11a and 5.12a, with no significant absorbance observed above 240 nm.

For the aerobically digested Rockland sludge sample conditioned using Flopolymer CA 4600, the results of the UV-Vis method and the laboratory methods are shown in Figure 5.11d. A minimum absorbance value was observed at polymer dosage of 5.0 g/kg DS, corresponding to the optimum dosage. The laboratory methods tested did not produce the expected trends. Instead, a positive trend was seen for the CST test times, and a negative trend was seen for the filtration test volumes. Optimum polymer dosages could not be determined from the CST times and filtrate volumes due to the lack of minimum and maximum values, respectively. This was an indication of the limitations of these laboratory methods. The rheograms obtained using the TTQ method, shown in Figure 5.11b, and the corresponding TTQ values, shown in Figure 5.11e, do not show any overdose curves or distinct maximum TTQ value. Accordingly, an optimum polymer dose cannot be determined here using this method. Likewise, the rheograms obtained using the direct injection method, shown in Figure 5.11c, and the peak values, shown in Figure 5.11e, also do not show any overdose curves or distinct maximum peak value. An optimum polymer dosage could therefore not be determined using the direct injection method. These were indications of the limitations of the torque rheological methods. These results are summarized in Table 5.6 and further discussed below.

For the aerobically digested Rockland sludge sample conditioned using Flopolymer CB 4350, the results of the UV-Vis method and the laboratory methods are shown in Figure 5.12d. It should be noted that the optimum dosages measured for this polymer in Rockland

sludge were an order of magnitude lower than those for the other polymer in Rockland sludge. The reason for this was unknown but was likely a result of the characteristics of the Flopolymer CB 4350 polymer. A minimum absorbance value was observed at polymer dosage of 0.75 g/kg DS, corresponding to the optimum dosage. The results of the CST test deviate slightly from this, as a minimum CST value was observed at a polymer dosage of 0.50 g/kg. However, an optimum polymer dosage could not be determined from the filtrate volumes due to the lack of a maximum value. This was an indication of the limitations of the filtration test. The rheograms obtained using the TTQ method, shown in Figure 5.12b, and the corresponding TTQ values, shown in Figure 5.12e, do not show any overdose curves or distinct maximum TTQ value. Accordingly, an optimum polymer dose cannot be determined here using this method. Likewise, the rheograms obtained using the direct injection method, shown in Figure 5.12c, and the peak values, shown in Figure 5.12e, also do not show any overdose curves or distinct maximum peak value. An optimum polymer dosage could therefore not be determined using the direct injection method. These were indications of the limitations of the torque rheological methods. These results are summarized in Table 5.6 and further discussed below.

Table 5.6: Summary of optimum polymer dosage predictions by method for a varying digested sludge samples using two different polyacrylamide conditioners.

Sludge sample	Polymer conditioner	Optimum polymer dose measurement by method (g/kg DS)				
		CST	Filtration	UV-Vis Spectroscopy	TTQ	Direction Injection
ROPEC	CA 4600	7.5	7.5	7.5	7.5	5.0 – 7.5
	CB 4350	5.0	5.0	7.5	7.5	5.0*
Gatineau	CA 4600	N/I**	N/I	10.0 – 12.5	10.0	5.0 – 7.5
	CB 4350	N/I	N/I	7.5	7.5	5.0
Rockland	CA 4600	N/I	N/I	5.0	N/I	N/I
	CB 4350	0.50	N/I	0.75	N/I	N/I

**indicates a degree of uncertainty regarding optimum dose, see above explanation.*
***N/I (Non-identifiable)*

As discussed in the previous section, the polymer dose optimization tests for the sludge samples from ROPEC conditioned with Flopolymer CA 4600 and Flopolymer CB 4350 showed that the TTQ rheological and UV-Vis spectrophotometry methods were consistent with one another. The laboratory tests using the CA 4600 polymer were consistent with the TTQ rheological and UV-Vis spectrophotometry methods. The laboratory tests using the CB 4350 polymer predicted lower optimum dosages than the UV-Vis spectrophotometry and TTQ rheological methods, but this was an effect of the lower molecular weight of the Flopolymer CB 4350 polymer. Furthermore, it was previously established that the direct injection torque rheological method consistently predicted a lower optimum polymer dose than the other methods (see previous discussions with regards to the ROPEC and Gatineau WWTP sludges).

Like the ROPEC sludge, the Gatineau sludge used for the dewatering optimization tests was anaerobically digested. However, as shown in Table 5.5 above, the Gatineau sludge sample had a much lower TS content than the ROPEC sludge, 0.99% compared with

1.88%, respectively. As a result of this low TS content, the overall filterability of the unconditioned Gatineau sludge was much higher than that of the ROPEC sludge. This can explain the 'S' curves seen in the CST and filtration test data in Figures 5.9d and 5.10d above. The CST and filtration tests measure and use the filterability of the conditioned sludge samples as a measure of their dewaterability. In the Gatineau sludge with a low TS content, the lower-than-optimum polymer dosed samples already had high filterability due to low TS content. This caused the initial low CST and high filtration volumes observed, respectively. At higher polymer dosages, however, the filterability of the samples was reduced, and as expected the CST increased and the filtration volumes decreased accordingly. This resulted in the 'S' curves seen in Figures 5.9d and 5.10d, and as such, an optimum polymer dosage could not reliably be determined for the Gatineau sludge using the laboratory methods tested here.

The in-line UV-Vis spectrophotometry and torque rheological methods were still able to determine an optimum polymer dosage for the Gatineau sludge despite its low TS content. Furthermore, as was the case for the ROPEC sludge samples, the UV-Vis spectrophotometry and the TTQ rheological methods were consistent with one another in optimum polymer dose measurements. The direct injection torque rheological method accordingly predicted a lower optimum polymer dosage. This was all consistent with the findings of the polymer dose optimization tests discussed in previous sections.

Compared with the anaerobically digested sludge from ROPEC and Gatineau, the Rockland sludge used for the dewatering optimization tests was aerobically digested. Aerobically digested sludge generally has poor mechanical dewatering characteristics compared with anaerobically digested sludge. Furthermore, the Rockland sludge samples

had a low TS content compared with that of the ROPEC sludge, 1.12% compared with 1.88%. A combination of these effects result in the lack of distinct minima and maxima in the CST and filtration volume values seen in Figures 5.11d and 5.12d. The exception to this is the CST test for the Rockland sludge conditioned using Flopolymer CB 4350, where an optimum polymer dosage of 0.50 g/kg was predicted by a minimum CST value. Overall, however, the CST and filtration tests were found to be limited in their usefulness for prediction of optimum polymer dose in the Rockland sludge, similarly to as they were for the Gatineau sludge.

For the Rockland sludge, the torque rheological methods were consistently unable to determine an optimum polymer dosage. This was most likely attributable to the Rockland sludge being aerobically digested. The torque rheological methods were able to determine optimum polymer dosages for both of the anaerobically digested sludge samples, ROPEC and Gatineau. The reason that the torque rheological methods could not measure an optimum polymer dose in the aerobically digested sludge sample was likely due to the physical properties of the aerobically digested sludge. Aerobic digestion processes are based on the activated sludge process often employed as a secondary treatment process at wastewater treatment facilities. These processes, and thus aerobic digestion as well, result in a product sludge with a flocculant appearance. These natural flocs in the sludge are both weak under shear and interfere with the uniformity of polymer floc formation, leading to inconsistent torque readings using the rheometer. The conclusion from this was that torque rheological methods were determined not to be useful for polymer dose optimization in aerobically digested sludges.

The UV-Vis spectrophotometry method, however, was still able to measure optimum polymer doses in the Rockland sludge. This was evidence of the reliability of this method in non-optimal conditions where every other method did not function. It also showed that a two-stage in-line and real-time polymer dose optimization method is beneficial where one system may operate sub-optimally. For example, if the pre-dewatering torque rheological method became incapable of determining an optimum polymer dose, the post-dewatering UV-Vis spectrophotometry method would still be able to provide a measurement, adding a layer of redundancy to the system.

5.4 Conclusion

The objective of this study was to investigate the feasibility of a two-stage feed-forward and feed-back control system using torque rheology and UV-Vis spectrophotometry for polymer dose optimization in sludge dewatering processes using lab-scale experiments.

The TTQ rheological method and the UV-Vis spectrophotometry method were found to consistently measure the same optimum polymer dosage as one another in all anaerobically digested sludge samples. This internal consistency provided evidence that the two methods could work in tandem in a two-stage polymer dose optimization system.

These methods were also found to be consistent with the established laboratory methods (CST and filtration test) conducted for comparison for some sludges and polymers. The direct injection torque rheological method was found to consistently predict lower optimum polymer doses than the other methods tested.

The experiments found that the established laboratory tests, which are based on the filterability of the sludge, were incapable of determining an optimum polymer dose for

sludge samples with a low TS content. Further, it was found that the torque rheological methods were incapable of determining an optimum polymer dose for the aerobic sludge samples. This was attributed to the natural flocculant appearance of the aerobically digested sludge rendering rheological measurements inconsistent.

The results of this study showed that a two-stage in-line and real-time polymer dose optimization system using the TTQ rheological method pre-dewatering and UV-Vis spectrophotometry post-dewatering provided both reliable and internally consistent optimum polymer dose measurements under most conditions. It was also shown that this system provided a level of redundancy where if one monitor was unable to determine an optimum dosage, the other would still be able to provide the measurement.

Chapter 6 – Nutrient recovery optimization in sludge side-streams using a real-time ultraviolet/visible spectrophotometry system

Abstract

Nutrient recovery from wastewater treatment processes is rapidly becoming a larger concern around the world both in order to minimize eutrophication potential in receiving bodies and due to diminishing global phosphorus supply. Side-streams generated by sludge thickening and dewatering processes at wastewater treatment facilities are good locations for nutrient recovery processes due to their relatively low flowrates and high nutrient concentrations. Struvite ($MgNH_4PO_4 \cdot 6H_2O$) formation and precipitation is a commonly used nutrient recovery process due to its simplicity and reliability. Magnesium is usually the limiting component for struvite formation in wastewaters and is thus added to facilitate its formation. Maintaining an optimum magnesium dosage is desirable for these processes as underdosing will not achieve optimal recovery of the nutrients, while overdosing of magnesium is not cost-effective, could be detrimental to downstream wastewater treatment processes, and may result in particle restabilization. A method for real-time monitoring of struvite formation indirectly through measuring nitrate concentration using UV-Vis spectrophotometry was developed. The method was tested through struvite formation experiments in both laboratory sludge filtrate and full-scale sludge centrate samples. In both media, the UV-Vis spectrophotometric method was able to reliably and accurately determine an optimum magnesium dosage for struvite formation.

Keywords: Ultraviolet/visible spectrophotometry, sludge supernatant, struvite, nutrient recovery, real-time monitoring, side-stream.

6.1 Introduction

Sludge thickening and dewatering processes produce solid and liquid product side-streams. These liquid side-streams are often simply returned to the headworks of most wastewater treatment facilities. Alternatively, some facilities perform additional treatment on these side-streams prior to returning them to the headworks. Side-streams can have relatively high suspended solids (SS), biochemical oxygen demand (BOD), total Kjeldahl nitrogen (TKN), ammonium (NH_4), nitrogen oxide (NO_x), and phosphorus (P) concentrations compared with the influent wastewater. As a result, and due to their relatively low flows, side-streams provide tempting points for treatment processes which target these components.

One of the most common types of treatment processes for side-streams is nutrient recovery. These processes are performed with the goal of removing either or both phosphorus and ammonia in a recoverable form, usually for reuse as a fertilizer or in industrial applications (Fattah *et al.*, 2008; Tchobanoglous *et al.*, 2014; Vaneeckhaute *et al*., 2018). This is desirable as phosphorus demand is expected to outstrip supply by the year 2035 (Cordell *et al*., 2009). Furthermore, removal of nutrients is often required by discharge regulations in order to minimize the potential for eutrophication of receiving water bodies (Abel-Denee *et al.*, 2018; Doyle and Parsons, 2002; Korchef *et al*., 2011). Performing nutrient recovery in side-stream processes aids this in reducing the nutrient loading to the wastewater treatment facility.

Struvite ($MgNH_4PO_4 \bullet 6H_2O$) precipitation is an excellent and often employed method for nutrient recovery in side-streams at wastewater treatment facilities (Tchobanoglous *et al.*, 2014). This is due in part to the simplicity and cost-effectiveness of the process, as well as

that struvite can be used as a fertilizer and in certain industrial applications (Fattah *et al.*, 2008; Tchobanoglous *et al.*, 2014; Vaneeckhaute *et al*., 2018). Struvite contains both nitrogen in the form of ammonium and phosphorus in the form of phosphate, and therefore its recovery removes both of these nutrients from the side-stream. In wastewaters, magnesium is generally the limiting component for struvite formation (Abel-Denee *et al.*, 2018; Doyle and Parsons, 2002; Fattah *et al.*, 2008; Jaffer *et al*., 2002). Accordingly, it is generally added to wastewater side-stream processes for struvite formation and precipitation (Doyle *et al*., 2000; Fattah *et al*., 2008). Struvite formation processes are highly dependent upon the pH of the wastewater, the turbulence of the mixing process, and the Mg:P ratio (Doyle *et al*., 2000; Fattah *et al*., 2008; Ohlinger *et al*., 1999).

Real-time and in-line monitoring has the potential for cost savings and improved process efficiency for nutrient recovery processes utilizing struvite formation and precipitation. Through achieving an optimum dosage of magnesium, excess chemical is not wasted, reducing cost. Additionally, an overdose of magnesium may be detrimental to downstream wastewater treatment processes (Fattah *et al*., 2008) and may result in particle restabilization. Particle restabilization is the phenomenon whereby an overdose of a cationic conditioning chemical has occurred. This causes sufficient conditioner to be adsorbed onto the surfaces of the anionic organic particles in solution to give them net positive charges, thus preventing their coagulation through charge neutralization (Bolto and Gregory, 2007).

Ultraviolet/visible (UV-Vis) spectrophotometry is a simple and reliable method for real-time monitoring of sludge treatment processes (Al Momani and Örmeci, 2014b). Ideally, a real-time and in-line UV-Vis spectrophotometric monitoring system does not rely on the

use of any reagents and can simply relay useful information based on normal measurements and minimal human interaction. For monitoring struvite formation, ideally the limiting component would be measured in order to directly measure when it has been fully consumed. As magnesium is being added to facilitate struvite formation, this makes phosphorus, or more specifically phosphate, the limiting component in most wastewaters. However, neither phosphorus nor phosphate can be measured in water using UV-Vis spectrophotometry without the use of chemical reagents prior to measurement. This leaves one other component of struvite as a potential monitor, nitrogen in the form of ammonium. Hypothetically, as struvite formation begins, ammonium concentration will begin to decrease. This continues until the limiting component is depleted, whereupon ammonium concentration will reach an equilibrium and become approximately constant. Through monitoring for this point, an optimum magnesium dose can be achieved, and thus optimum struvite formation. However, ammonium is not directly detectable using UV-Vis spectrophotometry either.

The UV-Vis spectrophotometric method developed in this study centred on the detection of nitrate, which has a peak absorbance at a wavelength of 224 nm (Ferree and Shannon, 2001). The developed methodology was based on the oxidation of the ammonium in a given sample to nitrate, and then the subsequent absorbance measurement thereof. As ammonium becomes bound in struvite crystals through magnesium addition, less of it would theoretically be oxidized to nitrate, thereby reducing the absorbance of the sample in question. This decrease would theoretically continue until the maximum struvite formation was reached, after which the change in oxidized ammonium would stop, and the absorbance would reach a minimum value.

The goal of this study was to develop a methodology by which struvite formation could be effectively monitored in real-time on a side-stream treatment train by using UV-Vis spectrophotometry to measure nitrate concentration. Maintaining an optimum magnesium dosage is desirable for these processes as underdosing will not achieve optimal recovery of the nutrients, while overdosing of magnesium is not cost-effective, could be detrimental to downstream wastewater treatment processes (Fattah *et al*., 2008), and result in particle restabilization. The first phase of this study developed calibration curves for nitrate dissolved in deionized water. Following this, struvite formation experiments were undertaken in laboratory sludge filtrate and in sludge centrate obtained from full-scale bowl centrifuges. Maintaining an optimum magnesium dosage is desirable for these processes as underdosing will not achieve optimal recovery of the nutrients, while overdosing of magnesium is not cost-effective, could be detrimental to downstream wastewater treatment processes as a result of increased alkalinity, and may result in particle restabilization.

6.2 Materials and Methods

The experiments for this study were conducted to develop a method for optimization of magnesium dosage for struvite formation and precipitation in wastewater side-stream processes. This dosage optimization was determined indirectly through the measurement of nitrate using UV-Vis spectrophotometry.

6.2.1 Sodium nitrate dosed in deionized water

A stock solution of sodium nitrate ($NaNO_3$) was prepared through dissolving 1,000 mg $NaNO_3$ into 1 L of deionized (DI) water (Direct-Q UV Water Purification System,

Millipore Sigma, USA). The dosed solution was mixed at 200 rpm for 3 minutes using a Phipps and Bird PB-700 Jar-tester (Richmond, VA). This mixing rate and time were found to be sufficient to fully dissolve the anhydrous sodium nitrate powder in the DI water.

The concentration series used to produce the calibration curves were prepared in 250 mL samples of DI water. Sodium nitrate was dosed from the stock solution into the 250 mL DI water samples via pipette to the desired concentrations. The dosed sample was then mixed at 200 rpm for 2 minutes using a Phipps and Bird PB-700 Jar-tester. Each sample was then individually passed through an in-line UV-Vis spectrophotometer and their spectra were measured.

6.2.2 Sludge and sludge centrate samples

Anaerobically digested sludge samples were collected from the Robert O. Pickard Environmental Centre (ROPEC) (located in Ottawa, Ontario). This sludge was used to prepare sludge filtrate for use in struvite formation experiments described below.

Anaerobically digested sludge centrate samples were also collected from ROPEC. These samples were collected from the effluent of the bowl centrifuges operated by the facility.

6.2.3 Sludge filtrate samples

An optimum polymer dosage for the anaerobically digested sludge samples were determined using an in-line UV-Vis spectrophotometer (Real Spectrum PL Series, Real Tech Inc., Ontario, Canada). This was completed through measuring the absorbance spectra of the supernatant of a series of sludge samples conditioned with increasing polymer dosages. As described by Al Momani and Örmeci (2014b), the optimum polymer

dosage corresponded to the sludge supernatant sample with the lowest absorbance value at a wavelength of $\lambda = 190$ nm.

Sludge samples were then conditioned using Flopolymer CA 4600 (manufactured by SNF Canada) at the optimum dosage using a Phipps and Bird PB-700 Jar-tester. The sludge sample to be conditioned was placed in a 500 mL beaker and placed in the jar-tester with the paddle lowered. The polymer dose was then injected via pipette into the sludge sample, which was then mixed at 300 rpm for 30 seconds. This high mixing speed ensured polymer flocculation by being well mixed while the low mixing time reduced shear stress on the sludge, minimizing the effect of the thixotropic nature of the sludge.

The conditioned sludge samples were filtered through a Whatman No. 2 filter with a pore size of 8 μm (Whatman, UK). The samples were placed in a Buchner funnel which was placed above a 250 mL graduated cylinder with vacuum port. A constant vacuum pressure of 20 in. Hg was applied using a vacuum pump (Welch, USA), and the filtrate was collected in a common beaker. This process was repeated until 1 L of filtrate was collected for use in experiments.

6.2.4 Magnesium dosing and struvite formation in sludge filtrate and centrate

Struvite formation in the sludge filtrate and centrate samples was facilitated by the addition of magnesium. Magnesium sulfate ($MgSO_4$) was dosed incrementally into common samples of the sludge filtrate and centrate, each with initial volumes of 1 L. Following each addition of $MgSO_4$, the samples were mixed at 300 rpm for 1 minute using a Phipps and Bird PB-700 Jar-tester. This constant mixing rate and time also ensured that the mixing

turbulence applied to the dosed samples was kept constant so as to minimize the effect from that parameter in struvite formation. Between each addition of $MgSO_4$, the samples were mixed continuously at 100 rpm using the jar tester to ensure that the solutions remained mixed and homogenous.

After each dosing and mixing period, 50 mL samples of the filtrate or centrate were taken for analysis. Prior to analysis, these samples were aerated for 1 minute using an air diffuser in order to oxidize the ammonium in solution. Preliminary tests found this time and method to be sufficient for ammonium oxidation and reliable measurement using the UV-Vis spectrophotometry method outlined below.

6.2.5 Ultraviolet/visible spectrophotometry

For all UV-Vis spectrophotometry measurements in this study, an in-line UV-Vis spectrophotometer instrument (Real Spectrum PL Series, Real Tech Inc., Ontario, Canada) was employed. All spectrophotometry measurements of samples were performed in triplicates using a 4 mm path length flow cell. Due to the range of the instrument and the nature of the media, the sludge filtrate and centrate samples were diluted by a factor of 1:25 prior to the measurement of their spectra. The peak absorbance of NO_x species has been reported to be observed at a wavelength of $\lambda = 224$ nm (Ferree and Shannon, 2001). During measurement, samples were continuously mixed using a stirring rod to prevent settling of solid particles.

6.2.6 Turbidity

For all samples of sludge filtrate and centrate in this study, turbidity measurements were performed. Turbidity was measured using a HACH 2100AN Turbidimeter (Hach Company, Colorado, USA). The turbidimeter was calibrated using standard turbidity calibration samples as per the procedure described by the manufacturer. Individual 30 mL samples after each $MgSO_4$ dosage were individually poured into the same sample vial and placed in the turbidimeter. These 30 mL samples were returned to the 50 mL grab sample taken and mixed. This process was repeated two additional times to obtain triplicate turbidity values which were then averaged.

In this study, turbidity was an additional measurement method to support the results obtained from the UV-Vis spectrophotometry, particle counter, and microscopy methods. Struvite crystals scatter light, increasing turbidity, up until the point that increased magnesium dosage does not result in any additional struvite formation. Thus, achieving a constant and steady turbidity value would hypothetically correspond to an optimum magnesium dosage as struvite formation would have more or less halted at such a point. There are many factors which can impact the turbidity values of the samples, however, and it is for this reason that turbidity is simply a supportive measurement in this study.

6.2.7 Particle counter

Sludge centrate and filtrate samples were analyzed using a particle counter (Dynamic Particle Analyzer DPA 4100, Brightwell Technologies Inc., Ontario, Canada). This particle counter functions by drawing a sample out of a reservoir placed above an optical detector.

The sample fluid is passed through a flow cell where it is optically analyzed by the instrument.

A 10 mL sample reservoir was filled with the sample to be analyzed and a stir screw was placed in the reservoir to ensure that the sample remained homogenous during testing. The sample was then pumped at a rate of 0.22 mL/min for 2 minutes through a 400 μm flow cell. The instrument then measured the particle size distribution and the concentration of particles greater than the detection limit of the instrument. The detection limit was a particle diameter of 2.00 μm, and the bin size for the particle size distribution was 0.25 μm. This means that the smallest bin size for the particle size distribution contained particles between the sizes of 2.00 μm to 2.25 μm. This test was repeated and performed in duplicates for all samples.

6.2.8 Microscopy

Visual confirmation of struvite formation for all samples was achieved through the use of microscopy. In this study, a Nikon Eclipse Ti (Nikon, Quebec, Canada) inverted microscope was employed for this purpose. For each analysis, a 10 μL sample was placed on a 25 x 75 x 1 mm microscope slide, and a 22 x 22 mm No. 1.5 glass cover was placed on top. The prepared slide was placed on the microscope stage. Each sample was focused at the magnification in use, and multiple fields of view were analyzed to get a sense of the visual makeup of the sample. Once this was achieved, photos of the sample were taken as a record.

6.2.8.1 Microscopic semi-quantitative analysis

A semi-quantitative analysis of the struvite crystal distribution and concentration was performed using the microscopy technique described above. This semi-quantitative analysis observed a number of microscopic fields of view and determined an average number of struvite crystals per field of view in the sample. The value of thirteen fields of view was determined to be sufficient for this purpose. This was determined through trial and error, and it was found that this number of fields of view determined internally consistent values for the samples examined.

6.3 Results and Discussion

6.3.1 Nitrate absorbance calibration curves

As noted previously, it has been reported that nitrate has a peak absorbance at a wavelength of $\lambda = 224$ nm (Ferree and Shannon, 2001). The spectra of deionized water samples dosed with sodium nitrate were measured using the 4 mm path length flow cell in the in-line UV-Vis spectrophotometer. Sodium nitrate was dosed to concentrations of 1.0, 2.0, 3.0, 4.0, 5.0, 10.0, 15.0, and 20.0 mg/L NO_3 by pipette. The spectra obtained are shown in Figure 6.1 below.

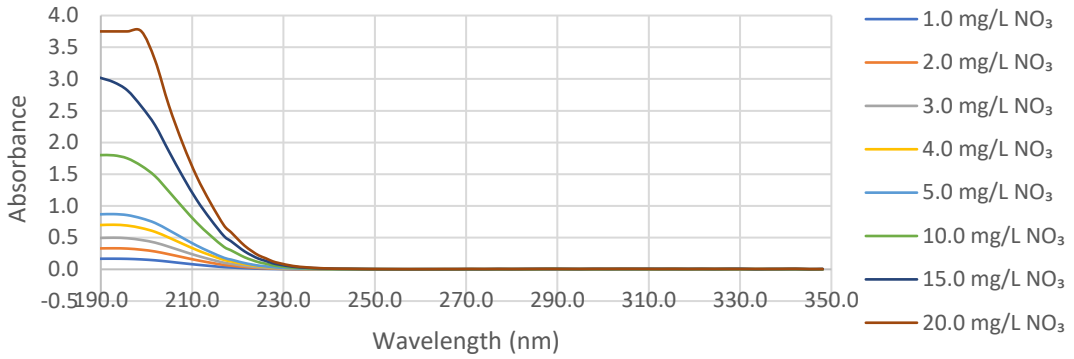

Figure 6.1: Absorbance spectra of sodium nitrate in deionized water using an in-line spectrophotometer with a flow cell path length of 4 mm.

Preliminary inspection of the absorbance spectra shown above in Figure 6.1 showed the expected increase in absorbance with increasing nitrate concentration was visible. However, the peak absorbance value was not observed that the expected wavelength of λ = 224 nm (Ferree and Shannon, 2001), but actually at the minimum wavelength of λ = 189.8 nm. This was determined to be attributable to the UV-Vis spectrophotometer itself. The Real Spectrum PL Series (Real Tech Inc.) is more sensitive at wavelengths closer to 190.0 nm. Accordingly, the peak absorbance was observed 189.8 nm, despite nitrate absorbing UV radiation more effectively at a wavelength of 224 nm.

The relationship between nitrate concentration and the magnitude of the absorbance of each sample at wavelengths of 189.8 nm and 224.6 nm are shown below in Figures 6.2a and 6.2b, respectively. Error bars are present on all data points, even if they are not visible. A summary of a linear regression analysis for the data shown in Figure 6.2 follows in Table 6.1. The data shown in Figure 6.2a and analyzed in Table 6.1 for the 189.8 nm wavelength does not include the 20.0 mg/L NO_3 datapoint. This is because the 20.0 mg/L NO_3 spectrum was over the maximum absorbance range of the spectrophotometer (abs = 3.75) between the wavelengths of λ = 189.8 nm and λ = 201.9 nm.

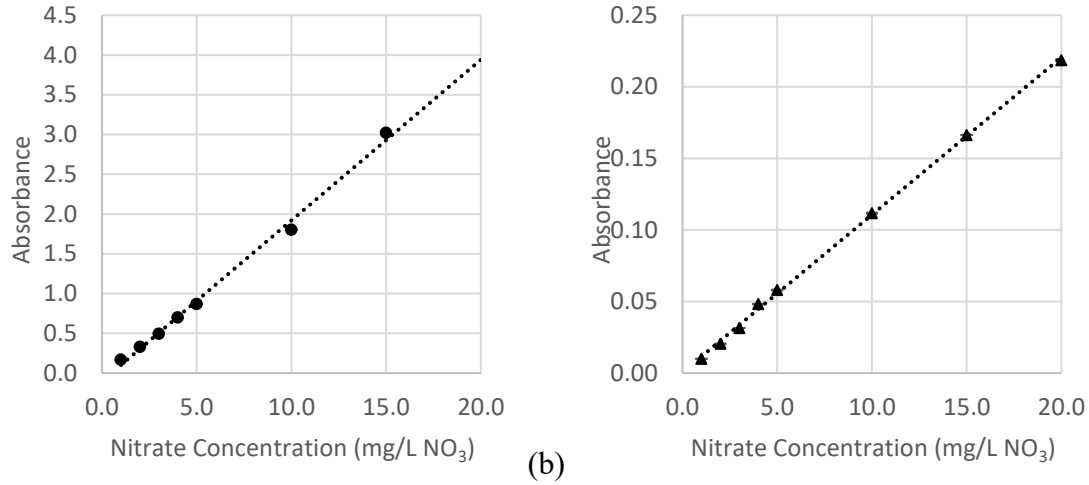

Figure 6.2: Relationship between nitrate concentration in deionized water and absorbance at a) λ = 189.8 nm and b) λ = 224.6 nm using flow cell path length of 4 mm.

Table 6.1: Summary of linear regression analysis of relationship between nitrate concentration in deionized water and absorbance at 189.8 nm and 224.6 nm using flow cell path length of 4 mm.

	Wavelength	
	λ = 189.8 nm	λ = 224.6 nm
Coefficient of Determination (R^2)	0.995	0.999
Residual Sum of Squares (RSS)	0.0295	$3.60*10^{-5}$
Total Sum of Squares (TSS)	6.210	0.0399
F statistic	1,047	6,652
F statistic P-value	$5.30*10^{-7}$	$2.29*10^{-10}$
Intercept	-0.101	0.000639
Slope	0.202	0.0110

Analysis of Figure 6.2 and Table 6.1 shows that the magnitude of the absorbances at both wavelengths increased as a factor of the increased path lengths, as expected. Using linear regression, the slope of the regression lines was observed to be greater at λ = 189.8 nm than at λ = 224.6 nm. A higher slope was indicative of a greater sensitivity to changes in nitrate concentration. However, the correlation between nitrate concentration and absorbance was observed to be higher at a wavelength of 224.6 nm (R^2 = 0.999) than at λ = 189.8 nm (R^2

= 0.995). This was consistent with what was expected as the peak absorbance of nitrate occurs at λ = 224.0 nm (Ferree and Shannon, 2001). The magnitude of the residual sum of squares (RSS) compared to that of the total sum of squares (TSS) was also lower for 224.6 nm wavelength, further indicative of a stronger relationship at the 224.6 nm wavelength. The P-value for both linear regressions showed that each regressed model was statistically significant (P-value < 0.05), with the stronger significance being seen at λ = 224.6 nm. Considering the greater correlation and significance seen in the λ = 224.6 nm data, subsequent experiments focussed on the 224.6 nm wavelength for the detection of nitrate using the UV-Vis spectrophotometer.

6.3.2 Struvite formation in sludge filtrate

Sludge filtrate obtained through laboratory filtration of conditioned anaerobically digested sludge was dosed with magnesium sulfate to facilitate the formation of struvite. Following each $MgSO_4$ dose increment, a 50 mL sample of the filtrate was taken for analysis. Figure 6.3 below shows the results of the quantitative analysis of the samples conducted. Figure 6.3a shows the spectra obtained for the samples of sludge filtrate taken from the 1 L common sample after dosages of 0, 250, 500, 750, 1,000, 1,250 and 1,500 mg $MgSO_4$. Figure 6.3b shows the relationship between the mass of $MgSO_4$ dosed with the turbidity and the absorbance of the samples at a wavelength of 224.6 nm. Figure 6.3c shows the relationship between the mass of $MgSO_4$ dosed and the results of the particle analysis, including the particle concentration (> 2.00 μm diameter) and the mean particle diameter (μm).

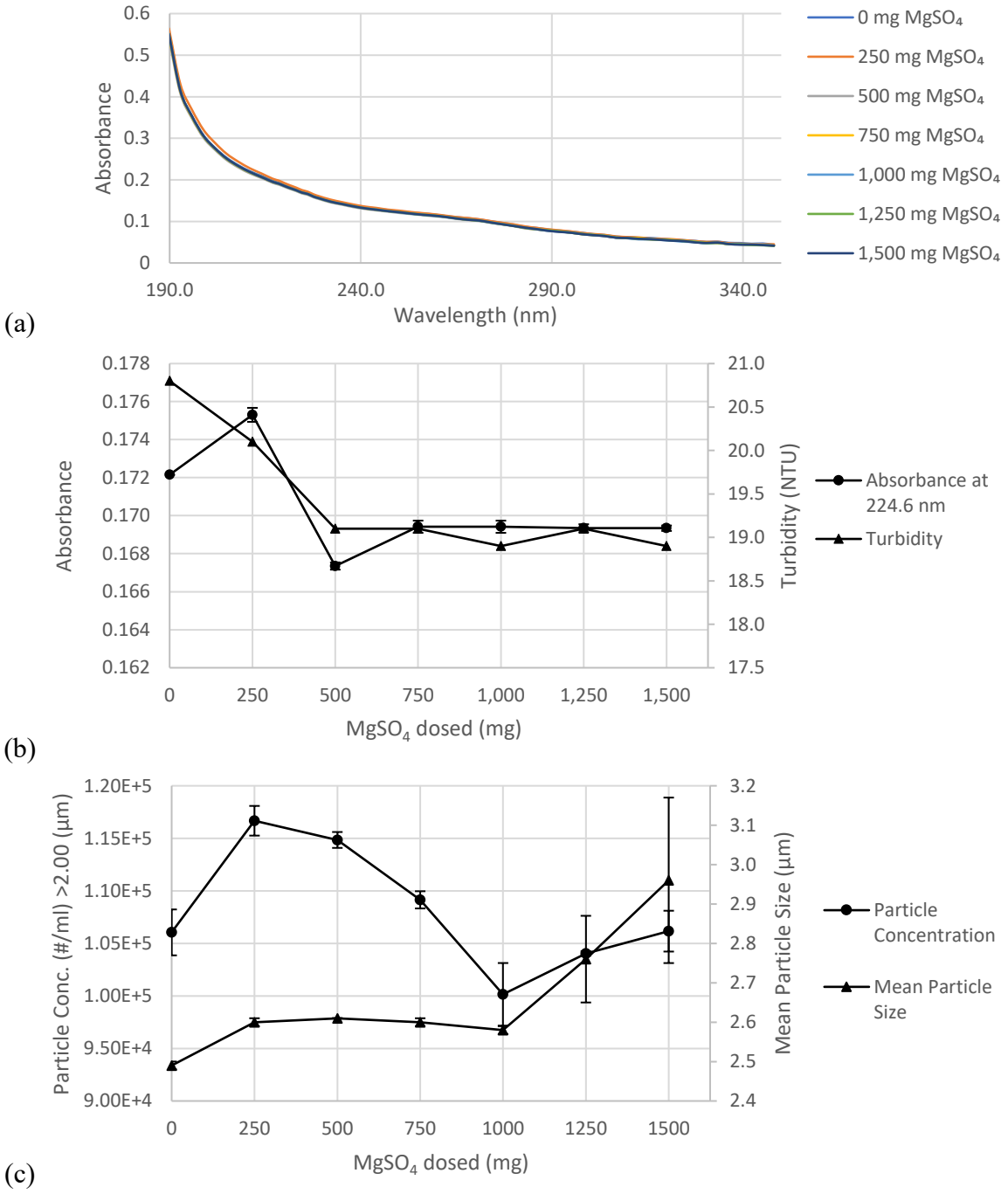

Figure 6.3: Results of struvite formation experiment in laboratory sludge filtrate a) Absorbance spectra; b) Absorbance values at 224.6 nm and turbidity (NTU) values; c) Particle analysis results.

Analysis of the results summarized in Figure 6.3 shows distinct minima and maxima from each of the experimental tests conducted on the sludge filtrate as magnesium was dosed.

The absorbance trend of the samples at λ = 224.6 nm showed an initial increase to a maximum of 0.175 abs at 250 mg $MgSO_4$, followed by a decrease to a minimum of 0.167 abs at 500 mg $MgSO_4$, followed by another increase to a constant value of approximately 0.169 abs starting at 750 mg $MgSO_4$. The difference between the minimum and maximum values of the absorbance measurements was only 0.08 abs, which is very small. This small absorbance magnitude is attributable to the small path length of the 4 mm flow cell employed. However, the expected trend was still visible. An initial increase in absorbance was expected as $MgSO_4$ was dosed due to the increase in particle concentration and size. This was expected to cause an increase in light scattering, increasing the apparent absorbance of the sample. Following this increase, a decrease in absorbance to a minimum value was expected. This was because as ammonium became fixed in struvite, less of it would be oxidized to nitrate prior to measurement. This lower nitrate concentration would thus result in a lower absorbance value measured at λ = 224.6 nm. A minimum measured absorbance value was expected to be seen once an optimum $MgSO_4$ dosage for struvite formation was reached. The subsequent increase in absorbance in $MgSO_4$ greater than 750 mg was expected for the same reason as the initial increase in absorbance, that as more $MgSO_4$ was dosed, more light was scattered, leading to an increase in apparent absorbance, until an equilibrium was achieved.

The turbidity data trend matched the UV-Vis absorbance trend well. A steady initial decrease in turbidity reached a near-constant minimum value of approximately 19 NTU at 500 mg $MgSO_4$. This was the same dosage at which the minimum absorbance value was observed.

A similar trend was observed for the particle concentration trend. An initial increase was seen to a maximum particle concentration of approximately 1.16 x 10^5 particles/mL (>2.00 μm) at 250 mg $MgSO_4$, followed by a decrease to a minimum of approximately 1.00 x 10^5 particles/mL (>2.00 μm) at 1,000 mg $MgSO_4$, followed again by a subsequent increase. The trend for mean particle size showed a slight maximum value of 2.61 μm at 500 mg $MgSO_4$, followed by a minimum value of 2.58 μm at 1,000 mg $MgSO_4$, followed by a subsequent increase.

The maxima and minima values observed in the particle concentration and mean particle size trends are explained through the nature of magnesium as an inorganic coagulant and the nature of struvite formation. Initially, as magnesium was added, coagulation of particles and soluble organics in the sludge filtrate occurred. This increased both the detectable particle concentration and the mean size of particles. Then, as more magnesium was added, these smaller particles coagulated into larger particles, decreasing the overall particle concentration. Further, as more magnesium became bound in struvite, which initially has relatively small crystal sizes, the mean particle size decreased slightly. Eventually, once an optimum magnesium dose for struvite formation was reached, further magnesium addition is hypothesized to have resulted in the restabilization of particles in solution. Restabilization is the phenomenon whereby sufficient cationic conditioner (i.e. Mg^{2+}) has adsorbed onto the surfaces of the anionic particles in solution to give them net positive charges and prevent their coagulation through charge neutralization. This increased the number of flocs, while struvite crystals continued to grow, resulting in the increased particle concentration and mean particle size observed.

Microscopic visual examinations of the sludge filtrate at the beginning and the end of the experiment were conducted to confirm the formation of struvite crystals. The images taken of the sludge filtrate prior to magnesium addition are shown in Figure 6.4 below. The images taken of the sludge filtrate after the addition of 1,500 mg $MgSO_4$ are shown in Figure 6.5 below. An interesting observation made from the images shown in Figure 6.5 was the tendency for struvite crystals to be bound into flocs in solution. Based on these images and comparison with available literature images of struvite (Doyle *et al*., 2000), struvite formation was confirmed visually.

(a) 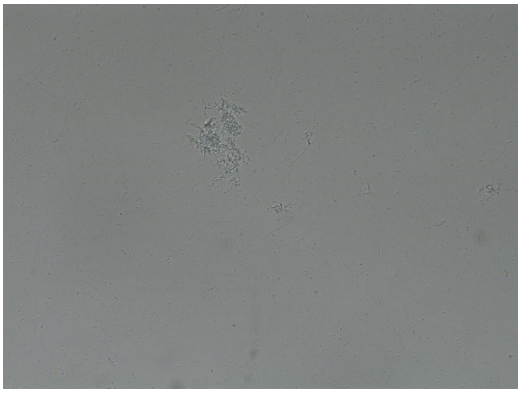 (b) 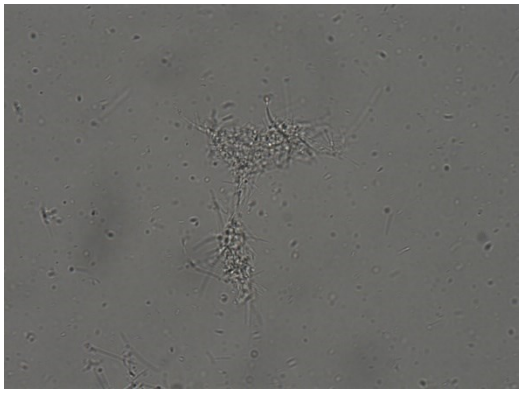

Figure 6.4: Microscopy images of sludge filtrate taken prior to magnesium addition a) 20X; b) 60X.

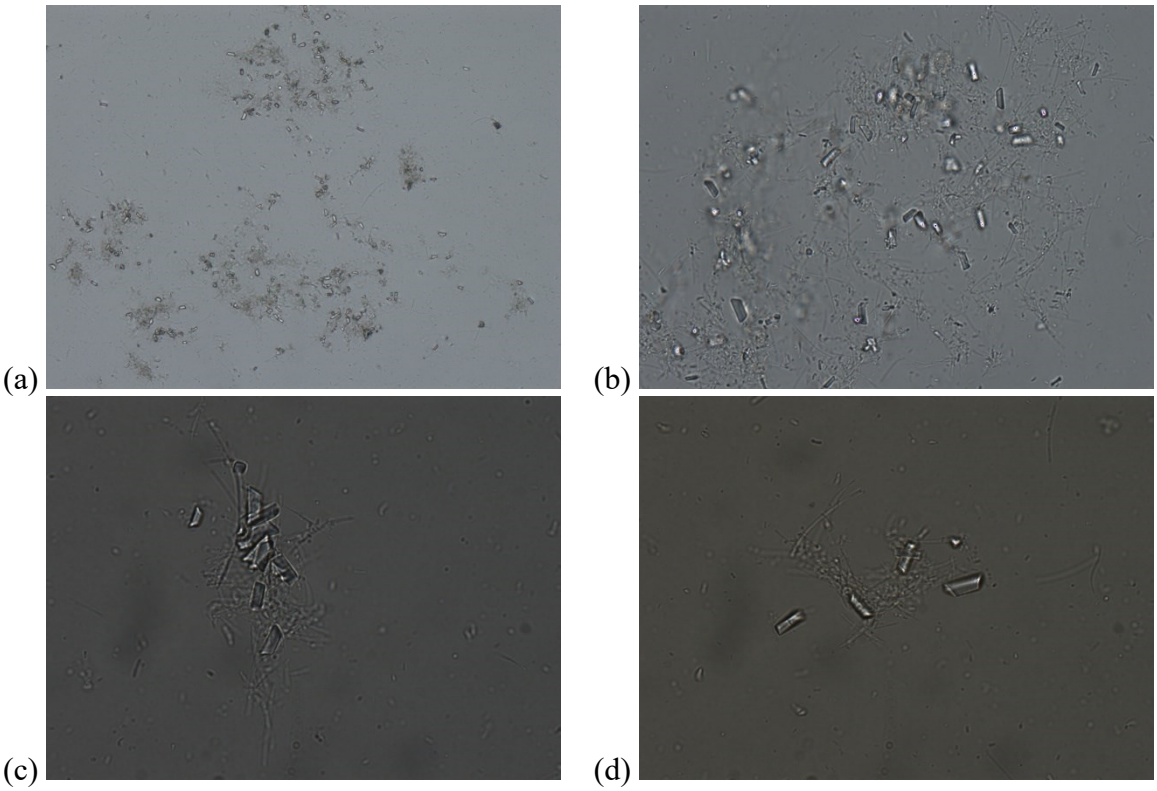

Figure 6.5: Microscopy images of sludge filtrate taken after the addition of 1,500 mg $MgSO_4$ a) 20X; b) 60X; c) 100X; d) 100X.

The same general trend was visible in the results of each of the experimental tests. However, the $MgSO_4$ dosages at which the maxima and minima values for absorbance, particle concentration, and mean particle size were measured differed between the different tests. The cause of this inconsistency was unknown, so a follow up experiment using full-scale sludge centrate obtained from ROPEC was undertaken.

6.3.3 Struvite formation in sludge centrate

Sludge centrate of conditioned anaerobically digested sludge obtained from full-scale bowl centrifuges was dosed with magnesium sulfate to facilitate the formation of struvite. Compared with the sludge filtrate of the previous experiment, the sludge centrate was

expected to have higher TS and BOD values. This was a more representative test of the methodology because it was working with centrate collected from a full-scale treatment facility. Following each $MgSO_4$ dose increment, a 50 mL sample of the filtrate was taken for analysis. Figure 6.6 below shows the results of the quantitative analysis of the experiment conducted. Figure 6.6a shows the spectra obtained for the samples of sludge centrate taken from the 1 L common sample after dosages of 0, 250, 500, 750, 1,000, 1,500, 2,000, 2,500 and 3,000 mg $MgSO_4$. Figure 6.6b shows the relationship between the mass of $MgSO_4$ dosed with the turbidity and the absorbance of the samples at a wavelength of 224.6 nm. Figure 6.6c shows the relationship between the mass of $MgSO_4$ dosed and the results of the particle analysis, including the particle concentration (> 2.00 μm diameter) and the mean particle diameter (μm). Further, a semi-quantitative analysis of the struvite crystal concentration was undertaken using microscopy. The average number of struvite crystals observed per microscopic field of view is shown for each sample in Figure 6.6c. A total of thirteen fields of view were observed for each sample to obtain these values. Representative microscopic images of each of the samples is shown in Figure 6.7 below.

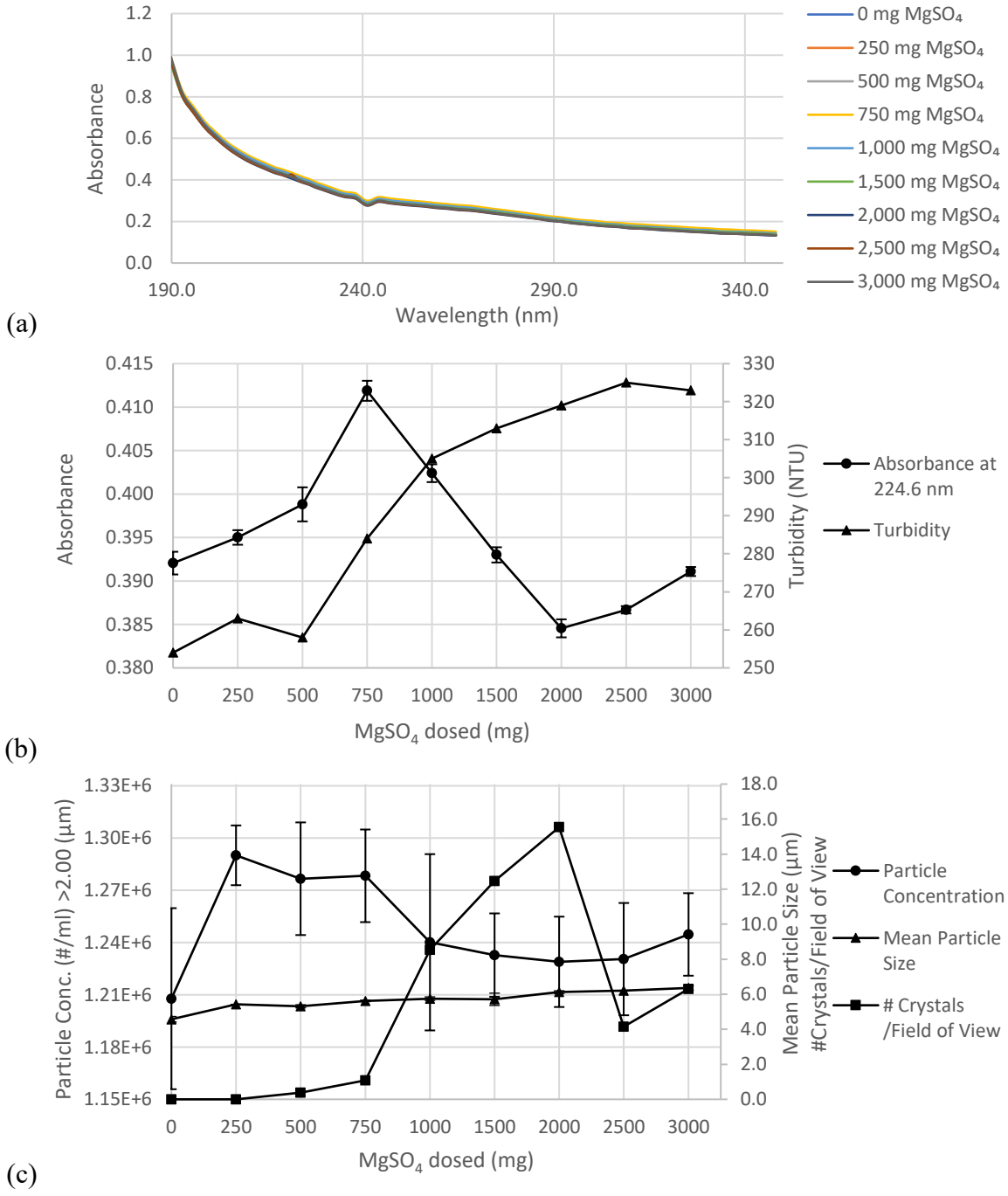

Figure 6.6: Results of struvite formation experiment in full-scale sludge centrate a) Absorbance spectra; b) Absorbance values at 224.6 nm and turbidity (NTU) values; c) Particle analysis results and microscopic semi-quantitative analysis results.

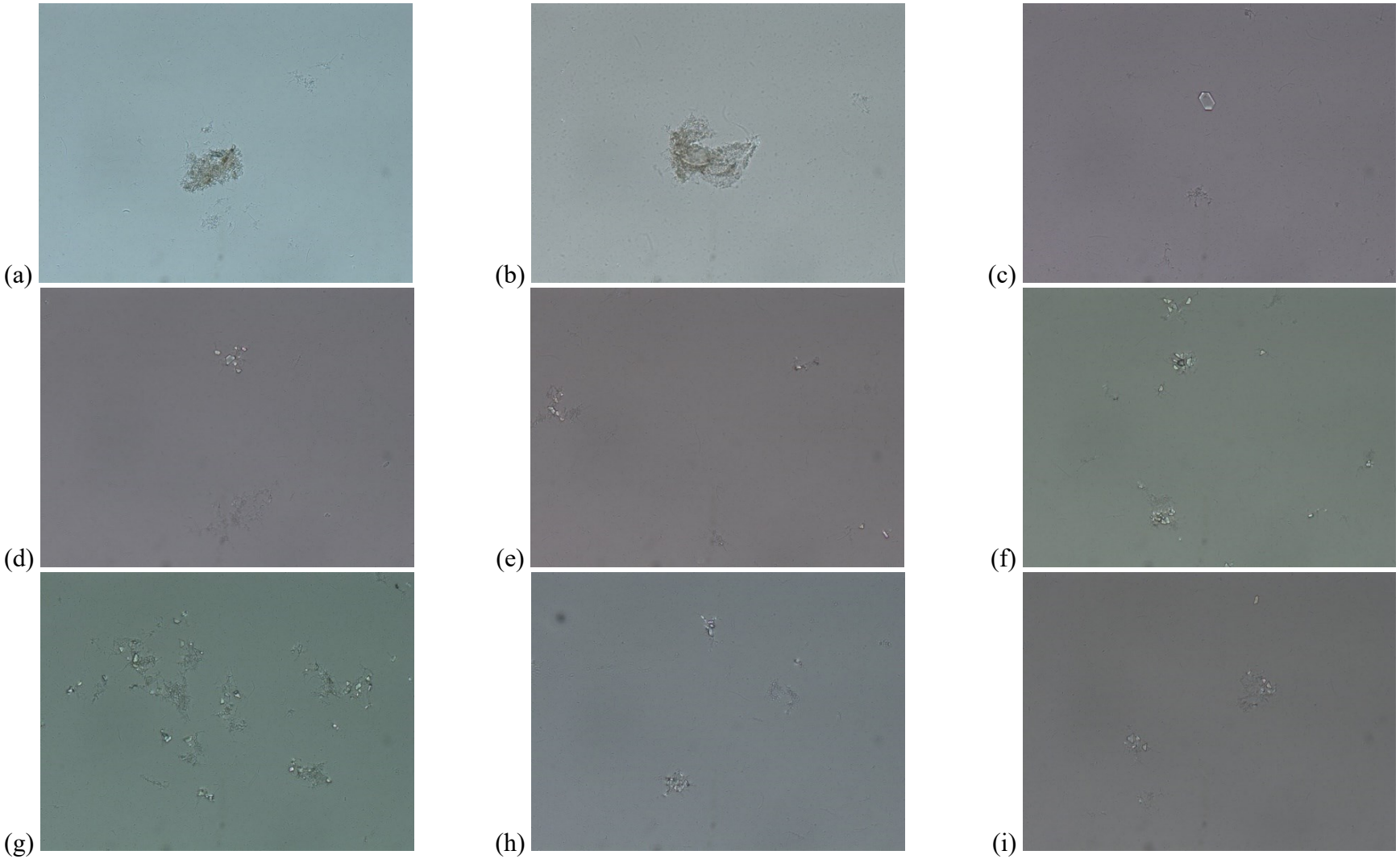

Figure 6.7: Microscopy images of sludge centrate taken at 20X magnification a) prior to $MgSO_4$ addition; and after $MgSO_4$ addition of b) 250 mg; c) 500 mg; d) 750 mg; e) 1,000 mg; f) 1,500 mg; g) 2,000 mg; h) 2,500 mg; i) 3,000 mg.

Analysis of the absorbance data shown in Figure 6.6b showed that the same trend was present as was observed in the previous section. Likewise, analysis of the particle concentration data shown in Figure 6.6c showed an identical trend. As magnesium was dosed, particle coagulation occurred at the same time as struvite crystal formation. These trends reached maximum values for absorbance and for particle concentration of 0.412 abs and 1.29 x 10^6 particles/mL (>2.00 μm) at $MgSO_4$ dosages of 750 mg and 250 mg, respectively. Then, with additional magnesium dosage, more struvite crystals began to form and grow. Accordingly, the absorbance and particle concentration values both decreased to minimum values of 0.384 abs and 1.28 x 10^6 particles/mL (>2.00 μm), respectively, at an $MgSO_4$ dosage of 2,000 mg. The particle concentration values measured had high levels of uncertainty, resulting in only an approximate minimum value in the range of 1,500 to 2,500 mg $MgSO_4$ dosed, but the trend observed does point to a dosage of 2,000 mg $MgSO_4$ as an apparent minimum. After this point, both absorbance and particle concentration began to increase again. This was the result of the magnesium being overdosed, as discussed previously. It was observed here that the difference between the maximum and minimum absorbance values was 0.028 abs, which is much more significant than the 0.08 abs difference than was observed in the previous experiment. Even though the differences in the magnitudes of the absorbance measurements small at λ = 244.6 nm, they are still detectable and reproducible with the Real Spectrum PL Series (Real Tech Inc.), as per the previous section. It is also noteworthy that this small difference in magnitude is again attributable to the employment of the 4 mm path length flow cell employed in the UV-Vis spectrophotometer in this study. Compared with a larger path length, such as that of 10 mm cuvettes employed by many desktop spectrophotometers, the

absorbance magnitude measured using a 4 mm path length is expected to be smaller. Based on both absorbance and particle concentration, the optimum $MgSO_4$ dosage for the sludge centrate appeared to be 2,000 mg.

The turbidity measurements support this and follow a curve which appears to level off after the predicted optimum magnesium dosage, as shown in Figure 6.6b. This trend showed an increase in turbidity with increased magnesium dosage, which was expected as more coagulated particles and struvite crystals formed. When the turbidity values measured appeared to begin to level off, this was interpreted as a balance point being reached between magnesium addition and particle formation. This was observed at around the same $MgSO_4$ dosage as the minimum absorbance particle concentration values, within the range of 2,000 mg to 2,500 mg $MgSO_4$. The mean particle size data was not as clear in predicting an optimum magnesium dose as it was in the previous experiment. As shown in Figure 6.6c, a slow but steady increase in mean particle size was observed consistently as additional magnesium was dosed. The lack of a defined minimum value in the mean particle size measurements could be the result of struvite crystal growth counteracting the effect of particle restabilization in the solution.

The optimum magnesium dosage predicted by these indirect measurements was confirmed through microscopic analysis of the dosed centrate samples. Through visual comparison of the images shown for the various samples in Figure 6.7, it is evident that the struvite crystal concentration reaches a maximum at the 2,000 mg $MgSO_4$ dosage. This was the same dosage as the optimum magnesium dose predictions made through the absorbance and particle concentration measurements. Since these images are merely representative images of an average field of view for the given samples, further analysis was conducted through

a semi-quantitative analysis of the microscopy data. The maximum number of crystals per field of view was observed to be approximately 15.5 crystals per field of view at a dosage of 2,000 mg $MgSO_4$, as shown in Figure 6.6c. The visual microscopic analysis of the dosed sludge centrate samples therefore found the same optimum magnesium dosage for struvite formation as was predicted by both the UV-Vis spectrophotometry method and the particle analysis.

The hypothesized causes of the maximum and minimum values observed in the absorbance and particle concentration trends was confirmed through the microscopic analysis. Through analysis of the images shown in Figure 6.7 and the results of the semi-quantitative analysis shown in Figure 6.6c, it was evident that struvite crystal formation began to occur much more rapidly after the maximum particle concentration and absorbance values were measured. Furthermore, as the minimum particle concentration and absorbance values were approached, struvite crystal concentration rapidly increased, pointing to more magnesium being consumed in struvite formation, as was predicted. Finally, after the minimum particle concentration and absorbance values were passed, noticeably smaller floc sizes were observed, pointing to the occurrence of particle restabilization. Also, as previously discussed and predicted, struvite concentration decreased.

6.4 Conclusion

The goal of this study was to develop a method for real-time and in-line monitoring of optimum magnesium dosage for struvite formation in wastewater side-stream processes. This was achieved using UV-Vis spectrophotometry to measure the residual nitrate concentration post-struvite formation.

Calibration curves were generated for nitrate dosed in deionized water and its data was linearly regressed. It was shown that when using the in-line UV-Vis spectrophotometer, while it was not the peak absorbance, the wavelength of 224.6 nm was best suited for measuring nitrate concentration.

The results of the struvite formation experiments showed that UV-Vis spectrophotometry could identify an optimum magnesium dosage in sludge filtrate and centrate samples. This was achieved through the oxidation of residual ammonium in solution and the measurement of minimum absorbance values where residual nitrate concentration reached a minimum. This is indicative that the phosphate available for struvite formation had been consumed, and that additional magnesium dosing would overdose the solution, leading to lower struvite concentrations. This identification of an optimum magnesium dosage was supported by the correlating measurements of particle concentration from a particle analysis and by turbidity measurements. The formation of struvite and confirmation of the optimum magnesium dosage was achieved visually through a microscopy and a semi-quantitative microscopic analysis of the struvite crystals.

Based on these results, an in-line and real-time UV-Vis spectrophotometer measuring residual nitrate concentrations following a struvite formation and precipitation process could be used to effectively monitor and maintain an optimum magnesium dosage. This would provide real-time assurance that optimal struvite formation and nutrient recovery were constantly taking place in side-stream processes. This system is also beneficial as it could provide cost savings on chemicals and improved performance of downstream processes through reduced magnesium usage.

Chapter 7 – Conclusions

The general conclusions of this thesis are as follows:

- The 4 mm path length flow cell was the optimal path length for residual polymer detection in deionized water and sludge supernatant using the in-line UV-Vis spectrophotometer. Smaller path lengths were shown to result in too much variability in the absorbance measurements for reliable polymer concentration quantification, while interference from other parameters such as solids was shown to reduce the sensitivity of larger path lengths. It was also shown that the in-line UV-Vis spectrophotometer was superior to the desktop UV-Vis spectrophotometer for residual polymer detection in sludge supernatant due to a higher sensitivity at lower wavelengths where polyacrylamide polymer best absorb radiation.
- It was shown that the UV-Vis spectrophotometry method was sensitive to particle concentration through tests varying dilution factor and filter size. This was seen through the lower relative linearity in the regressed data of the samples with higher TS content (no or lower filtration and less dilution) compared with those of lower TS content. Filtration through smaller pore sized filters was observed to reduce the sensitivity of residual polymer detection using the UV-Vis spectrophotometer due to the reduced particle size and concentration. Likewise, increased dilution reduced the impact of particles and again resulted in a lower sensitivity for residual polymer detection. This combined with the increased sensitivity of the smaller 4 mm path length reduces the need for filtration and lowers the amount of dilution required for sludge centrate in full-scale applications.

- The feasibility of a feed-forward and feed-back control system for polymer dose optimization using torque rheology and UV-Vis spectrophotometry was shown through conducting lab-scale dewatering experiments on different samples of anaerobically and aerobically digested sludges and different polymer conditioners. The TTQ rheological method and the UV-Vis spectrophotometry method were found to consistently measure the same optimum polymer dosage as one another in all anaerobically digested sludge samples. This showed that a two-stage in-line and real-time polymer dose optimization system using the TTQ rheological method pre-dewatering and UV-Vis spectrophotometry post-dewatering provided both reliable and internally consistent optimum polymer dose measurements under most conditions.
- These methods were also found to be consistent with the established laboratory methods (capillary suction time and filtration tests) conducted for comparison for some sludges and polymers. The direct injection torque rheological method was found to consistently predict lower optimum polymer doses than the other methods tested.
- The experiments found that the established laboratory tests, which are based on the filterability of the sludge, were incapable of determining an optimum polymer dose for sludge samples with a low TS content. Further, it was found that the torque rheological methods were incapable of determining an optimum polymer dose for the aerobic sludge samples. This was attributed to the natural flocculant appearance of the aerobically digested sludge rendering rheological measurements inconsistent. This showed that the proposed two-stage polymer dose optimization

system provides a level of redundancy where if one monitor is unable to determine an optimum dosage, the other would still be able to provide the measurement.

- It was shown that showed that UV-Vis spectrophotometry could identify an optimum magnesium dosage in sludge filtrate and centrate samples in lab-scale struvite formation experiments. This was achieved through the measurement of minimum absorbance values corresponding to achieving a minimum residual nitrate concentration. This was indicative that the phosphate available for struvite formation had been consumed, and that additional magnesium dosing would overdose the solution, leading to lower struvite concentrations.
- This identification of an optimum magnesium dosage was supported by the correlating measurements of particle concentration from a particle analysis and by turbidity measurements. The formation of struvite and confirmation of the optimum magnesium dosage was achieved visually through a microscopy and a semi-quantitative microscopic analysis of the struvite crystals.
- Based on these results, an in-line and real-time UV-Vis spectrophotometer measuring residual nitrate concentrations following a struvite formation and precipitation process could be used to effectively monitor and maintain an optimum magnesium dosage. This would provide real-time assurance that optimal struvite formation and nutrient recovery were constantly taking place in side-stream processes.

References

Abel-Denee, M., Abbott, T., and Eskicioglu, C. (2018). Using mass struvite precipitation to remove recalcitrant nutrients and micropollutants from anaerobic digestion dewatering centrate. *Water Research, 132*, 292-300. Doi:10.1016/j.watres.2018.01.004

Abu-Orf, M. M., and Dentel, S. K. (1999). Rheology as tool for polymer dose assessment and control. *Journal of Environmental Engineering, 125*(12), 1133-1141. Doi:10.1061/(asce)0733-9372(1999)125:12(1133)

Abu-Orf, M. M., and Örmeci, B. (2005). Measuring sludge network strength using rheology and relation to dewaterability, filtration, and thickening – laboratory and full-scale experiments. *Journal of Environmental Engineering, 131*(8), 1139-1146. Doi:10.1061/(asce)0733-9372(2005)131:8(1139)

Aghamir-Baha, S., and Örmeci, B. (2014). Determination of optimum polymer dose using UV-vis spectrophotometry and its comparison to filtration based tests. *Journal of Residuals Science and Technology, 11*(3), 79-84. Doi:10.1016/j.petrol.2016.05.004

Aguado, D., Barat, R., Soto, J., and Martínez-Mañez, R. (2016). Monitoring dissolved orthophosphate in a struvite precipitation reactor with a voltammetric electronic tongue. *Talanta, 159*, 80-86. Doi:10.1016/j.talanta.2016.06.002

Al Momani, F. A., and Örmeci, B. (2014a). Measurement of polyacrylamide polymers in water and wastewater using an in-line UV-vis spectrophotometer. *Journal of Environmental Chemical Engineering, 2*(2), 765-772. Doi:10.1016/j.jece.2014.02.015

Al Momani, F. A., and Örmeci, B. (2014b). Optimization of polymer dose based on residual polymer concentration in dewatering supernatant. *Water, Air, & Soil Pollution*, *225*(11). Doi:10.1007/s11270-014-2154-z

APHA, AWWA, and WEF (2005). *Standard Methods for the Examination of Water and Wastewater* (21st edition). Washington: APHA/AWWA/WEF.

Arryanto, Y., and Bark, L. (1992). Reineckate ions as a precipitant for the determination of trace amounts of polyacrylamides in potable waters. *Analytica Chimica Acta*, *263*(1-2), 119–129. Doi: 10.1016/0003-2670(92)85433-7

Baudez, J. C. (2008). Physical aging and thixotropy in sludge rheology. *Applied Rheology, 18*(1), 13495-1-13495-8. Doi:10.1515/arh-2008-0003

Becker, N., Bennett, D., Bolto, B., Dixon, D., Eldridge, R., Le, N., and Rye, C. (2004). Detection of polyelectrolytes at trace levels in water by fluorescent tagging. *Reactive and Functional Polymers*, *60*, 183–193. Doi: 10.1016/j.reactfunctpolym.2004.02.022

Bhuiyan, M. I., Mavinic, D. S., and Beckie, R. D. (2009). Determination of temperature dependence of electrical conductivity and its relationship with ionic strength of anaerobic digester supernatant, for struvite formation. *Journal of Environmental Engineering, 135*(11), 1221-1226. Doi:10.1061/(asce)0733-9372(2009)135:11(1221)

Bolto, B., and Gregory, J. (2007). Organic polyelectrolytes in water treatment. *Water Research, 41*(11), 2301-2324. Doi:10.1016/j.watres.2007.03.012

Campbell, H. W., and Crescuolo, P. J. (1982). The use of rheology for sludge characterization. *Water Science and Technology, 14*(6-7), 475-489. Doi:10.2166/wst.1982.0120

Chang, L.-L., Bruch, M. D., Griskowitz, N. J., and Dentel, S. K. (2002). NMR spectroscopy for determination of cationic polymer concentrations. *Water Research*, *36*(9), 2255–2264. Doi: 10.1016/s0043-1354(01)00444-4

Chhabra, R. P., and Richardson, J. F. (2008). Rheometry for non-newtonian fluids. In R. P. Chhabra and J. F. Richardson, *Non-Newtonian Flow and Applied Rheology – Engineering Applications* (2nd ed.) (pp. 56-109). Butterworth-Heinemann.

Chmilenko, F. A., Korobova, I. V., and Nazarenko, S. V. (2004). Spectrophotometric setermination of polyacrylamide in aqueous solutions using cationic dyes. *Journal of Analytical Chemistry*, *59*(2), 124–128. Doi: 10.1023/b:janc.0000014737.11478.e5

Cordell, D., Drangert, J. O., and White, S. (2009). The story of phosphorus: global food security and food for thought. *Global Environmental Change, 19*(2), 292-305. Doi:10.1016/j.gloenvcha.2008.10.009

Cormier, R. (2019). *UV-vis spectroscopy as a tool for the detection of residual polymer and optimization of polymer dose in drinking water treatment applications* (Unpublished master's thesis). Carleton University, Ottawa, Canada.

Dentel, S. K., Abu-Orf, M. M., and Walker, C. A. (2000a). Optimization of slurry flocculation and dewatering based on electrokinetic and rheological phenomena. *Chemical Engineering Journal*, *80*(1-3), 65-72. Doi:10.1016/s1383-5866(00)00078-2

Dentel, S. K., Chang, L. L., Raudenbush, D. L., Junnier, R. W., and Abu-Orf, M. M. (2000b). *Analysis and fate of polymers in wastewater treatment*. Alexandria, VA: Water Environment Research Foundation.

Dentel, S. K. (2001). Conditioning. In L. Spinosa, and P. A. Vesilind, *Sludge into Biosolids: Processing, Disposal, Utilization* (pp. 279-311). London: IWA Publishing.

Doyle, J. D., and Parsons, S. A. (2002). Struvite formation, control and recovery. *Water Research, 36*(16), 3925-3940. Doi:10.1016/s0043-1354(02)00126-4

Doyle, J. D., Philp, R., Churchley, J., and Parsons, S. A. (2000). Analysis of struvite precipitation in real and synthetic liquors. *Process Safety and Environmental Protection, 78*(6), 480-488. Doi:10.1205/095758200531023

Fattah, K. P., Mavinic, D. S., Koch, F. A., and Jacob, C. (2008). Determining the feasibility of phosphorus recovery as struvite from filter press centrate in a secondary wastewater treatment plant. *Journal of Environmental Science and Health, Part A, 43*(7), 756-764. Doi:10.1080/10934520801960052

Ferree, M. A., and Shannon, R. D. (2001). Evaluation of a second derivative UV/visible spectroscopy technique for nitrate and total nitrogen analysis of wastewater samples. *Water Research, 35*(1), 327–332. Doi: 10.1016/s0043-1354(00)00222-0

Gardner, K. L., Murphy, W. R., and Geehan, T. G. (1978). Polyacrylamide solution ageing. *Journal of Applied Polymer Science 22*(3), 881-882. Doi:10.1002/app.1978.070220330

Gehr, R., and Kalluri, R. (1983). The effects of short-term storage and elevated temperatures on the flocculation activity of aqueous polymer solutions. *Water Quality Research Journal*, *18*(1), 23–44. Doi: 10.2166/wqrj.1983.002

Gibbons, M. K., and Örmeci, B. (2013). Quantification of polymer concentration in water using UV-Vis spectroscopy. *Journal of Water Supply: Research and Technology – Aqua, 62*(4), 205-213. Doi:10.2166/aqua.2013.032

Hammadi, L., Ponton, A., and Belhadri, M. (2012). Temperature effect on shear flow and thixotropic behaviour of residual sludge from wastewater treatment. *Mechanics of Time-Dependent Materials, 17*(3), 401-412. Doi:10.1007/s11043-012-9191-z

Hansen, L. D., and Eatough, D. J. (1987). Determination of ammonia, amides, and the degree of hydrolysis of partially hydrolyzed polyacrylamide by thermometric titration and direct injection enthalpimetry. *Thermochimica Acta*, *111*, 57–65. Doi: 10.1016/0040-6031(87)88034-6

Jaffer, Y., Berry, T., Pearce, P., and Parsons, S. A. (2002). Potential phosphorus recovery by struvite formation. *Water Research, 36*(7), 1834-1842. Doi:10.1016/S0043-1354(01)00391-8

Jungreis, E. (1981). A simple microdetermination of polymer flocculants (polyacrylamides and guar) in mine water. *Analytical Letters*, *14*(14), 1177–1183. Doi: 10.1080/00032718108059814

Keenan, K. E., Papavasilopoulos, E. N., and Bache, D. H. (1998). Measurement of polymer residuals in an alum sludge. *Water Research*, *32*(10), 3173–3176. Doi: 10.1016/s0043-1354(98)00141-9

Kirinovic, E., Leichtfuss, A. R., Navizaga, C., Zhang, H., Christus, J. D., and Baltrusaitis, J. (2017). Spectroscopic and microscopic identification of the reaction products and intermediates during the struvite ($MgNH_4PO_4 \cdot 6H_2O$) formation from magnesium

oxide (MgO) and magnesium carbonate ($MgCO_3$) microparticles. *ACS Sustainable Chemistry & Engineering, 5*(2), 1567-1577. Doi:10.1021/acssuschemeng.6b02327

Korchef, A., Saidou, H., and Amor, M. B. (2011). Phosphate recovery through struvite precipitation by CO_2 removal: Effect of magnesium, phosphate and ammonium concentrations. *Journal of Hazardous Materials, 186*(1), 602-613. Doi:10.1016/j.jhazmat.2010.11.045

Kulicke, W. M., and Kniewske, R. (1981). Long-term change in conformation of macromolecules in solution: 2.Poly(acrylamide-co-sodium acrylate)s. *Macromolecular Chemistry and Physics, 182*(8), 2277-2287.

Lu, J., and Wu, L. (2003). Polyacrylamide quantification methods in soil conservation studies. *Journal of Soil and Water Conservation, 58*(5), 278-289.

Mortimer, D. A. (1991). Synthetic polyelectrolytes—a review. *Polymer International, 25*(1), 29-41. Doi:10.1002/pi.4990250107

Moulessehoul, A., Gallart-Mateu, D., Harrache, D., Djaroud, S., Guardia, M. D., and Kameche, M. (2017). Conductimetric study of struvite crystallization in water as a function of pH. *Journal of Crystal Growth, 471*, 42-52. Doi:10.1016/j.jcrysgro.2017.05.011

Murray, A., and Örmeci, B. (2008). Impact of polymer-sludge interaction on rheogram peaks and optimum dose determination. *Water Science and Technology, 57*(3), 389-394. doi:10.2166/wst.2008.018

Nadler, A., Magaritz, M., and Leib, L. (1994). Pam application techniques and mobility in soil. *Soil Science*, *158*(4), 249–254. Doi: 10.1097/00010694-199410000-00004

Novak, J. T., and O'Brien, J. H. (1975). Polymer conditioning of chemical sludges. *Journal (Water Pollution Control Federation), 47*(10), 2397-2410.

Nowak, O. (2006). Optimizing the use of sludge treatment facilities at municipal WWTPs. *Journal of Environmental Science and Health, Part A*, *41*(9), 1807–1817. Doi: 10.1080/10934520600778986

Ohlinger, K. N., Young, T. M., and Schroeder, E. D. (1999). Kinetics effects on preferential struvite accumulation in wastewater. *Journal of Environmental Engineering, 125*(8), 730-737. Doi:10.1061/(asce)0733-9372(1999)125:8(730)

Örmeci, B. (2007). Optimization of a full-scale dewatering operation based on rheological characteristics of wastewater sludge. *Water Research*, *41*, 1243-1252. Doi:10.1016/j.watres.2006.12.043

Örmeci, B., and Abu-Orf, M. M. (2005). Protocol to measure network strength of sludges and its implications for dewatering. *Journal of Environmental Engineering, 131*(1), 80-85. Doi:10.1061/(asce)0733-9372(2005)131:1(80)

Örmeci, B., Cho, K., and Abu-Orf, M. (2004). Development of a laboratory protocol to measure network strength of sludges using torque rheology. *Journal of Residuals Science and Technology, 1*(1), 35-44.

Owen, A. T., Fawell, P. D., Swift, J. D., and Farrow, J. B. (2002). The impact of polyacrylamide flocculant solution age on flocculation performance. *International Journal of Mineral Processing, 67*(1-4), 123-144. Doi:10.1016/s0301-7516(02)00035-2

Owen, A. T., Fawell, P. D., and Swift, J. D. (2007). The preparation and ageing of acrylamide/acrylate copolymer flocculant solutions. *International Journal of Mineral Processing, 84*(1-4), 3-14. Doi:10.1016/j.minpro.2007.05.003

Owen, T. (1996). *Fundamentals of UV-visible spectroscopy*. Germany: Hewlett-Packard Company.

Scholz, M. (2005). Review of recent trends in capillary suction time (CST) dewaterability testing research. *Industrial & Engineering Chemistry Research, 44*(22), 8157-8163. Doi:10.1021/ie058011u

Scoggins, M., and Miller, J. (1979). Determination of water-soluble polymers containing primary amide groups using the starch-triiodide method. *Society of Petroleum Engineers Journal*, *19*(03), 151–154. Doi: 10.2118/7664-pa

SNF Floerger (2002). *Preparation of Organic Polymers*, SNF Floerger, Andrézieux-Bouthéon, FR.

SNF Floerger (2003). *Sludge Dewatering*, SNF Floerger, Andrézieux-Bouthéon, FR.

Taylor, K., Burke, R., Nasr-El-Din, H., and Schramm, L. (1998). Development of a flow injection analysis method for the determination of acrylamide copolymers in brines. *Journal of Petroleum Science and Engineering*, *21*(1-2), 129–139. Doi: 10.1016/s0920-4105(98)00042-4

Taylor, K. C., and Nasr-El-Din, H. A. (1994). Acrylamide copolymers: A review of methods for the determination of concentration and degree of hydrolysis. *Journal of Petroleum Science and Engineering. 12*(1), 9-23. Doi:10.1016/0920-4105(94)90003-5

Tchobanoglous, G., Stensel, H., Tsuchihashi, R., Burton, F., Abu-Orf, M., Bowden, G., and Pfrang, W. (2014). *Wastewater Engineering: Treatment and Resource Recovery* (5th ed.). New York, NY: McGraw Hill.

US EPA. (1987). Design manual: Dewatering municipal wastewater sludges. *U.S. EPA CERI/ORD, EPA 652/1-87-014*, Environmental Protection Agency, Cincinnati, OH.

Vaneeckhaute, C., Belia, E., Meers, E., Tack, F. M., and Vanrolleghem, P. A. (2018). Nutrient recovery from digested waste: towards a generic roadmap for setting up an optimal treatment train. *Waste Management, 78*, 385-392. Doi:10.1016/j.wasman.2018.05.047

WEF (2012). *Solids Process Design and Management*, Water Environment Federation, Alexandria, VA.